Clp-Mediated Regulation of the Mycobacterial Cell Cycle

Clp-Mediated Regulation of the Mycobacterial Cell Cycle

A dissertation presented

by

Jemila Caplan Kester

to

The Committee on Higher Degrees in Biological Sciences in Public Health

in partial fulfillment of the requirements
for the degree of

Doctor of Philosophy

in the subject of
Biological Sciences in Public Health

Harvard University
Cambridge, Massachusetts

March 2017

Clp-Mediated Regulation of the Mycobacterial Cell Cycle

Abstract

Tuberculosis is currently the most deadly infectious disease worldwide. Given the high rates of treatment failure, new antibiotics are desperately needed. Antibacterial drugs typically target DNA replication, cell growth, and cell division processes, yet regulators of the mycobacterial cell cycle remain undiscovered. In my thesis work, I sought to identify key players in mycobacterial cell cycle control, potentially leading to new antibacterial targets.

Mycobacteria share a unique pattern of asymmetric growth and division with the model bacterium *Caulobacter crescentus*. *C. crescentus* initiates its cell cycle through proteolysis of key cell cycle regulators using the housekeeping protease complex ClpXP. Therefore, we postulated that a Clp-dependent mechanism might underlie cell cycle control in mycobacteria as well.

In order to measure changes to the cell cycle brought about by modulations to Clp family proteins, I first developed a suite of quantitative microscopy tools to analyze each period of the cell cycle. During validation of this toolset, I discovered a post-division phase where the new pole—created at the site of division—does not initially grow. The identification of this "lag phase" clarified an outstanding question in the field as to the origin of asymmetric growth.

To understand the role of Clp proteins (ClpC, ClpX, and ClpP) in the cell cycle, I systematically depleted each protein *in vivo*, and used my suite of image analysis tools to quantify changes.

Loss of the ATPase ClpC and the protease ClpP lead to similar morphologies, notably loss of asymmetric growth and division. Conversely, depletion of the ATPase ClpX resulted in loss of cell division and DNA integrity. These cells eventually lyse and die, providing the first experimental evidence for ClpX's predicted essentiality. To identify proteins interacting with ClpX, we designed a novel methodology and biochemically validated a top hit from this screen as an adaptor of ClpX. Our data suggest a link between ClpX and DNA replication.

This is the first functional demonstration of a mycobacterial Clp adaptor. My work provides a framework for understanding the unique essentiality of multiple Clp proteins in mycobacteria: their non-redundant regulatory roles in DNA replication, cell growth, and division.

Table of Contents

Dedication

To my husband, for your never-ending support, compassion,

friendship, respect, and love.

I love you with all that I have and all that I am.

Acknowledgements

This work would not have been possible without the academic, financial, and mental health support of my faculty advisor, Prof. Sarah Fortune. Sarah, you are one of a kind! Thank you for standing by me and believing in me. ENFJs are the best.

We in the Fortune lab call ourselves Fortunates, because we recognize how special it is to work along side such a fabulous team. I feel ever so fortunate to have gotten to work with all of you for the last 5 years. I am eternally grateful to current and former members of the lab, especially Bree Aldridge, Scarlet Shell, Alex Sakatos, Connie Martin, Bryan Bryson, and Allison Carey. And a special thanks goes to the people who directly contributed to this work: Mike Chase, Alex Dills, and Vivian Leung.

The Fortune lab works in parallel with Eric Rubin's lab, and I am thankful for Eric's support, as well as the guidance (commiseration?) of members of his lab. Particularly past and current members Katie Wu, Annie Park, Ravi Raju, Cara Boutte, Kasia Baranowski, Alissa Myrick, and Karen Kieser, who contributed intellectually, scientifically, emotionally, or all three.

Beyond the Fortunates and Rubinites, our circle extends to the Sassetti lab. I thank you all for your support, but I must especially thank Kadamba "Sundaram" Papavinasasundaram, Christina Baer, Xavier Meniche, and Aditya "Adi" Bandekar.

I received wonderful scientific feedback and emotional support from my dissertation advisory committee and preliminary qualifying exam committee members: Barbara Burleigh, Marcia Goldberg, Christopher Sassetti and Jay Mitchell. Thank you to my defense exam committee members for their time and effort: Barbara Burleigh, Eric Rubin, Yonatan Grad, and Simon Dove.

I was lucky enough to work closely with Olga Kandror in Fred Goldberg's lab. My science mom. Tov, toda. I have learned everything biochemistry from you, and you are the most gracious person I know. A thanks also goes to Tatos Akopian in Fred's lab for your help on all things pharma.

I managed to spend a limited amount of time in the BL3, but thanks to the wonderful folks caring for all the nitty gritty details at HSPH and the Ragon. Yong, you are working wonders on the scope—thank you so much.

I worked closely with Paula Montero Llopis in David Rudner's lab at HMS on a side project. While those data didn't make the cut for this, I am very thankful to Paula for her patience and generosity with her high throughput imaging platform.

To my undergraduate and post-bac advisors, Professors Shubha Govind and Johanna Joyce: You both taught me to enjoy science but be rigorous at the same time. Johanna, you demonstrated how to be scientist who is a woman (not simply a female scientist) every day. Shubha, you showed me how to be a mom and a brilliant thinker, without having to compromise on either. Thank you both.

I am grateful to the administrative support at HSPH. In the BPH Program, Marianne Wessling-Resnick and Deirdre Duckett have been extremely supportive. In the grants program, I literally would not have managed to submit my F31 without Monica Patel.

My fellow BPH2011 class was an amazing cohort with whom to traverse the perils and pleasures of grad school. Including the BPH2011 honorary member, Deepali. My friends in BPH classes above and below were also wonderful supports throughout, especially Kasia, Perrine, Alex, Karelle, and Regina.

People always ask, how can you go to grad school and do so much yoga? And I always reply, how can you go to grad school and *not* do so much yoga? Thanks to my yoga family at O2, especially my fellow TTs, Ann, Sarah, Lynne, and Elliott. To my students: you might think I'm teaching you, but you are teaching me. I learn from you in every class and continue to be wowed by your strength and power. Mimi, you inspire me as a teacher, a parent, an entrepreneur, and a professional bad-ass.

Lear. I love you. You kept me sane, kept me from dropping out (at least twice), financed my Netflix-watching, and made me laugh. I am not exaggerating to say I would not have gotten this far without you. You are the hardest working person in science (she really is, it's insane), yet you always had time to get a coffee with me, listen to my complaints, give me a hug, tell me I'm being crazy, or just sit with me. I thank you from the bottom of my heart.

I have the best friends. Thanks to all of you who kept me from losing it. Like, a lot. Jenn (my unpaid therapist), Lindsey (for all the Tom Collinses), Erin (woman, 3 is enough!), Lear (see above), Bryan (you taught me the care face), Allison (you taught me the skeptical face), Audrey (gym bud), Alex (real zing), Jess B. (now Professor Jess), Jess (aka tall girl), Kassie, Nicole, Sarah W. (you plank like a beast). You guys rock!

Thanks to my mom and sister. They say it takes a village to raise a child. I say, it takes one Nana and one Auntie to raise two of 'em. How many times did I desperately beg you to babysit at the very last minute? More than anyone can count. Mom, thanks for always believing in me. You are my biggest fan. You gave me the foundation from which I could spread my wings; you made it possible for me to fly. I love you both.

My beautiful girls, who make it all worth it, thank you for constantly reminding me what really matters. (And I don't mean movie night and chocolate. Although those are some of the

best things in the world.) You are my life's purpose. While I *sometimes* complained about the difficulty of raising kids in grad school, the truth is I couldn't have done this without you both, because what then would have been the point? You are my babies, my heart and soul, my everything. I love you to the moon and back.

Chapter 1

Introduction

Adapted from:

Kester JC[1], Fortune SM[1]. 2014. Crit Rev Biochem Mol Biol.49(2):91-101. Persisters and beyond: mechanisms of phenotypic drug resistance and drug tolerance in bacteria.

[1]Department of Immunology and Infectious Diseases, Harvard School of Public Health, Boston, MA, USA.

Declaration of Interests/Acknowledgements

The authors report no declarations of interest. Funding support from NSF GRFP DGE-1144152 awarded to JCK and Burroughs Wellcome Fund 2010054, Doris Duke Charitable Foundation, and NIH 1DP2OD001378-01 awarded to SMF.

Abstract

One of the challenges in clinical infectious diseases is the problem of chronic infections, which can require long durations of antibiotic treatment and often recur. An emerging explanation for the refractoriness of some infections to treatment is the existence of subpopulations of drug tolerant cells. While typically discussed as "persister" cells, it is becoming increasingly clear that there is significant heterogeneity in drug responses within a bacterial population and that multiple mechanisms underlie the emergence of drug tolerant and drug resistant subpopulations. Many of these parallel mechanisms have been shown to affect drug susceptibility at the level of a whole population. Here we review mechanisms of phenotypic drug tolerance and resistance in bacteria with the goal of providing a framework for understanding the similarities and differences in these cells.

keywords: population heterogeneity, efflux pumps, permeability, cellular differentiation, chronic infections, biofilm, asymmetric growth and division.

I. Introduction

Classically, bacterial response to antibiotics is defined in terms of drug susceptibility and resistance. For some organisms, like *Mycobacterium tuberculosis* (Mtb), drug susceptibility and resistance are treated clinically as binary classifiers. For other organisms, susceptibility is considered along a spectrum in terms of the minimum concentration of drug required to inhibit growth. These metrics share an important common feature: in these assays, the bacterial population is considered to be homogeneously susceptible or resistant.

However, since the 1940's it has been recognized that the members of a bacterial population are not phenotypically homogeneous, even where they are, to a large extent, genetically clonal. Importantly, in considering responses to antibiotics, studies have revealed subpopulations of bacterial cells that vary in their susceptibility to antibiotic. One well recognized class of these cells are the so-called "persister" cells, which are classically defined as a stochastically arising, nonreplicative subpopulation of cells that are phenotypically tolerant of antibiotics. More recently, studies have demonstrated that there can be multiple phenotypically distinct subpopulations within a given bacterial population. These subpopulations vary in their physiologic state, size, frequency, the degree to which they are less susceptible to drug as well as their mechanistic basis. Importantly, the known mechanisms by which a subpopulation of cells becomes less susceptible to drug are conceptually similar to mechanisms that play out, in other circumstances, at a population level. It is therefore likely that we can learn from population level studies of drug responses what other, as yet undiscovered, paths to drug tolerant subpopulations might encompass.

Ia. Key terminology

While the terms "drug susceptible" and "drug resistant" seem self evident, there is often some confusion in their use. The uncertainty becomes more apparent when "drug tolerance" is used in contrast to "drug resistance". Thus, we begin by clarifying the terminology used in this review.

We use **drug resistance** to mean that the bacterial cell continues to replicate in a given concentration of drug (Fig 1.1). Drug resistance is therefore explicitly relative to the concentration of drug in question. The minimum inhibitory concentration (MIC) of drug is the smallest amount sufficient to inhibit growth of a population of bacteria in a defined window of time. Thus, a simpler way to codify drug resistance is to say that it reflects an increase in MIC; yet the magnitude of this increase is not inherent in the definition. As the relative nature of drug resistance implies, there can be higher-level drug resistance or lower-level drug resistance. In clinical microbiology, drug response is typically assessed according to MIC thresholds. In the best cases, these MIC thresholds have been validated clinically as to whether a bacterium, with a given MIC, can be successfully treated with a given drug. However, even what is clinically considered high-level drug resistance is rarely absolute. For example, clinical isolates of *M. tuberculosis* are considered to have high-level resistance to the cell wall-acting antibiotic isoniazid (INH) if their MIC exceeds 0.4 mg/ml, though INH concentrations of up to 5 mg/ml are achievable in plasma. Recently, a survey of clinical isolates revealed that over 80% of samples considered to be isoniazid resistant on clinical testing had MICs of less than 5 mg/ml and thus might respond to high dose isoniazid therapy (Schaaf et al. 2007).

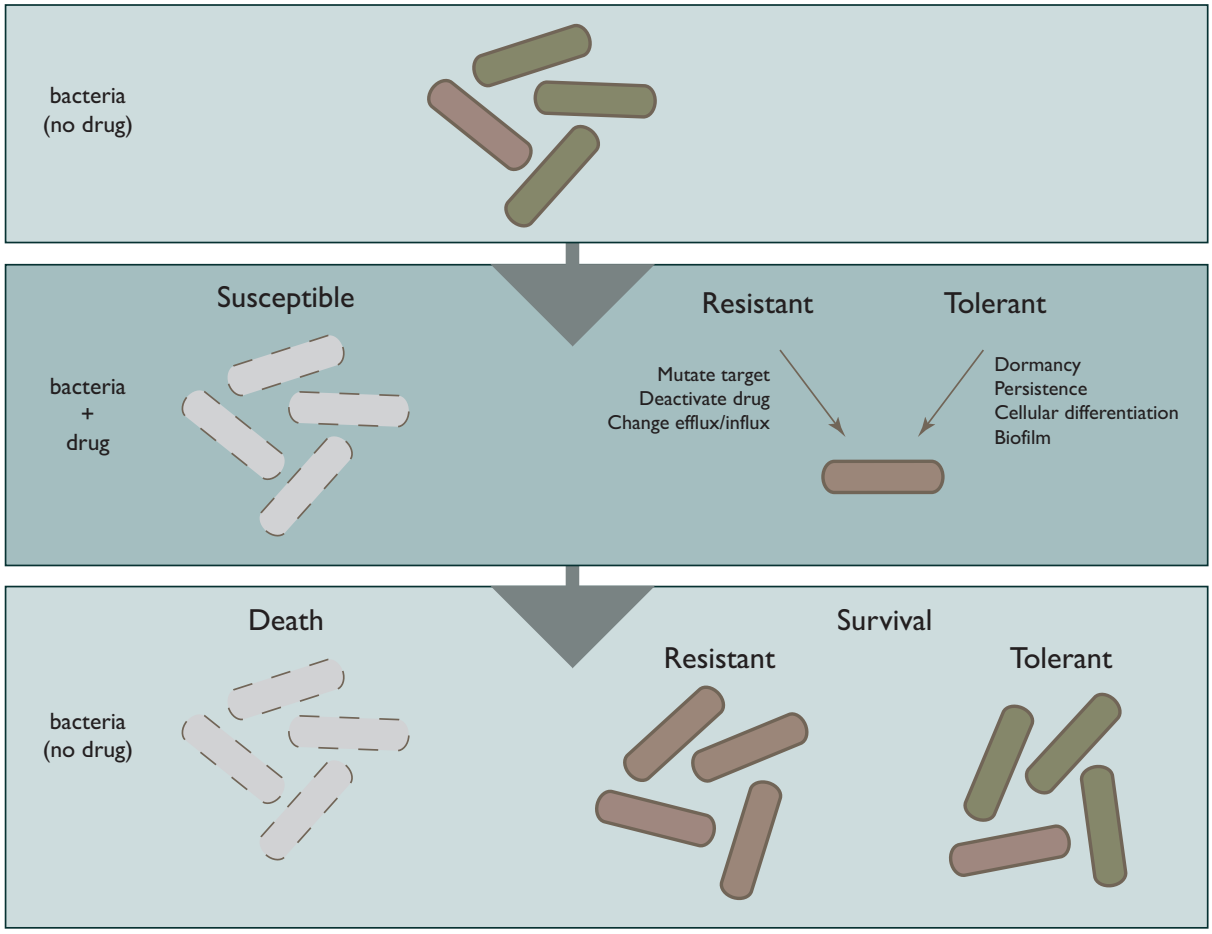

Figure 1.1 Resistance vs. tolerance. Bacterial resistance refers to continued growth in the presence of antibiotic, whereas tolerance refers to survival without replication.

Drug resistance typically arises through mechanisms that block the interaction of a drug and its target. There are many ways to achieve drug resistance. These include genetic mutation of the target, enzymatic deactivation of the drug or loss of an enzyme required to activate a prodrug. They also include mechanisms that prevent a drug from reaching the target, for example drug export by efflux pumps or changes that reduce the cell's permeability of the drug.

In contrast, we use **drug tolerance** to mean that a bacterium survives but does not grow in the face of a given concentration of drug (Fig 1.1). Drug tolerance is therefore a relevant descriptor of bacterial response to cidal antibiotics. In contrast, for biostatic drugs—that is, drugs that inhibit bacterial growth but do not kill—the term makes little sense. The term *resistance* still holds for these drugs: cells continue to grow at the same antibiotic concentration and require higher MICs to inhibit growth. However, all cells surviving static drugs without growth would be considered tolerant.

Drug resistance and drug tolerance are often, though not necessarily correctly, distinguished according to their mechanistic basis. Thus, drug resistance is often considered to arise primarily through genetic change, and is described as **genotypic**. Drug tolerant states are thought to arise because of a change in bacterial physiology and thus be **phenotypic**. From this perspective, subpopulations of bacterial cells that differ in their drug susceptibilities have typically been described as **phenotypically drug tolerant**. However, these associations are not perfect. We discuss several examples of **phenotypic drug resistance** and we anticipate that more such examples will be identified in the future. Using these sorts of definitions will mean that a broad range of phenotypically drug tolerant/resistant cells are included in discussions of the different types of drug responses within populations of bacterial cells.

Ib. Paths to phenotypic drug tolerance and resistance

There are multiple mechanisms by which subpopulations of bacterial cells, with varying susceptibilities to drug, are generated. We describe first mechanisms of phenotypic drug tolerance originating along a population spectrum from whole population, as with growth phase dynamics, to large subpopulations, as with asymmetric growth and division, and finally to rare

cells, as persister cells. We then proceed with phenotypic resistance mechanisms of whole populations, specifically changes in influx, efflux, and antibiotic deactivating enzymes. We continue coverage of phenotypic resistance with several vignettes on specialized cases of topical studies providing windows into mechanisms by which single cells contribute to population-level susceptibility. These include stochastic gene expression, swarming behavior, bacterial altruism, and phenotypic switching. We conclude with a discussion of how many of these mechanisms play out in bacterial biofilms.

II. Drug tolerance at a population and subpopulation level: growth arrest from stationary phase to persister cells

This section describes phenotypic mechanisms of drug tolerance where growth phase or metabolic rate affect a cell's ability to survive antibiotic treatment. Three main topics are covered: dormancy, asymmetric growth and division, and persister cells. We discuss the phenotypic appearance of these variants as well as the molecular mechanisms used to create them.

IIa. Stationary phase and metabolic quiescence

When cells in bulk culture experience limited nutrients, they enter into a phase of slowed growth balanced with cell death called late or prolonged stationary phase (Finkel 2006). When challenged with antibiotics in this phase, cells have increased survival compared to logarithmically growing cells (Spoering & Lewis 2001; Tenover 2006; Herbert et al. 1996) (Anderl et al. 2003; Eng et al. 1991). Upon reintroduction of nutrient-rich media or removal of antibiotics, surviving cells resume rapid growth. Stationary phase survival is not limited to

antibiotic challenge, however. *Bordetella pertussis* stationary phase cultures evade host complement-mediated killing (Barnes & Weiss 2002) and stationary phase cultures of *E. coli* are resistant to serum-induced death (Allen & Scott 1980).

What is the mechanism for stationary phase survival of antibiotics? One proposed mechanism for gram-negative bacteria is that cells experience decreased dependence on or lowered availability of the drug's target during stationary phase. For example, slowed growth confers tolerance to the cell wall-acting β-lactams due to a decreased need for cell wall synthesis (Tenover 2006). Similarly, quinolones – which target topoisomerase II to create unresolved nicks in the bacterial chromosome – generally require highly active transcription or DNA replication in order to kill bacteria (Gradelski et al. 2002). Cellular quiescence does not create universally drug tolerant cells, however. There is evidence for bacterial dependence on ATP synthesis and the proton motive force during dormancy (Schaaf et al. 2007; Rao et al. 2008), presumably reflected in the increased potency on quiescent cells of certain drugs, like ATP-synthase-targeting diarylquinolones (Finkel 2006; Koul et al. 2008; Sala et al. 2010) and the lipopeptide daptomycin, which acts by depolarizing the membrane (Spoering & Lewis 2001; Silverman et al. 2003).

Growth arrest is likely a more prominent contributor to changes in antibiotic susceptibility in some infections versus others. In *M. tuberculosis*, for example, it is thought that persistent, non-replicative states both allow the prolonged survival of the organism in the host environment and contribute to the long duration of treatment required to clear the infection. In *M. tuberculosis*, a non-replicative state can be induced by a variety of triggers, including those commonly encountered by Mtb in the host environment, such as starvation, hypoxia, and reactive nitrogen or oxygen species. These stressors trigger a common signaling pathway, mediated by the

dormancy survival (Dos) regulatory system, the sensor kinase DosS and its cognate transcription factor DosR (Tenover 2006; Park et al. 2003; Kendall et al. 2004). Dos activation induces expression of 48 genes, including triacylglycerol synthase (*tgs1*), which directs carbon flux away from the TCA cycle and into storage lipid synthesis (Herbert et al. 1996; Shi et al. 2010; Daniel et al. 2004). This stress-induced metabolic remodeling decreases *M. tuberculosis* susceptibility to many different classes of antibiotics both *in vitro* and *in vivo* (Anderl et al. 2003; Deb et al. 2006; Daniel et al. 2004). Mutants that specifically redirect carbon flux back to the TCA cycle under stress conditions are more susceptible to antibiotics than wild type cells (Eng et al. 1991; Baek et al. 2011).

IIb. Asymmetric growth and division

A more nuanced form of growth phase-dependent antibiotic survival is seen in the differential growth states of dividing mycobacteria. Asymmetric growth and division has recently been described in mycobacteria (Barnes & Weiss 2002; Aldridge et al. 2012) (Allen & Scott 1980; Joyce et al. 2012) (Tenover 2006; Singh et al. 2013). Mycobacteria are rod shaped cells that elongate from their poles. Within a single cell, the new pole, created by cytokinesis, grows slower than the previously established, or old, pole (Gradelski et al. 2002; Aldridge et al. 2012). Aldridge et al. showed that this growth polarization creates sister cells with distinct phenotypes: cells inheriting the older pole grow faster than cells inheriting the newer pole, and this creates dimorphism with each division. Importantly, aging and asymmetry lead to differential susceptibility to antibiotics (Aldridge et al. 2012). Faster growing cells, termed accelerators, are more susceptible to cell wall-acting antibiotics, while slower growing cells, termed alternators, are more susceptible to transcription-targeting drugs (Aldridge et al. 2012). These studies were not performed in such a way that one could assess the MIC's of alternator

and accelerator cells. However, the change in MIC is likely to be relatively small but affect many cells in the population.

Mycobacteria are not alone in having dimorphic progeny with distinct antibiotic susceptibilities. The non-pathogenic, soil-dwelling *Paenibacillus vortex* has two discrete morphotypes within differentiated swarmer cells, each with different susceptibility to antibiotics (Roth et al. 2013). Unlike mycobacteria, susceptibility is fixed by morphotype and does not appear to be dependent upon drug: slower-growing, lower ATP-containing morphotypes are more resistant to both kanamycin and rifampin (Roth et al. 2013). The dynamics of *P. vortex* morphotype creation and durability are similar to asymmetric growth and division in that a colony can change from a single type to a mixed population in a few hours, though the actual mechanism of switching has not been found (Roth et al. 2013). These high frequency phenotypic variants represent a new class of heterogeneity-based mechanisms for surviving stress, discovered through single-cell analysis.

IIc. Persisters

An extreme example of growth state-dependent tolerance is the persister phenotype. Joseph Bigger coined the term *persisters* in 1944 to describe the small percentage of phenotypically tolerant cells causing a lack of sterilizing ability of penicillin on *Staphylococcus* cultures (Bigger 1944). Currently, the field defines persister cells as phenotypic variants that survive MIC of antibiotics in a non-growing, non-dividing state (Keren, Kaldalu, et al. 2004). Intrinsic to their definition, following re-initiation of growth and division, resulting progeny have the same susceptibility to that drug as the parent culture (Keren, Shah, et al. 2004; Bigger 1944). Persistence is thus an example of phenotypic tolerance, as persister cells neither divide nor die during challenge and survivors have similar survival dynamics and MIC as the parental strain.

The persister phenotype has been extensively described. The addition of lethal amounts of antibiotics to a culture elicits a biphasic kill curve, where the majority of the population dies quickly, but a small percentage of cells survive (Falla & Chopra 1998; Keren, Shah, et al. 2004). When conditions are again favorable, these persister cells restart growth and division cycles. In an elegant series of papers from Moyed and collaborators using a mutant strain with higher rates of persister formation, *Escherichia coli* persisters were shown to survive in the presence of different classes of drugs (Moyed & Bertrand 1983; Moyed & Broderick 1986; Scherrer & Moyed 1988). This multidrug tolerant phenotype was further supported in later work from another group (Correia et al. 2006). In works from Keren, Spoering, Lewis, and coworkers, *Staphylococcus aureus* and *Pseudomonas aeruginosa* persisters are enriched in stationary phase cultures and contribute significantly to the survival of both stationary and biofilm cultures (Spoering & Lewis 2001; Keren, Kaldalu, et al. 2004; Keren, Shah, et al. 2004).

One described mechanism for the formation of persister cells is toxin-dependent slowed growth in a subset of cells that survive antibiotic treatment. In *E. coli* persister cells, toxin-antitoxin genes are enriched (Shah et al. 2006) and can be exploited therapeutically to aid in bacterial killing (Williams & Hergenrother 2012). In the *hipA* mutant, persisters display prototypical biphasic killing (Moyed & Bertrand 1983). HipA is the toxin in the HipBA toxin-antitoxin module. The presence of HipA without HipB is sufficient to induce persistence (Korch & Hill 2006; Korch et al. 2003). In a seminal work from Balaban and colleagues, a *hipA* mutant was used to observe high levels of persisters; their generation dynamics, β-lactam survival, and growth characteristics were assayed (Balaban et al. 2004). Using microfluidic-based live cell imaging, the authors characterized the growth dynamics of cells that would go on to survive, demonstrating that slow growth was protective. When compiled with their wild type *E. coli* data,

a model evolved whereby persistence is achieved through slow or absent growth of cells (Balaban et al. 2004). The mechanism for hipA-mediated and other TA system-mediated persistence in *E. coli* was recently tied to stochastic production of the alarmone (p)ppGpp (Maisonneuve et al. 2013; Germain et al. 2013).

In some cases, the emergence of persister cells appears to be metabolically regulated. One gene implicated in metabolism-based persistence is *glpD*, a G3P dehydrogenase involved in the utilization of glucose as a carbon source. Using an ingenious method for isolating persister cell RNA, Keren et al looked at expression profiles to identify genes responsible for persister development or survival (Keren, Shah, et al. 2004). In a follow up paper, the same group found *glpD* deletion drastically decreased persister development (Spoering et al. 2006), pointing to a link between carbon metabolism and persister formation. Recently, another group corroborated a role for *glpD* in *E. coli* persister formation. In this latest study, using microarray-based genetic footprinting, Girgis et al found that mutations in *glpD* led to drastic increases in persistence enacted through slowed growth from changes to metabolic flux (Girgis et al. 2012). In a study suggestive of similar links in other organisms, *M. tuberculosis* biosynthetic and energy catabolic pathway transcripts were in significantly lower abundance in isolated persisters than in vegetatively growing cultures (Keren et al. 2011). *S. aureus* small colony variants, which are specially adapted to persistence in the host environment, display lowered biosynthesis of nucleotides (reviewed in (Martínez & Rojo 2011)).

Despite the potential clinical implications of persister cells (Fauvart et al. 2011) and the efforts in describing them, there is no consensus on the mechanisms by which persisters arise or the basis of their drug tolerance (Balaban et al. 2013). This may be because persistence is not a single state of being; persistent cells might be created by various mechanisms and survival

ensured via different paths. Further studies into the mechanisms by which they are generated as well as ways to perturb persisters are needed in order to define their functional relevance in treatment failure.

III. Drug resistance through altered access: influx, efflux, and deactivating enzymes

We now switch gears from drug tolerance to mechanisms of phenotypic resistance. Conceptually, mechanisms that lead to resistance differ from those that lead to tolerance in that they reduce the interaction of the drug and its target.

It is not surprising that bacteria have evolved myriad ways of limiting entry and increasing expulsion of antibiotic from the cell given the abundance of targets and mechanisms of action. There are two main types of access restriction: intrinsic and inducible. Intrinsic defenses are constitutively expressed or expressed without external stimuli, whereas inducible defenses are environmentally initiated and maintained. Consequently, it is the durability of the mechanism that separates one from the other, rather than the mechanism itself. For both intrinsic and inducible changes in drug access to target, mechanisms include impermeable cell walls, efflux pumps, and drug-deactivating enzymes. All three modes are described below.

Whether intrinsic or inducible, influx and efflux changes shift intracellular drug concentration, but whether resistance is due to altered permeability or antibiotic export has been difficult to distinguish and a topic of debate. Resistance-conferring changes in intracellular antibiotic concentration were classically attributed to permeability (Zimmermann & Rosselet 1977; Nikaido 1989) (Scudamore et al. 1979). β-lactam antibiotics, which inhibit cell wall synthesis, were shown to enter gram negative bacteria primarily through porins (Yoshimura &

Nikaido 1985). In the gram negative *P. aeruginosa*, barrier-dependent β-lactam exclusion had been attributed to the absence or closing of porins, as their deletion led to increased MIC (Nicas & Hancock 1983). But in 1991, Livermore and Davy showed that, at least for *P. aeruginosa*, permeability-based estimates were not sufficient to explain β-lactam resistance (Livermore & Davy 1991). Livermore and Davy used cell lines with a range of permeability capacities and introduced the *β-lactamase* gene on a plasmid, conferring resistance to β-lactam antibiotics to these cells. If permeability were the major resistance driver, they should find an inverse correlation between resistance and permeability. Strikingly, they found that resistance was not correlated with permeability, disproving the model for *P. aeruginosa* (Livermore & Davy 1991) and paving the way for rethinking intrinsic resistance models.

In fact, studies suggest that a combination of porins, efflux pumps, and deactivating enzymes confers resistance in *P. aeruginosa* to β-lactams (Li, Ma, et al. 1994; Li, Livermore, et al. 1994). Efflux pumps also actively rid the cell of drugs such as tetracycline, chloramphenicol, and norfloxacin (Li, Livermore, et al. 1994), but this is dependent upon efficient cooperativity between permeability through the outer membrane and efflux pumps (Nikaido 1994). Finally, a link was shown between β-lactamases and efflux, where inhibitors of the former are substrates of the latter (Li et al. 1998), and where co-regulation of β-lactamase and efflux pump genes has been demonstrated (Li et al. 2002).

These findings have been recapitulated in many other organisms. For example, in *M. tuberculosis*, efflux pumps represent an important participant in intrinsic resistance to cell wall-acting antibiotics. This year, through the step-wise deletion of each class of efflux pump in *M. tuberculosis*, Dinesh et al demonstrated the reliance of *M. tuberculosis* on efflux as a resistance

mechanism against cell wall inhibiting drugs, including penicillin, ampicillin, meropenem, and vancomycin (Dinesh et al. 2013).

Although the initial focus upon permeability has waned as interest in efflux pumps emerged, recent studies encourage us to reconsider the role of cell permeability in surviving antibiotics through porins and other membrane components. In a study of drug killing mechanisms, the most significant contributor to *E. coli* survival of aminoglycosides was influx across the cell membrane in a proton motive force-dependent manner (Ezraty et al. 2013). In another work, silver was found to change cell permeability and improve efficacy of three classes of antibiotics as well as rescuing sensitivity of a drug resistant mutant strain of *E. coli* (Morones-Ramirez et al. 2013).

The importance of stationary phase-associated drug tolerance was discussed in terms of slow growth, but there is also evidence from three recent studies that changes in permeability may contribute to growth phase-dependent changes in antibiotic susceptibility. In the first, starved and dormant *M. tuberculosis* exhibited resistance to fluoroquinolones, rifamycins, and linezolid in the presence of efflux pump inhibitors, suggesting a role for cell wall permeability at least in stationary culture unique from efflux mechanisms (Sarathy et al. 2013). In another study, stationary cultures of *S. aureus* were shown to have thicker cell walls with lowered integrity as evidenced by the presence of non-bridge-linked peptidoglycan stems by NMR spectroscopy and HPLC-MS (Zhou & Cegelski 2012). Finally, in the bacterial cause of community-acquired pneumonia, *Klebsiella pneumoniae*, efflux and influx modulation creates resistance to multiple drugs and has differing effects on virulence simultaneously (Bialek et al. 2010). Bialek et al found efflux overexpression increased virulence in a nematode model, while reduced porin levels had the opposite effect on virulence; yet both mechanisms led to increased survival during

exposure to several drugs. From these studies it becomes clear we need to further examine cell wall changes to definitively assign a resistance role for permeability without efflux.

Bacteria are able to augment their intrinsic restrictions with inducible changes in efflux pump activity and permeability as the need arises. Decreased influx and increased efflux can be provoked by several different stresses, including antibiotics, environmental demands, and intracellular life. Gram-negatives are the classically studied genera for efflux resistance mechanisms, in particular the resistance-nodulation-cell division (RND) family of efflux pumps (reviewed extensively in (Alvarez-Ortega et al. 2013)). An interesting example is the MexXY-OprM RND multidrug efflux pump of *P. aeruginosa* (Poole 2001). When *P. aeruginosa* is treated with ribosome inhibitors, the interaction of the drug and its target induces the overproduction of the MexXY-OprM pump and allows for survival and proliferation in the presence of drug (Jeannot et al. 2005; Masuda et al. 2000; Morita et al. 2006). Importantly, pump overexpression is found in recalcitrant clinical infections (Beaudoin et al. 2010) (Wu et al. 2012), underlining the physiologic and public health relevance of efflux pumps. Compounding the issue, by changing efflux or influx rates, cells reduce their intracellular and/or periplasmic drug concentration, not only allowing for their survival and growth but also establishing a continuous low level of antibiotic inside the cell. Prolonged sub-inhibitory concentration of antibiotic may lead to mutations conferring heritable drug resistance (Kohanski et al. 2010) and increase the formation of persister cells (Johnson & Levin 2013).

In addition to antibiotic exposure, environmental pressures have been shown to affect rates of drug influx and efflux (Bornet et al. 2003; Ghisalberti et al. 2005; Rodrigues et al. 2012). In *E. coli*, environmental stresses such as acidic conditions can change the expression levels of outer membrane proteins OmpP and OmpX leading to increased survival (Dupont et al. 2007). The

expression change is environmentally maintained, as removal of the stress returns cells to their previous susceptibilities (Dupont et al. 2007). In a study of *Enterobacter aerogenes*, bacteria returned to their original antibiotic sensitivity in the absence of antibiotic pressure, as seen through consecutive isolates from patients (Bornet et al. 2000). In contrast, continuous antibiotic pressure selects for cells with increased efflux pump expression, leading to a phenotypically resistant population of cells (Alonso et al. 1999).

In *M. tuberculosis*, efflux is also likely to contribute to differences in antibiotic susceptibility and may be specifically upregulated by the stressors in the host environment. First, upregulation of three of the known classes of efflux pumps leads to increased MICs of several antibiotics including all first line drugs *in vitro* (Balganesh et al. 2012; Dinesh et al. 2013). An additional pump was recently described in mycobacteria, a member of the sodium-dependent multidrug and toxic compound extrusion (MATE) family (Mishra & L. Daniels 2013), and future studies may show it contributes to resistance as well. Antibiotic resistant clinical isolates display higher efflux pump expression (Wang et al. 2012), underscoring the potential importance of this survival mechanism in treatment failure. Further studies are needed in order to establish a causal link between increased MIC and efflux expression levels, however.

Importantly, mycobacteria upregulate efflux pumps when living intracellularly (Adams et al. 2011). Using a model system of zebrafish larvae and *M. marinum* in conjunction with *Mtb*-infected macrophages, Adams et al demonstrate that intracellular bacteria upregulate efflux pump expression even in the absence of antibiotic exposure. This efflux expression contributes to bacterial survival of antibiotics in both models, and is ablated by the addition of efflux pump inhibitors (Adams et al. 2011). This work provides a potentially clinically relevant treatment alternative and demonstrates the role of efflux pumps in antibiotic resistance.

IV. Subpopulation resistance due to variable gene expression

As persisters are rare, highly drug tolerant cells that exist within a population, recent work suggests that there are also mechanisms by which rare, highly phenotypically drug resistant cells can arise within a population. Recently, a study in *Msm* identified a novel mechanism by which a subpopulation of phenotypically drug resistant cells arises within the population (Wakamoto et al. 2013). They found stochastic or pulsatile gene expression affecting susceptibility to isoniazid (INH) (Wakamoto et al. 2013), a cell wall biosynthesis inhibitor that is part of the first-line treatment for tuberculosis. INH is delivered as a prodrug that is converted to its active form within the mycobacterial cell by the catalase-peroxidase, KatG. In the absence of *katG*, cells are resistant to INH. In a recent work, Wakamoto and colleagues describe pulsatile expression of *katG* in mycobacteria at the single-cell level, with associated increase in INH susceptibility of KatG-pulsing cells (Wakamoto et al. 2013). The mechanistic basis for the pulsatile expression remains undefined, but could potentially come about in several ways. Interestingly, this new data could suggest a mechanism, either nondeterministic or with an as yet undetermined pattern of expression, where population heterogeneity increases survival during numerous stressful conditions. The concept of variation increasing survival is not new in bacteriology (Adam et al. 2008; Veening et al. 2008; Levy et al. 2012; Hsieh et al. 2013), but stochastic expression of genes on so short a time scale is provocative and an important area of further study.

V. Subpopulation escape from drug: Swarming

One of the more fascinating mechanisms bacteria have evolved to survive stressful environments is to simply relocate. Swarming is a group motility behavior employed by some flagellate

bacteria in response to excessive cell density and low nutrient availability (Henrichsen 1972). When cells are crowded or nutrients are scarce, cells signal to initiate swarm behavior and move to a region with better a resource:cell ratio (R. Daniels et al. 2004). Evasion of antibiotic by swarming behavior is also an established drug resistance mechanism (Lai et al. 2009).

In addition to survival through evasion, swarming groups are more impervious to drug (Lai et al. 2009), allowing them to move through a region of antibiotic to an antibiotic-free environment. For example, *Salmonella enterica* serovar Typhimurium phenotypically differentiates into motile swarm cells on agar when limited in certain nutrients or if exposed to acidic conditions (Kox et al. 2000) (Soncini & Groisman 1996). Kim et al found serovar Typhimurium swarming led to increased resistance to a wide range of antibiotic classes, with MICs from five to 100 times higher than vegetative colonies (Kim et al. 2003). One possible mechanism is through changes in the lipopolysaccharides (LPS) essential for differentiation into the swarm cell phenotype (Toguchi et al. 2000), which is often characterized by hyperflagellated, elongated, and multinucleate cells. Kim et al suggest the change in LPS may decrease permeability of antibiotics into swarming serovar Typhimurium cells, though the study did not conclusively distinguish between permeability and efflux changes (Kim et al. 2003).

VI. Response to secreted cues: bacterial altruism and selfishness

As we have discussed, population-wide drug susceptibility is not necessarily representative of every individual's MIC. With a few exceptions, the mechanisms by which this occurs are not well understood. One intriguing mechanism first described by a team lead by James Collins is bacterial altruism. Enacted by a single cell but done in benefit of the whole population, altruism, like kin selection, is characterized by a small subset of cells suffering a fitness cost in order to

increase the likelihood of population-wide survival (West et al. 2006). In the study (Lee et al. 2010), Lee, Collins, and colleagues continuously cultured *E. coli* in increasing concentrations of norfloxacin, a bactericidal fluoroquinolone that inhibits gyrase A. As concentrations of norfloxacin increased, so too did the population-level MIC, which they defined as the concentration inhibiting 60% of growth. Strikingly, the majority of individual isolates had resistance levels below the population, while a small minority had significantly higher MICs, and emerged prior to the raising of the collective's MIC (Lee et al. 2010). By using a combination of mass spectrometry, genetic mutation, whole genome sequencing, and transcriptional profiling, Lee et al demonstrated that these high resistance isolates (HRIs) were genetically resistant due to mutations in *gyrA*, the drug's target. Strikingly, HRIs secrete a metabolite, indole, which provided less resistant neighbors with a signal to increase efflux pump expression and other phenotypic resistance products (Lee et al. 2010). Repeating these experiments using another drug, the ribosome-targeting gentamicin, they demonstrated that altruism is a survival tactic for bacteria spanning multiple classes of antibiotics (Lee et al. 2010).

On the opposite end of the spectrum from altruism is selfish behavior, where the action is beneficial for the actor and detrimental for the recipient (West et al. 2006). An example of this is between-colony competition. In the normally rod-shaped, social bacterium *Paenibacillus dendritiformis*, competing colonies respond to overcrowding and nutrient limitation by secreting a cell wall-acting toxin, Slf, that kills neighbors at colony interfaces (Be'er et al. 2009; Be'er et al. 2010). Amazingly, at the sub-lethal doses of toxin found within one's own colony, a small percentage of motile rod cells is triggered to switch to non-motile, replicating cocci that are resistant to the toxin (Be'er et al. 2011). When conditions again favor a rod-shaped existence, cocci secrete an inducer, Ris, and switch back to replicating, motile rods (Be'er et al. 2011).

Here we have presented evidence for both preexisting and inducible phenotypic variation at the subpopulation level that leads to the enhanced survival of an entire population with implications for survival in harsh environments, including inside the host. As single-cell analysis methods become more and more advanced, it is likely additional mechanisms will be revealed for a broader range of species.

VII. Pulling it all together, or—how these mechanisms unite in a biofilm

In the sections above, we have focused on individual mechanisms of altered drug susceptibility as they enable the survival of a subpopulation of bacterial cells in the face of antibiotic treatment. Our goal has been to highlight determinants of drug susceptibility—growth state, efflux/permeability and antibiotic response-related gene expression—that can vary at a subpopulation level. As this review has emphasized, changes in these factors can occur at both high and low frequency within a bacterial population through a variety of mechanisms. However, this structure artificially implies that there are single mechanisms to bacterial survival at play at any given time and that any given population is in two discrete states. Instead, it is perhaps more accurate to think of bacterial populations as a complex collection of individuals that can vary for any given phenotype through many mechanisms and through that multifaceted phenotypic heterogeneity acquire the ability to withstand various stresses.

One of the best-studied examples of this is bacterial biofilms. Biofilms are complex communities of bacterial cells that develop upon a solid surface. Both in medicine and experimentally, biofilms are notoriously insensitive to antibiotics (Prosser et al. 1987; Nichols et al. 1989; Gristina et al. 1987; Holmes & Evans 1989). Various lines of research have implicated

many paths to altered drug susceptibility. In addition, it is clear that these mechanisms impact drug susceptibility to some degree both at a population level and in specialized subpopulations of drug tolerant cells. While biofilms have been the focus of many excellent reviews, here we discuss the literature pertinent to phenotypic drug tolerance and resistance.

Drug access: Biofilms are made up of individually drug susceptible cells that become refractory to drug as the biofilm forms and matures (Stewart & Costerton 2001). Several features of biofilm growth contribute to drug tolerance. The most obvious may be the features of the biofilm that reduce drug access, namely matrix and associated three-dimensional structure of the biofilm (Mah & O'Toole 2001). These are thought to reduce antibiotics' ability to reach the bacterial cells themselves. The importance of matrix-based drug exclusion was directly tested in early studies such as Hoyle and colleagues. Using physiologically relevant levels of Ca^{2+} to induce structural rearrangements in biofilm matrices of *Pseudomonas aeruginosa*, Hoyle et al. found complete loss of diffusion of the β-lactam piperacillin into the biofilm (Hoyle et al. 1992), supporting a role for drug exclusion in biofilm associated antibiotic resistance, though this may be compound-specific (Kirby et al. 2012). Importantly, the biofilm matrix broadly shields the cells in the biofilm population. This enables non-matrix producing cells to arise and prosper without the cost of matrix production—and as such represents one example of phenotypic differentiation (Billings et al. 2013) and bacterial altruism within the biofilm.

However, the protective effects of the matrix can be more complex than simply serving a generic barrier function. For example, in a study of *K. pneumoniae* where ampicillin was shown to be unable to penetrate the biofilm, this was shown to be dependent on β-lactamase production by the bacteria; essentially, the biofilm trapped and thus concentrated the effect of β-lactamases secreted by resident bacteria (Anderl et al. 2000). In addition, matrix sugars may limit bacterial

cell exposure to drug – and presumably other toxins – through other, more cognate means. For example, in *P. aeruginosa* (PsA), synthesis of a periplasmic glucan by biofilm cells appears to protect the cell by specifically sequestering antibiotic (Mah et al. 2003). Similarly, recent studies in PsA have implicated a specific matrix polysaccharide, Psl (containing repeats of D-mannose, D-glucose and L-rhamnose) in antibiotic resistance (Billings et al. 2013). Finally, cells within a biofilm may also alter their effective drug exposure through regulation of efflux mechanisms similar to those discussed above. This is best established in PsA biofilms where efflux by the MexAB-OprM pump as well as by other MDR pumps in the BrlR operon contribute to biofilm drug tolerance (Billings et al. 2013; Liao et al. 2013).

Growth characteristics: In addition, bacterial growth patterns change markedly within the biofilm, both in bulk and, as will be described below, in specialized subpopulations of cells. Indeed, slow growth was an early explanation of bacterial drug tolerance in biofilms (Allison et al. 1990). Subsequent studies have confirmed that many *K. pneumoniae* mature biofilms exhibit slowed growth (Wentland et al. 1996), likely due to limited nutrient access and waste removal. In *K. pneumoniae*, this phenomenon was shown to cause resistance to the β-lactam ampicillin and ciprofloxacin, a quinolone (Anderl et al. 2003). Mathematical modeling also supports the role of slow growth in biofilm resistance (Roberts & Stewart 2003). In addition to causing slow growth, nutrient limitation also induces the SOS response (Janion et al. 2002). Recently, the SOS response in *E. coli* was implicated in increasing biofilm resistance to another quinolone, ofloxacin (Bernier et al. 2013). Taken together, these studies highlight a role for slow growth and the SOS response in biofilm recalcitrance to treatment.

Subpopulation biology: The programs to slow cell growth are not enacted homogeneously across the biofilm. Even biofilms made up of a single species can harbor several phenotypically

distinct cell types. Cellular differentiation into functionally specialized cells has been demonstrated in biofilms of several different bacterial species (Verhamme et al. 2009; Serra et al. 2013). This differentiation allows cells to functionally specialize in a variety of ways. One subpopulation of cells that emerge in biofilm conditions is classic persister cells (Kwan et al. 2013), which are more abundant in biofilms than planktonic cultures. It has been proposed that persister cell formation is a major determinant of biofilm-associated antibiotic treatment failure (Römling & Balsalobre 2012; Spoering & Lewis 2001; Lewis 2006).

Not only is there phenotypic diversification within a biofilm population, there are several lines of evidence indicating bacteria within biofilms have increased capacity to genetically diversify. In *E. faecalis*, cells within a biofilm exhibit greater plasmid copy number variation with associated increases in population heterogeneity in antibiotic resistance cassettes (Cook & Dunny 2013). In *S. pneumonia*, biofilm formation favors exchange of genetic material and recombinatorial diversity (Narisawa et al. 2011).

Concluding remarks

A framework for considering drug resistance and drug tolerance

The definitions of drug resistance and drug tolerance emphasize the fact that drug responses are relative to a given drug concentration. One way to distinguish drug resistance from drug tolerance is the extent of change in MIC. However, other characteristics of these changes in drug susceptibility are also important, including the percent population affected, and durability of the mechanism (Fig 1.2). With the advent of single-cell analysis techniques and considering the clinical significance of durable resistance and tolerance mechanisms, it is increasingly clear that these other dimensions may be important determinants of the ultimate response to drug. While

there may be only a few fundamental paradigms by which cells escape antibiotic killing, they can play out over a small number of cells or a large number of cells, be fully or partially penetrant and be durable or transient. Thus, we anticipate that for cases where mechanisms of tolerance and resistance have only been described at a population level, future studies will uncover specialized subpopulations of cells that exploit them, and will require us to consider all three axes.

Bacterial infections remain an issue of global importance. Recalcitrant and recrudescent infections, either due to tolerant cells able to reactivate upon drug removal or resistant ones that continue growth in the presence of drug, are likely to be an important problem in this century. To better treat bacterial infections, we must rationally design combination therapies targeting multiple aspects of an infection. To do this, we will need to understand why seemingly identical cells behave differently, how cells differentiate, and how to efficaciously treat all bacterial subpopulations, likely by employing logical combinations of different classes of drugs to target different aspects of cell physiology. Of particular urgency is an understanding of how phenotypic resistance and tolerance mechanisms beget mutation-based, heritable resistance, and how stresses such as antibiotics and host factors can induce such phenotypic adaptations.

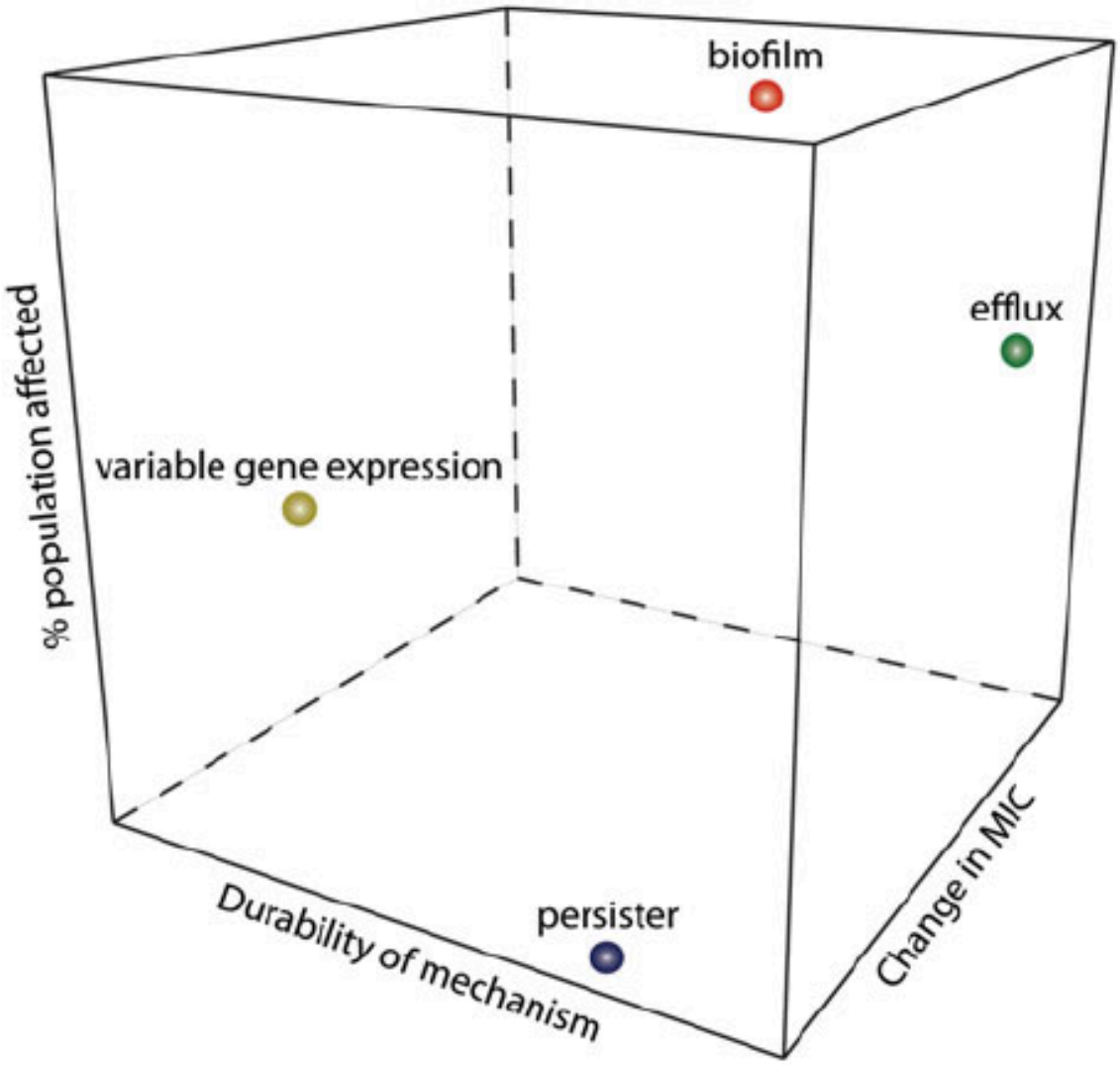

Figure 1.2 3D diagram for mechanisms of survival. Considering all factors contributing to resistance and tolerance, a new diagram emerges with three axes: percent population affected, change in MIC, and durability of mechanism. Axes are illustrated using four examples of mechanisms from the text.

References for Chapter 1

Adam, M. et al., 2008. Epigenetic inheritance based evolution of antibiotic resistance in bacteria. *BMC Evolutionary Biology*, 8(1), p.52.

Adams, K.N. et al., 2011. Drug Tolerance in Replicating Mycobacteria Mediated by a Macrophage-Induced Efflux Mechanism. *Cell*, 145(1), pp.39–53.

Aldridge, B.B. et al., 2012. Asymmetry and Aging of Mycobacterial Cells Lead to Variable Growth and Antibiotic Susceptibility. *Science*, 335(6064), pp.100–104.

Allen, R.J. & Scott, G.K., 1980. The effect of purified lipopolysaccharide on the bactericidal reaction of human serum complement. *Journal of general microbiology*, 117(1), pp.65–72.

Allison, D.G. et al., 1990. Surface hydrophobicity and dispersal of Pseudomonas aeruginosa from biofilms. *FEMS Microbiology Letters*, 59(1-2), pp.101–104.

Alonso, A., Campanario, E. & Martınez, J.L., 1999. Emergence of multidrug-resistant mutants is increased under antibiotic selective pressure in Pseudomonas aeruginosa. *Microbiology*, 145, pp.2857–2862.

Alvarez-Ortega, C., Olivares, J. & Martínez, J.L., 2013. RND multidrug efflux pumps: what are they good for? *Frontiers in microbiology*, 4, p.7.

Anderl, J.N. et al., 2003. Role of nutrient limitation and stationary-phase existence in Klebsiella pneumoniae biofilm resistance to ampicillin and ciprofloxacin. *Antimicrobial Agents and Chemotherapy*, 47(4), pp.1251–1256. Available at: http://eutils.ncbi.nlm.nih.gov/entrez/eutils/elink.fcgi?dbfrom=pubmed&id=12654654&retmo

de=ref&cmd=prlinks.

Anderl, J.N., Franklin, M.J. & Stewart, P.S., 2000. Role of antibiotic penetration limitation in Klebsiella pneumoniae biofilm resistance to ampicillin and ciprofloxacin. *Antimicrobial Agents and Chemotherapy*, 44(7), pp.1818–1824.

Baek, S.-H., Li, A.H. & Sassetti, C.M., 2011. Metabolic regulation of mycobacterial growth and antibiotic sensitivity. *PLoS Biology*, 9(5), p.e1001065.

Balaban, N.Q. et al., 2004. Bacterial Persistence as a Phenotypic Switch. *Science*, 305(5690), pp.1622–1625.

Balaban, N.Q. et al., 2013. PERSPECTIVES. *Nature Reviews Microbiology*, 11(8), pp.587–591.

Balganesh, M. et al., 2012. Efflux Pumps of Mycobacterium tuberculosis Play a Significant Role in Antituberculosis Activity of Potential Drug Candidates. *Antimicrobial Agents and Chemotherapy*, 56(5), pp.2643–2651.

Barnes, M.G. & Weiss, A.A., 2002. Growth Phase Influences Complement Resistance of Bordetella pertussis. *Infection and Immunity*, 70(1), pp.403–406.

Be'er, A. et al., 2009. Deadly competition between sibling bacterial colonies. *Proceedings of the National Academy of Sciences*, 106(2), pp.428–433.

Be'er, A. et al., 2010. Lethal protein produced in response to competition between sibling bacterial colonies. *Proceedings of the National Academy of Sciences*, 107(14), pp.6258–6263.

Be'er, A. et al., 2011. Surviving Bacterial Sibling Rivalry: Inducible and Reversible Phenotypic

Switching in Paenibacillus dendritiformis. *mBio*, 2(3), pp.e00069–11–e00069–11.

Beaudoin, T. et al., 2010. Characterization of clonal strains of Pseudomonas aeruginosa isolated from cystic fibrosis patients in Ontario, Canada. *Canadian journal of microbiology*, 56(7), pp.548–557.

Bernier, S.P. et al., 2013. Starvation, Together with the SOS Response, Mediates High Biofilm-Specific Tolerance to the Fluoroquinolone Ofloxacin P. H. Viollier, ed. *PLoS Genetics*, 9(1), p.e1003144.

Bialek, S. et al., 2010. Membrane Efflux and Influx Modulate both Multidrug Resistance and Virulence of Klebsiella pneumoniae in a Caenorhabditis elegans Model. *Antimicrobial Agents and Chemotherapy*, 54(10), pp.4373–4378.

Bigger, J.W., 1944. Treatment of Stphylococcal infections with penicillin by intermittent sterilisation. *The Lancet*, pp.497–500.

Billings, N. et al., 2013. The Extracellular Matrix Component Psl Provides Fast-Acting Antibiotic Defense in Pseudomonas aeruginosa Biofilms. *PLoS Pathogens*, 9(8), p.e1003526.

Bornet, C. et al., 2003. Imipenem and expression of multidrug efflux pump in Enterobacter aerogenes. *Biochemical and Biophysical Research Communications*, 301(4), pp.985–990.

Bornet, C. et al., 2000. Imipenem Resistance of *Enterobacter aerogenes* Mediated by Outer Membrane Permeability. *Journal of Clinical Microbiology*, 38(3), pp.1048–1052.

Cook, L.C. & Dunny, G.M., 2013. Effects of biofilm growth on plasmid copy number and

expression of antibiotic resistance genes in Enterococcus faecalis. *Antimicrobial Agents and Chemotherapy*, 57(4), pp.1850–1856.

Correia, F.F. et al., 2006. Kinase Activity of Overexpressed HipA Is Required for Growth Arrest and Multidrug Tolerance in Escherichia coli. *Journal of Bacteriology*, 188(24), pp.8360–8367.

Daniel, J. et al., 2004. Induction of a novel class of diacylglycerol acyltransferases and triacylglycerol accumulation in Mycobacterium tuberculosis as it goes into a dormancy-like state in culture. *Journal of Bacteriology*, 186(15), pp.5017–5030.

Daniels, R., Vanderleyden, J. & Michiels, J., 2004. Quorum sensing and swarming migration in bacteria. *FEMS Microbiology Reviews*, 28(3), pp.261–289. Available at: http://eutils.ncbi.nlm.nih.gov/entrez/eutils/elink.fcgi?dbfrom=pubmed&id=15449604&retmode=ref&cmd=prlinks.

Deb, C. et al., 2006. A novel lipase belonging to the hormone-sensitive lipase family induced under starvation to utilize stored triacylglycerol in Mycobacterium tuberculosis. *The Journal of biological chemistry*, 281(7), pp.3866–3875.

Dinesh, N., Sharma, S. & Balganesh, M., 2013. Involvement of Efflux Pumps in the Resistance to Peptidoglycan Synthesis Inhibitors in Mycobacterium tuberculosis. *Antimicrobial Agents and Chemotherapy*, 57(4), pp.1941–1943.

Dupont, M. et al., 2007. An Early Response to Environmental Stress Involves Regulation of OmpX and OmpF, Two Enterobacterial Outer Membrane Pore-Forming Proteins. *Antimicrobial Agents and Chemotherapy*, 51(9), pp.3190–3198.

Eng, R.H. et al., 1991. Bactericidal effects of antibiotics on slowly growing and nongrowing bacteria. *Antimicrobial Agents and Chemotherapy*, 35(9), pp.1824–1828.

Ezraty, B. et al., 2013. Fe-S Cluster Biosynthesis Controls Uptake of Aminoglycosides in a ROS-Less Death Pathway. *Science*, 340(6140), pp.1583–1587.

Falla, T.J. & Chopra, I., 1998. Joint Tolerance to β-Lactam and Fluoroquinolone Antibiotics in *Escherichia coli* Results from Overexpression of *hipA*. *Antimicrobial Agents and Chemotherapy*, 42(12), pp.3282–3284.

Fauvart, M., De Groote, V.N. & Michiels, J., 2011. Role of persister cells in chronic infections: clinical relevance and perspectives on anti-persister therapies. *Journal of Medical Microbiology*, 60(6), pp.699–709.

Finkel, S.E., 2006. Long-term survival during stationary phase: evolution and the GASP phenotype. *Nature Reviews Microbiology*, 4(2), pp.113–120.

Germain, E. et al., 2013. Molecular Mechanism of Bacterial Persistence by HipA. *Molecular Cell*, 52(2), pp.248–254.

Ghisalberti, D. et al., 2005. Chloramphenicol and expression of multidrug efflux pump in Enterobacter aerogenes. *Biochemical and Biophysical Research Communications*, 328(4), pp.1113–1118.

Girgis, H.S., Harris, K. & Tavazoie, S., 2012. Large mutational target size for rapid emergence of bacterial persistence. *Proceedings of the National Academy of Sciences*, 109(31), pp.12740–12745.

Gradelski, E. et al., 2002. Bactericidal mechanism of gatifloxacin compared with other quinolones. *The Journal of antimicrobial chemotherapy*, 49(1), pp.185–188.

Gristina, A.G. et al., 1987. Adhesive colonization of biomaterials and antibiotic resistance. *Biomaterials*, 8(6), pp.423–426.

Henrichsen, J., 1972. Bacterial surface translocation: a survey and a classification. *Bacteriological reviews*, 36(4), pp.478–503.

Herbert, D. et al., 1996. Bactericidal action of ofloxacin, sulbactam-ampicillin, rifampin, and isoniazid on logarithmic- and stationary-phase cultures of Mycobacterium tuberculosis. *Antimicrobial Agents and Chemotherapy*, 40(10), pp.2296–2299.

Holmes, C.J. & Evans, R.C., 1989. Resistance of bacterial biofilms to antibiotics. *The Journal of antimicrobial chemotherapy*, 24(1), p.84.

Hoyle, B.D., Alcantara, J. & Costerton, J.W., 1992. Pseudomonas aeruginosa biofilm as a diffusion barrier to piperacillin. *Antimicrobial Agents and Chemotherapy*, 36(9), pp.2054–2056.

Hsieh, Y.-Y., Hung, P.-H. & Leu, J.-Y., 2013. Hsp90 Regulates Nongenetic Variation in Response to Environmental Stress. *Molecular Cell*, 50(1), pp.82–92.

Janion, C. et al., 2002. Induction of the SOS response in starved Escherichia coli. *Environmental and molecular mutagenesis*, 40(2), pp.129–133. Available at: http://eutils.ncbi.nlm.nih.gov/entrez/eutils/elink.fcgi?dbfrom=pubmed&id=12203406&retmode=ref&cmd=prlinks.

Jeannot, K. et al., 2005. Induction of the MexXY efflux pump in Pseudomonas aeruginosa is dependent on drug-ribosome interaction. *Journal of Bacteriology*, 187(15), pp.5341–5346.

Johnson, P.J.T. & Levin, B.R., 2013. Pharmacodynamics, Population Dynamics, and the Evolution of Persistence in Staphylococcus aureus H. S. Malik, ed. *PLoS Genetics*, 9(1), p.e1003123.

Joyce, G. et al., 2012. Cell division site placement and asymmetric growth in mycobacteria. *PLoS ONE*, 7(9), p.e44582.

Kendall, S.L. et al., 2004. The Mycobacterium tuberculosis dosRS two-component system is induced by multiple stresses. *Tuberculosis (Edinburgh, Scotland)*, 84(3-4), pp.247–255.

Keren, I. et al., 2011. Characterization and Transcriptome Analysis of Mycobacterium tuberculosis Persisters. *mBio*, 2(3), pp.e00100–11–e00100–11.

Keren, I., Kaldalu, N., et al., 2004. Persister cells and tolerance to antimicrobials. *FEMS Microbiology Letters*, 230(1), pp.13–18.

Keren, I., Shah, D., et al., 2004. Specialized Persister Cells and the Mechanism of Multidrug Tolerance in Escherichia coli. *Journal of Bacteriology*, 186(24), pp.8172–8180.

Kim, W. et al., 2003. Swarm-cell differentiation in Salmonella enterica serovar typhimurium results in elevated resistance to multiple antibiotics. *Journal of Bacteriology*, 185(10), pp.3111–3117.

Kirby, A.E., Garner, K. & Levin, B.R., 2012. The relative contributions of physical structure and cell density to the antibiotic susceptibility of bacteria in biofilms. *Antimicrobial Agents and*

Chemotherapy, 56(6), pp.2967–2975.

Kohanski, M.A., DePristo, M.A. & Collins, J.J., 2010. Sublethal antibiotic treatment leads to multidrug resistance via radical-induced mutagenesis. *Molecular Cell*, 37(3), pp.311–320.

Korch, S.B. & Hill, T.M., 2006. Ectopic overexpression of wild-type and mutant hipA genes in Escherichia coli: effects on macromolecular synthesis and persister formation. *Journal of Bacteriology*, 188(11), pp.3826–3836.

Korch, S.B., Henderson, T.A. & Hill, T.M., 2003. Characterization of the hipA7 allele of Escherichia coli and evidence that high persistence is governed by (p)ppGpp synthesis. *Molecular Microbiology*, 50(4), pp.1199–1213.

Koul, A. et al., 2008. Diarylquinolines are bactericidal for dormant mycobacteria as a result of disturbed ATP homeostasis. *The Journal of biological chemistry*, 283(37), pp.25273–25280.

Kox, L.F.F., Wosten, M.M.S.M. & Groisman, E.A., 2000. A small protein that mediates the activation of a two-component system by another two-component system. *The EMBO Journal*, 19(8), pp.1861–1872.

Kwan, B.W. et al., 2013. Arrested protein synthesis increases persister-like cell formation. *Antimicrobial Agents and Chemotherapy*, 57(3), pp.1468–1473.

Lai, S., Tremblay, J. & Déziel, E., 2009. Swarming motility: a multicellular behaviour conferring antimicrobial resistance. *Environmental Microbiology*, 11(1), pp.126–136.

Lee, H.H. et al., 2010. Bacterial charity work leads to population-wide resistance. *Nature*, 467(7311), pp.82–85.

Levy, S.F., Ziv, N. & Siegal, M.L., 2012. Bet Hedging in Yeast by Heterogeneous, Age-Correlated Expression of a Stress Protectant L. D. Hurst, ed. *PLoS Biology*, 10(5), p.e1001325.

Lewis, K., 2006. Persister cells, dormancy and infectious disease. *Nature Reviews Microbiology*, 5(1), pp.48–56.

Li, X.-Z. et al., 1998. Beta-lactamase inhibitors are substrates for the multidrug efflux pumps of Pseudomonas aeruginosa. *Antimicrobial Agents and Chemotherapy*, 42(2), pp.399–403.

Li, X.-Z., Livermore, D.M. & Nikaido, H., 1994. Role of efflux pump(s) in intrinsic resistance of Pseudomonas aeruginosa: resistance to tetracycline, chloramphenicol, and norfloxacin. *Antimicrobial Agents and Chemotherapy*, 38(8), pp.1732–1741.

Li, X.-Z., Ma, D., et al., 1994. Role of efflux pump(s) in intrinsic resistance of Pseudomonas aeruginosa: active efflux as a contributing factor to beta-lactam resistance. *Antimicrobial Agents and Chemotherapy*, 38(8), pp.1742–1752.

Li, X.-Z., Zhang, L. & Poole, K., 2002. SmeC, an Outer Membrane Multidrug Efflux Protein of Stenotrophomonas maltophilia. *Antimicrobial Agents and Chemotherapy*, 46(2), pp.333–343.

Liao, J., Schurr, M.J. & Sauer, K., 2013. The MerR-like regulator BrlR confers biofilm tolerance by activating multidrug efflux pumps in Pseudomonas aeruginosa biofilms. *Journal of Bacteriology*, 195(15), pp.3352–3363.

Livermore, D.M. & Davy, K.W., 1991. Invalidity for Pseudomonas aeruginosa of an accepted

model of bacterial permeability to beta-lactam antibiotics. *Antimicrobial Agents and Chemotherapy*, 35(5), pp.916–921.

Mah, T.-F. et al., 2003. A genetic basis for Pseudomonas aeruginosa biofilm antibiotic resistance. *Nature Cell Biology*, 426(6964), pp.306–310.

Mah, T.-F.C. & O'Toole, G.A., 2001. Mechanisms of biofilm resistance to antimicrobial agents. *Trends in Microbiology*, 9(1), pp.34–39.

Maisonneuve, E., Castro-Camargo, M. & Gerdes, K., 2013. (p)ppGpp Controls Bacterial Persistence by Stochastic Induction of Toxin-Antitoxin Activity. *Cell*, 154(5), pp.1140–1150.

Martínez, J.L. & Rojo, F., 2011. Metabolic regulation of antibiotic resistance. *FEMS Microbiology Reviews*, 35(5), pp.768–789.

Masuda, N. et al., 2000. Contribution of the MexX-MexY-oprM efflux system to intrinsic resistance in Pseudomonas aeruginosa. *Antimicrobial Agents and Chemotherapy*, 44(9), pp.2242–2246.

Mishra, M.N. & Daniels, L., 2013. Characterization of the MSMEG_2631 Gene (mmp) Encoding a Multidrug and Toxic Compound Extrusion (MATE) Family Protein in Mycobacterium smegmatis and Exploration of Its Polyspecific Nature Using Biolog Phenotype MicroArray. *Journal of Bacteriology*, 195(7), pp.1610–1621.

Morita, Y., Sobel, M.L. & Poole, K., 2006. Antibiotic inducibility of the MexXY multidrug efflux system of Pseudomonas aeruginosa: involvement of the antibiotic-inducible PA5471

gene product. *Journal of Bacteriology*, 188(5), pp.1847–1855.

Morones-Ramirez, J.R. et al., 2013. Silver Enhances Antibiotic Activity Against Gram-Negative Bacteria. *Science Translational Medicine*, 5(190), pp.190ra81–190ra81.

Moyed, H.S. & Bertrand, K.P., 1983. hipA, a newly recognized gene of Escherichia coli K-12 that affects frequency of persistence after inhibition of murein synthesis. *Journal of Bacteriology*, 155(2), pp.768–775.

Moyed, H.S. & Broderick, S.H., 1986. Molecular cloning and expression of hipA, a gene of Escherichia coli K-12 that affects frequency of persistence after inhibition of murein synthesis. *Journal of Bacteriology*, 166(2), pp.399–403.

Narisawa, N. et al., 2011. Competence-dependent endogenous DNA rearrangement and uptake of extracellular DNA give a natural variant of Streptococcus mutans without biofilm formation. *Journal of Bacteriology*, 193(19), pp.5147–5154.

Nicas, T.I. & Hancock, R.E., 1983. Pseudomonas aeruginosa outer membranepermeability: isolation of aporin protein F-deficient mutant. *Journal of Bacteriology*, 153(1), pp.281–285.

Nichols, W.W. et al., 1989. The penetration of antibiotics into aggregates of mucoid and non-mucoid Pseudomonas aeruginosa. *Journal of general microbiology*, 135(5), pp.1291–1303.

Nikaido, H., 1989. Outer membrane barrier as a mechanism of antimicrobial resistance. *Antimicrobial Agents and Chemotherapy*, 33(11), pp.1831–1836.

Nikaido, H., 1994. Prevention of drug access to bacterial targets: permeability barriers and active efflux. *Science*, 264(5157), pp.382–388.

Park, H.-D. et al., 2003. Rv3133c/dosR is a transcription factor that mediates the hypoxic response of Mycobacterium tuberculosis. *Molecular Microbiology*, 48(3), pp.833–843.

Poole, K., 2001. Multidrug efflux pumps and antimicrobial resistance in Pseudomonas aeruginosa and related organisms. *Journal of Molecular Microbiology and Biotechnology*, 3(2), pp.255–264.

Prosser, B.L. et al., 1987. Method of evaluating effects of antibiotics on bacterial biofilm. *Antimicrobial Agents and Chemotherapy*, 31(10), pp.1502–1506.

Rao, S.P.S. et al., 2008. The protonmotive force is required for maintaining ATP homeostasis and viability of hypoxic, nonreplicating Mycobacterium tuberculosis. *Proceedings of the National Academy of Sciences*, 105(33), pp.11945–11950.

Roberts, M.E. & Stewart, P.S., 2003. Modeling Antibiotic Tolerance in Biofilms by Accounting for Nutrient Limitation. *Antimicrobial Agents and Chemotherapy*, 48(1), pp.48–52.

Rodrigues, L. et al., 2012. Infection, Genetics and Evolution. *Infection, Genetics and Evolution*, 12(4), pp.695–700.

Roth, D. et al., 2013. Identification and characterization of a highly motile and antibiotic refractory subpopulation involved in the expansion of swarming colonies of Paenibacillus vortex. *Environmental Microbiology*, 15(9), pp.2532–2544.

Römling, U. & Balsalobre, C., 2012. Biofilm infections, their resilience to therapy and innovative treatment strategies. *Journal of Internal Medicine*, 272(6), pp.541–561.

Sala, C. et al., 2010. Simple Model for Testing Drugs against Nonreplicating Mycobacterium

tuberculosis. *Antimicrobial Agents and Chemotherapy*, 54(10), pp.4150–4158.

Sarathy, J. et al., 2013. Reduced Drug Uptake in PhenotypicallyResistant Nutrient-Starved Nonreplicating Mycobacterium tuberculosis. *Antimicrobial Agents and Chemotherapy*, 57(4), pp.1648–1653.

Schaaf, H.S. et al., 2007. Minimal inhibitory concentration of isoniazid in isoniazid-resistant Mycobacterium tuberculosis isolates from children. *European journal of clinical microbiology & infectious diseases : official publication of the European Society of Clinical Microbiology*, 26(3), pp.203–205.

Scherrer, R. & Moyed, H.S., 1988. Conditional impairment of cell division and altered lethality in hipA mutants of Escherichia coli K-12. *Journal of Bacteriology*, 170(8), pp.3321–3326.

Scudamore, R.A., Beveridge, T.J. & Goldner, M., 1979. Outer-Membrane Penetration Barriers as Components of Intrinsic Resistance to Beta-Lactam and Other Antibiotics in Escherichia coli K-12. *Antimicrobial Agents and Chemotherapy*, 15(2), pp.182–189.

Serra, D.O. et al., 2013. Microanatomy at Cellular Resolution and Spatial Order of Physiological Differentiation in a Bacterial Biofilm. *mBio*, 4(2), pp.e00103–13–e00103–13.

Shah, D. et al., 2006. Persisters: a distinct physiological state of E. coli. *BMC Microbiology*, 6, p.53.

Shi, L. et al., 2010. Carbon flux rerouting during Mycobacterium tuberculosis growth arrest. *Molecular Microbiology*, 78(5), pp.1199–1215.

Silverman, J.A., Perlmutter, N.G. & Shapiro, H.M., 2003. Correlation of daptomycin bactericidal

activity and membrane depolarization in Staphylococcus aureus. *Antimicrobial Agents and Chemotherapy*, 47(8), pp.2538–2544.

Singh, B. et al., 2013. Asymmetric growth and division in Mycobacterium spp.: compensatory mechanisms for non-medial septa. *Molecular Microbiology*, 88(1), pp.64–76.

Soncini, F.C. & Groisman, E.A., 1996. Two-component regulatory systems caninteract to process multiple environmental signals. *Journal of Bacteriology*, 178(23), pp.6796–6801.

Spoering, A.L. & Lewis, K., 2001. Biofilms and Planktonic Cells of Pseudomonas aeruginosa Have Similar Resistance to Killing by Antimicrobials. *Journal of Bacteriology*, 183(23), pp.6746–6751.

Spoering, A.L., Vulic, M. & Lewis, K., 2006. GlpD and PlsB Participate in Persister Cell Formation in Escherichia coli. *Journal of Bacteriology*, 188(14), pp.5136–5144.

Stewart, P.S. & Costerton, J.W., 2001. Antibiotic resistance of bacteria in biofilms. *The Lancet*, 358(9276), pp.135–138.

Tenover, F.C., 2006. Mechanisms of antimicrobial resistance in bacteria. *The American journal of medicine*, 119(6 Suppl 1), pp.S3–10– discussion S62–70.

Toguchi, A. et al., 2000. Genetics of Swarming Motility in Salmonella enterica Serovar Typhimurium: Critical Role for Lipopolysaccharide. *Journal of Bacteriology*, 182(22), pp.6308–6321.

Veening, J.-W. et al., 2008. Bet-hedging and epigenetic inheritance in bacterial cell development. *Proceedings of the National Academy of Sciences*, 105(11), pp.4393–4398.

Verhamme, D.T., Murray, E.J. & Stanley-Wall, N.R., 2009. DegU and Spo0A jointly control transcription of two loci required for complex colony development by Bacillus subtilis. *Journal of Bacteriology*, 191(1), pp.100–108.

Wakamoto, Y. et al., 2013. Dynamic Persistence of Antibiotic-Stressed Mycobacteria. *Science*, 339(6115), pp.91–95.

Wang, K. et al., 2012. The Expression of ABC Efflux Pump, Rv1217c–Rv1218c, and Its Association with Multidrug Resistance of Mycobacterium tuberculosis in China. *Current Microbiology*, 66(3), pp.222–226.

Wentland, E.J. et al., 1996. Spatial variations in growth rate within Klebsiella pneumoniae colonies and biofilm. *Biotechnology progress*, 12(3), pp.316–321.

West, S.A. et al., 2006. Social evolution theory for microorganisms. *Nature Reviews Microbiology*, 4(8), pp.597–607.

Williams, J.J. & Hergenrother, P.J., 2012. Artificial activation of toxin–antitoxin systems as an antibacterial strategy. *Trends in Microbiology*, 20(6), pp.291–298.

Wu, Y. et al., 2012. Role of Oxidative Stress in Persister Tolerance. *Antimicrobial Agents and Chemotherapy*, 56(9), pp.4922–4926.

Yoshimura, F. & Nikaido, H., 1985. Diffusion of beta-lactam antibiotics through the porin channels of Escherichia coli K-12. *Antimicrobial Agents and Chemotherapy*, 27(1), pp.84–92.

Zhou, X. & Cegelski, L., 2012. Nutrient-dependent structural changes in S. aureus peptidoglycan

revealed by solid-state NMR spectroscopy. *Biochemistry*, 51(41), pp.8143–8153.

Zimmermann, W. & Rosselet, A., 1977. Function of the outer membrane of Escherichia coli as a permeability barrier to beta-lactam antibiotics. *Antimicrobial Agents and Chemotherapy*, 12(3), pp.368–372.

Chapter 2

Creation of tools to describe the mycobacterial cell cycle

Abstract

Tuberculosis (TB) is the leading cause of death from an infectious agent globally. Cellular reproduction of *Mycobacterium tuberculosis* (Mtb), the etiologic agent of TB, is necessary for its pathogenesis. Yet regulators of the mycobacterial cell cycle—the process of going from one bacterium to two—remain undiscovered. In my thesis work, I sought to identify the molecular mechanisms regulating the cell cycle in mycobacteria. In order to do this, I developed a set of quantitative imaging and analysis tools to map the mycobacterial cell cycle at high resolution and allow for the critical analysis of perturbations. This chapter describes these tools and their validation.

Introduction

Tuberculosis (TB) remains a global health burden, with over 10 million incident cases each year worldwide (World Health Organization 2016). Infection requires, among many other factors, a bacterium to replicate itself. As such, each stage of the cell cycle—cell growth, DNA replication, and cell division—has been a successful target of antibacterials. Despite the multitude of successful drugs, over 1.5 million people die from TB annually (World Health Organization 2016). With the failures of current treatments, new medications and/or regimens are needed as well as a deeper understanding of the workings of the cell cycle. Yet despite the importance of the cell cycle, key regulators have not been identified in mycobacteria.

The term **cell cycle** refers to the ordered events leading up to and including the generation of daughter cells, notably DNA replication, cell growth, and cell division. In bacteria, there are three main periods of the cell cycle: growth (B), DNA replication (C), and cell division (D). The prokaryotic B, C, and D periods are analogous to the eukaryotic G1, S, and G2 phases; these are followed by cell division/M (Figure 2.1). Following is a brief overview of our current understanding of mycobacterial growth, division, and DNA replication.

Micro review of mycobacterial cell growth, division, and DNA replication

Mycobacteria are rod shaped bacteria. At the end of each cell cycle, a new pole is created by the resolution of the division site. The previously established pole is termed the old pole (Figure 2.1A). Mycobacteria synthesize and insert new cell wall components at or near their poles (Meniche et al. 2014). Growth poles are established by the DivIVA homolog Wag31 (Kang et al. 2008), which functions as an anchor for the polar growth machinery, termed the elongasome. Fluorescent fusions to Wag31 and other components of the elongasome have been used to

indicate growth directionality (Wakamoto et al. 2013; Meniche et al. 2014), while fluorescent dyes have been used to quantify total growth over the cell cycle (Aldridge et al. 2012) (Figure 2.1A).

The total growth from the old pole is greater than from the new pole across the cell cycle (Aldridge et al. 2012), though rates of growth from each pole were shown to be equal (Wakamoto et al. 2013). This seeming paradox could be due either to timing of growth or differences in baseline rates; this is addressed later in this chapter.

Mycobacteria also divide asymmetrically; the old pole-inheriting daughter cell is larger at birth than its new pole-inheriting sister (Vijay et al. 2014; Singh et al. 2013) (Figure 2.1A). Despite asymmetric birth sizes, the division sites themselves are established at or near midcell, though with a much larger range than in other related species (Joyce et al. 2012).

Division is carried out by the stepwise association and function of the group of proteins termed the divisome (Figure 2.1B). The primary step in nearly all bacteria, including mycobacteria, is the assembly of the Z ring. The tubulin homolog FtsZ localizes, polymerizes, and forms a Z ring at or near midcell.

Next, the ring matures by the addition of structural components. In *B. subtilis* and *E. coli*, the stabilizing proteins ZipA and FtsA, an actin homolog, arrive and form the proto-ring with FtsZ (Rico et al. 2013). Mycobacteria lack FtsA, and ZipA has only been described by sequence homology (Slayden et al. 2006). In mycobacteria, the remaining Fts proteins assemble in the order K, Q, W, I (Hett & Rubin 2008) along with the other known structural components, including the anchor protein Wag31, FhaB, CswA, and CrgA (Kieser & Rubin 2014).

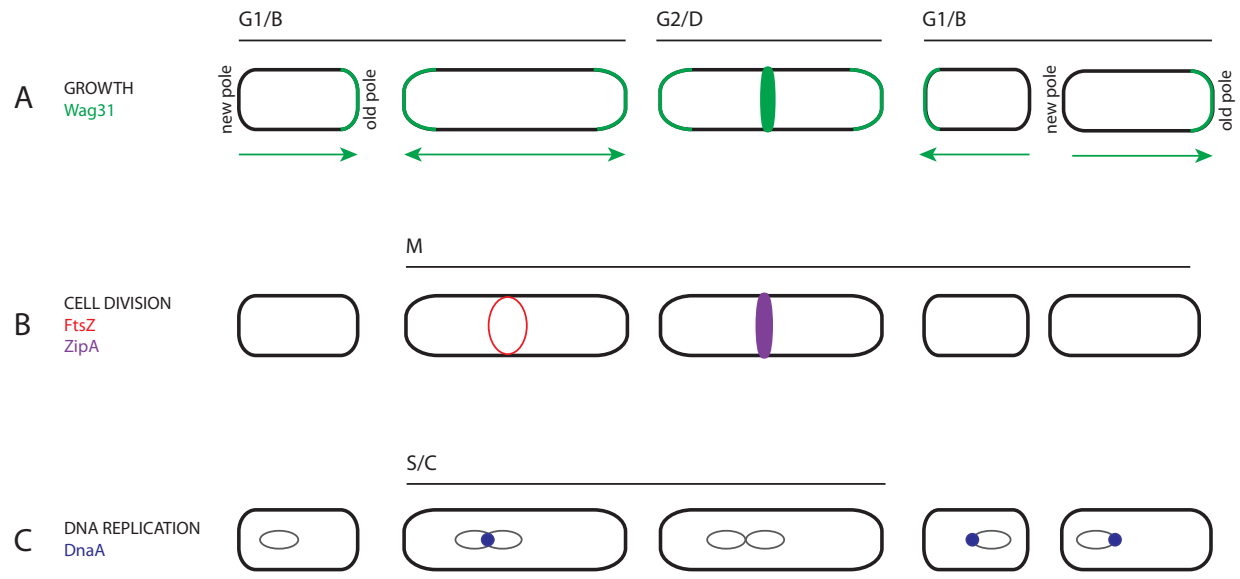

Figure 2.1 Current understanding of the mycobacterial cell cycle phases. (A) Growth machinery can be localized using fluorescently tagged Wag31, the mycobacterial DivIVA homolog. Growth is asymmetric in mycobacteria, with greater total growth occurring at the old pole. **(B)** Cell division occurs in a stepwise system. Early assembly of the divisome is visualized using fluorescently labeled FtsZ. Maturation proteins assemble after, as shown by ZipA fusions. **(C)** DnaA binds DnaA boxes within the *oriC*. Bi-directional replication proceeds from there, culminating at a *ter* locus near the end of the right arm. Chromosomes segregate prior to cell separation.

The final step is cleavage of the septum via synthesis and hydrolysis of peptidoglycan (PG). PG synthases and hydrolases perform a coordinated tug-of-war to separate the cells fully without compromising the integrity of the cell wall.

As compared to cell growth and division, less is known about DNA replication in mycobacteria. Initiation begins with the assembly of the replisome at the *ori*gin of replication on the *c*hromosome (*oriC*) (Figure 2.1C). The first proteins to assemble include the initiator AAA+ ATPase, DnaA; the replicative helicase, DnaB; and the single-stranded DNA (ssDNA) binding protein, SSB. The initiator proteins function together to unwind the double helix, and allow for the assembly of the DNA polymerase III holoenzyme and primosome complex.

DNA replication occurs bi-directionally from the *oriC* site, utilizing canonical leading and lagging strand synthesis mechanisms (Figure 2.1C). Termination of replication in mycobacteria has not been widely studied. In fact, there are no known homologs of termination machinery found in other species, i.e., Tus. Following termination, replicated chromosomes are segregated and disseminated to daughter cells (Figure 2.1C).

Regulation of the cell cycle in mycobacteria

Entry into each stage of the eukaryotic cell cycle is sequential and guarded by complex enzymatic circuitry. Like their eukaryotic counterparts, bacterial species have evolved elaborate regulatory systems for ensuring fidelity of cell component dissemination to daughter cells. These controls are termed checkpoints and there are two main checkpoints in bacteria. The first, which prevents DNA replication, is utilized under normal growth to prevent multiple rounds of replication per cell cycle, or to halt replication in the presence of DNA damage. The second inhibits ectopic cell division under normal growth. Cell division is also inhibited under certain hazardous circumstances, including DNA damage and major environmental stressors like heat or starvation.

Regulation of DNA replication

Prokaryotic DNA replication is generally controlled at the initiation stage. In mycobacteria, this is accomplished by negative regulation of binding of DnaA to DnaA boxes at *oriC*. $DnaA_{TB}$ only weakly binds its cognate $DnaA_{TB}$ boxes (Wolański et al. 2014; Zawilak-Pawlik et al. 2005; Madiraju et al. 2006). This low affinity is overcome by the spatial arrangement of $DnaA_{TB}$ boxes

at the Mtb *oriC* (Zawilak-Pawlik et al. 2005), ensuring oligomerization and cooperativity of DnaA molecules.

In eukaryotes, the helicase binds before the initiator protein, while most prokaryotes bind DnaA prior to DnaB (Bleichert et al. 2017). In *E. coli*, after DnaA binding, DnaB is loaded by DnaC (Bartosik & Jagura-Burdzy 2005). Mycobacteria do not have a DnaC homolog; DnaA or primase have been suggested to compensate (Warner et al. 2014). Furthermore, $DnaB_{TB}$ has been shown to regulate $DnaA_{TB}$ oligomerization (Xie & He 2010), potentially flipping the order of assembly. This would suggest mycobacteria might also utilize a mechanism for replication initiation regulation unique from other bacterial species.

Control at the *oriC* level has also been demonstrated in Mtb. The response regulator MtrA and replication inhibitor IciA bind to sites on or near the *oriC* and inhibit initiation through unknown mechanisms (Rajagopalan et al. 2010; Kumar et al. 2009). MtrA has been suggested potentially to have a positive regulatory role (Rajagopalan et al. 2010), but no other positive regulators of DNA replication have been identified in mycobacteria.

Other regulatory mechanisms established in other bacteria are absent in mycobacteria. For example, $DnaA_{TB}$ is not inhibited by ADP (Madiraju et al. 2006), as has been shown for *E. coli* (Mott & Berger 2007). And while DnaA turnover has been shown to be proteolytically regulated in *C. crescentus* (Gorbatyuk & Marczynski 2005; Jonas et al. 2013; Liu et al. 2016) and *B. subtilis* and *E. coli* (Schenk et al. 2017), this avenue of negative regulation has yet to be explored in mycobacteria. It is likely there are regulatory mechanisms in mycobacteria yet to be uncovered.

Regulation of cell division

Regulation of cell division in bacteria centers around negative control of septal site placement. Specifically, negative regulation of FtsZ has been broadly described in model organisms. This control can be essential for preventing premature or ectopic cell division, or it can be induced upon DNA damage or another major stress event.

Inhibition of premature or ectopic cell division is handled using two known mechanisms: nucleoid occlusion and the Min system. Nucleoid occlusion relies on the presence of a nucleoid-associated protein with negative control on FtsZ, thereby preventing FtsZ ring formation in areas where chromosome is present (reviewed in (Wu & Errington 2011)). *C. crescentus* has no nucleoid occlusion factor (Jensen 2006) and instead relies only on its nucleoid-independent placement system.

The Min system is the flagship nucleoid-independent septal placement control mechanism. The slightly differing Min systems of *E. coli* and *B. subtilis*, summarized here (Rowlett & Margolin 2013), utilize three Min proteins (plus DivIVA for *B. subtilis*) in various gradients to limit FtsZ ring formation to the cell's center. Similarly, *C. crescentus* employs a protein gradient of the FtsZ polymerization antagonist MipZ to regulate septal site placement (Thanbichler & Shapiro 2006).

In addition to the site placement restriction mechanisms active under normal conditions, DNA damage can induce inhibition of division via the SOS response. The SOS response in *E. coli* and *B. subtilis* induces production of FtsZ-specific inhibitors SulA and YneA, respectively (Higashitani et al. 1995; Mo & Burkholder 2010). These cells filament and lose FtsZ localization. In contrast, the *C. crescentus* target of the SOS response division inhibitor SidA is the late arrival protein FtsW, not FtsZ (Modell et al. 2011). This mechanism still results in

filaments, but with properly arranged FtsZ as division is blocked at a later stage (Modell et al. 2011).

No homologs of nucleoid occlusion factors, Min or MipZ, or SOS-induced FtsZ inhibitors have been shown experimentally in mycobacteria. Mycobacteria do contain an essential DivIVA protein, but studies to date have not found an anti-cell division role for it. Considering mycobacteria distribute complete sets of genetic material to their daughter cells and inhibit cell division upon DNA damage, we can assume some mechanism exists.

How do the stages of the cell cycle integrate?

Implicit in thinking about the bacterial cell cycle as individual periods, like eukaryotes, is the idea that B, C, and D occur sequentially and separately (Figure 2.1). Mycobacteria, like all prokaryotes, lack membrane-bound organelles. Therefore, the processes of the cell cycle happen in overlapping space. This necessitates unique control mechanisms but also allows for the simultaneous control of multiple processes, potentially by the same molecular machinery.

In addition to the difference in spatial separation in bacterial cells, there is not the same temporal division between events in prokaryotic as in eukaryotic cells. That is to say, G1, S, G2, and M happen in overlapping time and space. What does this mean for regulatory mechanisms? For mycobacteria especially, since the timing of cell cycle events is not fully established, this is an open question.

To understand the temporal and spatial relationship of the cell cycle components, I developed and validated a suite of microscopy-based tools to image key cell cycle events. Using this toolset, in this chapter I mapped the relative timing and localization of DNA replication and segregation, polar growth, and cell division in *Mycobacterium smegmatis* (Msm), a highly

conserved non-pathogenic and faster growing model mycobacterial species. In subsequent chapters, I will use this same toolset to describe the contributions of certain proteins to cell cycle progression.

Materials and Methods

Growth conditions

M. smegmatis mc^2155 was cultured in Middlebrook 7H9 salts supplemented with 10% ADC (5:2:3 albumin:dextrose:catalase), 0.25% glyercol, and 0.05% Tween-80 or plated on Middlebrook 7H10 agar supplemented with ADC, 0.25% glycerol, and 0.05% Tween-80. All cultures were grown at 37°C, unless otherwise noted.

Cloning

MCtH::ptb21-DnaN-eGFP and MCtH::ptb21-parB-mCherry constructs were made using a customized Invitrogen multi-site Gateway system created and generously donated by Christina Baer in Christopher Sassetti's lab at UMass Worcester Medical School, Worcester, MA, USA. PCR was performed using Phusion High Fidelity DNA polymerase (NEB Cat #M0530). The gene of interest was then subcloned into the appropriate entry vector (pDO), and final constructs were made by combining the gene of interest in the appropriate pDO with entry vectors containing promoter and appropriate tag, and the destination vector. All genes in entry and destination vectors were sequenced to confirm no mutations were introduced during PCR or subsequent cloning steps. MCtH::ptb21-FtsZ-mCherry was made by Cara Boutte in Eric Rubin's lab at Harvard University, Boston, MA, USA using the same Gateway system.

All BP and LR reactions were performed using the BP Clonase II enzyme mix (Invitrogen-Cat # 11789-020) or LR Clonase II Plus enzyme mix (Invitrogen-Cat # 12538-120) in 5µl total volume overnight at room temperature. Next, protein digestion was performed by adding 1ul Proteinase K for 15 minutes at 37C, and the entire 6ul reaction was electroporated into 15µl *DH5a* electrocompetent cells prepared in our laboratory, and plated on LB kanamycin

plates (50 μg/ml) or appropriate drug for destination vector. Plasmids were transformed into *M. smegmatis* mc^2155 cells made competent by three rounds of washing in 10% glycerol, and electroporated, followed by 3hr recovery in 7H9 at 37°C.

Imaging and analysis

Devices: As previously described (Aldridge et al. 2012), microfluidic devices were made of polydimethylsiloxane (PDMS) bonded to #1.5 cover glass substrates using soft lithography techniques. Additional baking in a conventional oven at 65 ºC for at least one week aided in reducing background fluorescence.

Microscope: As previously described (Aldridge et al. 2012), time-lapse images were acquired at 60X (Plan APO NA 1.42) using a DeltaVision PersonalDV microscope with an automated stage enclosed in an environmental chamber warmed to 37°C, unless otherwise noted. We used the InsightSSI Solid State Illumination system (461-489 nm; Applied Precision, Inc.) to illuminate and a CoolSnap HQ2 camera (Photometric) to take pictures. We used the Ultimate Focus System (Applied Precision, Inc.) to maintain focus in time-lapse imaging. Images were acquired every 10 or 15 minutes for 18-24 hours.

Analysis: Images were annotated using ImageJ (National Institutes of Health) with the ObjectJ plugin (Norbert Vischer and Stelian Nastase, University of Amsterdam, http://simon.bio.uva.nl/objectj/index.html). Cell elongation was measured as new unstained cell wall material; cell division was defined as the first frame when physical invagination of the cell wall was visible. We used an in-house Python script to analyze the annotations. The brightness and contrast were adjusted linearly and identically across each image in a series.

Dyes: Cells were pelleted and washed with PBS with 0.2% Tween 20 (PBS-T) and

resuspended in PBS-T in 1/10 of the original culture volume. Alexa Fluor 488 succinimidyl ester (ThermoFisher, Catalog number: A20100)was added to a final concentration of 0.05 mg/ml and gently mixed (Invitrogen). The cells were pelleted immediately, washed in PBST and resuspended in media. Cells were filtered through 10um filter membranes to remove clumps before loading into imaging chambers.

Growth rate assay: Images were taken every 10 minutes (unless otherwise noted), and undyed new cell growth from each pole was measured at each frame. Rate of growth over time was plotted, and the slopes of each line created by this plot was taken.

Total growth assay: Images were taken every 10 minutes (unless otherwise noted), and undyed cell growth from each pole was measured at the first frame where invagination is noted and the last frame before the next cell division is visible. Total growth is calculated as last minus first, and this is divided by total time for a rate approximation.

Data representation and statistical analysis

Prism 6.0a software (GraphPad Software, La Jolla, CA) was used to graph and analyze all growth data. Statistical tests of measurements were used as noted in figure legends from the Prism suite.

Results

2.1 Development of high-resolution assays to define phases of the cell cycle.

In order to determine any protein's contribution to cell cycle progression, it was necessary to first order key cell cycle events relative to each other. To do this, I used time-lapse imaging in devices I microfabricate and quantitative image analysis of each microcolony to order each event in time and place. I used fluorescent fusion proteins or cytologic dyes for each key event.

DNA replication initiation is shown as the appearance of DnaN-eGFP foci (Santi & McKinney 2015; Trojanowski et al. 2015). DnaN is the β-clamp, a member of the DNA pol III holoenzyme, and functions to hold the polymerase to the DNA. Chromosome segregation is seen with the separation of ParB-mCherry (Santi & McKinney 2015; Trojanowski et al. 2015). ParB attaches to *parS*, the centromere-like *ori*-proximal sequence on the chromosome; ParB-mCherry is therefore also a marker of the *oriC*. Together with ParA, ParB drives chromosome segregation. DNA replication termination is observed as resolution of DnaN-eGFP foci (Santi & McKinney 2015).

Cell growth and division are visualized as follows. Z ring initial formation and maturation is seen by dynamic and stable FtsZ-mCherry localization, respectively. Late functionality of the cytokinetic ring is shown by the invagination of cell wall in brightfield and fluorescent fusion to a ZipA-like protein in fluorescent imaging. This is one of two predicted ZipA homologs in Mtb (Slayden et al. 2006). While ZipA localizes directly following FtsZ in *E. coli* (Rico et al. 2013), this ZipA-like protein showed later assembly (Figure 2.2E). We therefore used ZipA-eGFP as a marker for mature Z rings.

Figure 2.2 Assays for cell cycle activities. (A) Pulse-chase dyeing of the cell wall allows for the quantification of new, undyed cell growth. **(B)** Replisomes are visible using DnaN-eGFP fusions (green). **(C)** Chromosome segregation is visible using ParB-mCherry fusions (green). These foci additionally indicate *oriCs*. **(D)** Early septation events are visible using FtsZ-mCherry (green). **(E)** Later division events are observed using ZipA-eGFP (green). FtsZ-mCherry is also visible in this image (red), showing temporality of the two proteins.

Ordering these processes relative to unipolar, bipolar, and septal growth was accomplished using pulse-chase labeling with cell wall dyes (Aldridge et al. 2012) (Figure 2.2A). To test if our assays were robust, we measured several factors and compared these to previously published data on the same processes.

2.2 DNA replication and cell division visualization tools are robust.

DnaN is part of DNA polymerase III holoenzyme responsible for DNA replication. DnaN specifically is the β-clamp and functions to maintain a connection of the holoenzyme to the DNA. ParB binds to an *oriC*-proximal site, termed *parS*, and uses the ATPase ParA as the energetic driver to segregate replicated chromosomes (Jakimowicz et al. 2007). Both proteins are predicted to be essential for *in vitro* growth in mycobacteria by high-density transposon mutagenesis (Sassetti et al. 2003). I therefore performed these assays as merodiploids, allowing for normal growth by the presence of the endogenous copy of *parB* or *dnaN*.

In this study, I created fluorescent translational fusions to both DnaN and ParB to visualize dynamics of chromosome replication and segregation. As was previously described (Santi & McKinney 2015; Trojanowski et al. 2015), I found WT cells to have 1 or 2 DnaN-eGFP foci (Figure 2.2B), as is expected with bidirectional replication from a single *ori*. DnaN-eGFP foci represent open replication forks; foci resolution is assumed to signify termination of replication (Santi & McKinney 2015). In my system, I found DNA replication initiation to occur prior to cell division, that is, in the final 10% of the cell cycle. This agrees with previous reports on DNA replication (Jakimowicz et al. 2007; Santi & McKinney 2015). WT cells seem to require ~75% of their cell cycle to replicate the chromosome, as DnaN-eGFP foci resolve on average 66% into a new cell cycle.

It is worth noting, though I was unable to make a single strain harboring both DnaN-eGFP and ParB-mCherry, I was able to image localization of each construct in cells relative to other landmarks, such as cell division and percent of cell cycle. Based on this relative measurement, we find ParB-mCherry foci to localize towards the poles throughout the cell cycle (Figure 2.2C). In the final 10% of the cell cycle, the two ParB-mCherry foci duplicate. One focus of each new pair moves towards the established poles (old and new). The other two foci move to midcell, where the new poles will eventually be in the daughter cells. This was also described before, validating this marker for DNA segregation (Jakimowicz et al. 2007; Santi & McKinney 2015).

FtsZ marks the early divisome in mycobacteria, as in nearly all bacteria. Early septation events are visible using an FtsZ-mCherry construct from Cara Boutte in Eric Rubin's lab at The Chan School of Public Health. C-terminal fluorescent tags on $FtsZ_{SM}$ have been previously validated (Rajagopalan et al. 2005).

2.3 Mycobacterial asymmetric growth is a result of a lag phase from the new pole.

Asymmetric division in mycobacteria has been established (Wakamoto et al. 2013; Aldridge et al. 2012; Singh et al. 2013; Vijay et al. 2014). Growth asymmetry is a little trickier. While total growth was shown to be asymmetric (Aldridge et al. 2012), this could be a result of temporal differences in growth or different absolute rates from each pole. To distinguish these possibilities, I have developed a dynamic growth assay. This assay measures growth from each pole at each frame of time-lapse imaging. This allowed us to calculate an absolute growth rate per pole, and therefore measure the difference between old and new pole growth (Figure 2.3A).

We find that, while there is asymmetry in total growth from each pole, there is no statistically significant difference in growth rates from poles once the new pole begins growing (Figure 2.3B). Instead, the asymmetry in total growth results from a temporal lag in growth from the new pole, which lasts ~100 minutes after each cell division (Figure 2.3A,C). We term this period the "lag phase" (Figure 2.3D).

Some model bacterium, like *C. crescentus* and *B. subtilis*, undergo asymmetric division under duress. Because mycobacteria, too, encounter stressful conditions, we asked if physiologically relevant stressors might perturb asymmetry in growth. The physiologically relevant stressors for pathogenic mycobacteria—limited carbon (data not shown) and reactive oxygen species (Figure 2.3C)—had no effect on the licensing period.

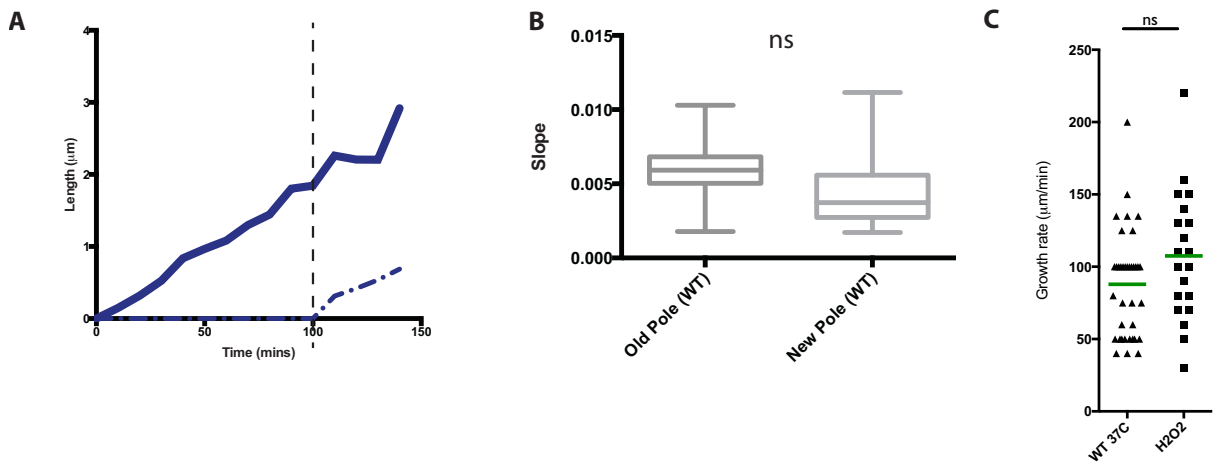

Figure 2.3 Licensing. A) Representative growth tracing showing licensing occurs ~100 minutes after division. **B)** No significant difference in growth rates, calculated as slopes, after licensing. **C)** Physiological stressors did not affect licensing time.

2.4 Conclusion

These assays give sufficient resolution into cell cycle growth dynamics to allow the identification of altered mycobacterial growth and division asymmetry as well as pinpoint perturbations to specific stages of the cell cycle. We have identified a lag phase at the start of each cell cycle. Combining the quantitative microscopy described here, we have contributed a detailed map of the cell cycle to the field (Figure 2.4).

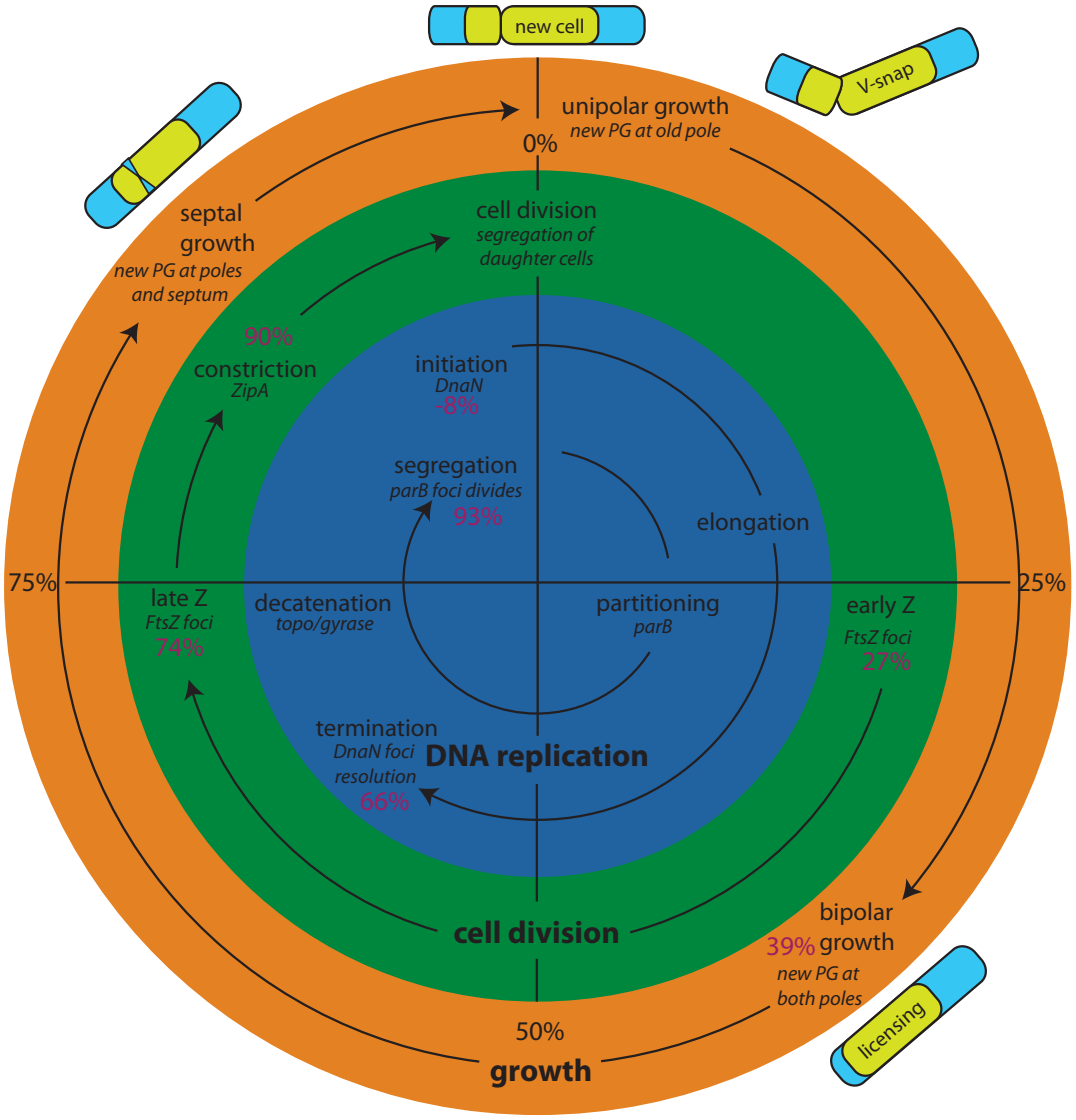

Figure 2.4 Detailed map of the mycobacterial cell cycle. Key findings from deep analysis of the cell cycle in *Mycobacterium smegmatis*. Cell growth: lag phase followed by equal growth rates upon licensing. DNA replication: lag between termination and segregation/initiation. Cell division: dynamism of Z ring in first half of cell cycle, followed by brighter, stable rings prior to constriction and division.

Discussion

This chapter described the quantitative microscopy assays I designed to use as tools to understand the mycobacterial cell cycle. Using this suite of probes, I ordered key events in the cell cycle relative to each other, including cell division, DNA replication, and cell growth.

The interplay between DNA replication and cell division

Previous studies of Msm have ordered ParB and DnaN events relative to cell division (Santi & McKinney 2015). This study from Santi & McKinney suggests ParB segregates ten minutes prior to cell separation and DnaN appears before cell division as marked by Wag31-GFP. In another paper published back-to-back, Trojanowski and colleagues similarly describe the dynamics of ParB and DnaN in Msm, but within the same cell (Trojanowski et al. 2015). In this work from Trojanowski et al., the authors observe DnaN foci after septation as marked by the earlier division marker Pbp1a, but still prior to invagination of the cell by brightfield imaging. I found a similar result using my DNA replication markers, and therefore consider these robust markers of DNA replication initiation and termination, as well as chromosome segregation.

In this tool development section I have described DnaN-eGFP foci appearance (DnaN-ON) and DnaN-eGFP resolution (DnaN-OFF). As has been previously reported (Santi & McKinney 2015; Trojanowski et al. 2015), DnaN-ON is likely DNA replication initiation, while DnaN-OFF probably marks the end of active replication. Here we show nearly 30% of the cell cycle remains between DnaN-OFF and the start of the next replication with DnaN-ON. What happens between these two events? It is tempting to speculate this is when replication termination takes place. Termination of replication in mycobacteria has not been widely studied. In fact, there are no known homologs of Tus or other termination machinery in other species.

Identification of the lag phase resolves an outstanding issue in the field.

As described earlier in this chapter, total growth per pole was shown to be asymmetric over the entire cell cycle (Aldridge et al. 2012), while the growth rates from each pole were not different (Wakamoto et al. 2013). How could these both be correct? In measuring the rate of growth from each pole every 10 minutes to create a slope for rate, I find that while the new pole has less total growth, its rate does not significantly differ from that of the old pole. The difference in total growth is explained by a lag phase. Following cell division, daughter cells' new poles do not have growth; this was also described by Wakamoto and colleagues. However, approximately 100 minutes after visible separation of daughter cells, the new pole begins growing.

What causes the new pole's lag phase? We found little to no effect on lag phase by several stress conditions (unpublished data obtained in collaboration with Bree Aldridge's lab at Tufts, Boston, MA, USA). Because mycobacteria grow from their poles rather than along the lateral wall like other rod shaped bacteria studied, a new elongasome must be established with each new division. As the old pole was growing already prior to division, this pole is able to continue. The new pole's elongasome must be created anew, and from the remains of the divisome; this is potentially the cause of the delay, though further inquiries are needed to establish this. Some proteins overlap between the two while other proteins must be exchanged (Kieser & Rubin 2014). It has therefore not escaped our notice that this is a potential point of cell cycle regulation.

References for Chapter 2

Aldridge, B.B. et al., 2012. Asymmetry and Aging of Mycobacterial Cells Lead to Variable Growth and Antibiotic Susceptibility. *Science*, 335(6064), pp.100–104.

Bartosik, A.A. & Jagura-Burdzy, G., 2005. Bacterial chromosome segregation. *Acta biochimica Polonica*, 52(1), pp.1–34.

Bleichert, F., Botchan, M.R. & Berger, J.M., 2017. Mechanisms for initiating cellular DNA replication. *Science*, 355(6327), p.eaah6317.

Gorbatyuk, B. & Marczynski, G.T., 2005. Regulated degradation of chromosome replication proteins DnaA and CtrA in Caulobacter crescentus. *Molecular Microbiology*, 55(4), pp.1233–1245.

Hett, E.C. & Rubin, E.J., 2008. Bacterial Growth and Cell Division: a Mycobacterial Perspective. *Microbiology and Molecular Biology Reviews*, 72(1), pp.126–156.

Higashitani, A., Higashitani, N. & Horiuchi, K., 1995. A cell division inhibitor SulA of Escherichia coli directly interacts with FtsZ through GTP hydrolysis. *Biochemical and Biophysical Research Communications*, 209(1), pp.198–204.

Jakimowicz, D. et al., 2007. Characterization of the mycobacterial chromosome segregation protein ParB and identification of its target in Mycobacterium smegmatis. *Microbiology (Reading, England)*, 153(Pt 12), pp.4050–4060.

Jensen, R.B., 2006. Coordination between Chromosome Replication, Segregation, and Cell Division in Caulobacter crescentus. *Journal of Bacteriology*, 188(6), pp.2244–2253.

Jonas, K. et al., 2013. Proteotoxic Stress Induces a Cell-Cycle Arrest by Stimulating Lon to Degrade the Replication Initiator DnaA. *Cell*, 154(3), pp.623–636.

Joyce, G. et al., 2012. Cell division site placement and asymmetric growth in mycobacteria. *PLoS ONE*, 7(9), p.e44582.

Kang, C.M. et al., 2008. Wag31, a homologue of the cell division protein DivIVA, regulates growth, morphology and polar cell wall synthesis in mycobacteria. *Microbiology*, 154(3), pp.725–735.

Kieser, K.J. & Rubin, E.J., 2014. How sisters grow apart: mycobacterial growth and division. *Nature Reviews Microbiology*, pp.1–13.

Kumar, S., Farhana, A. & Hasnain, S.E., 2009. In-Vitro Helix Opening of M. tuberculosis oriC by DnaA Occurs at Precise Location and Is Inhibited by IciA Like Protein D. M. Ojcius, ed. *PLoS ONE*, 4(1), p.e4139.

Liu, J. et al., 2016. ClpAP is an auxiliary protease for DnaA degradation in Caulobacter crescentus. *Molecular Microbiology*, 102(6), pp.1075–1085.

Madiraju, M.V.V.S. et al., 2006. The intrinsic ATPase activity of Mycobacterium tuberculosis DnaA promotes rapid oligomerization of DnaA on oriC. *Molecular Microbiology*, 59(6), pp.1876–1890.

Meniche, X. et al., 2014. Subpolar addition of new cell wall is directed by DivIVA in mycobacteria. *Proceedings of the National Academy of Sciences*, 111(31), pp.E3243–E3251.

Mo, A.H. & Burkholder, W.F., 2010. YneA, an SOS-Induced Inhibitor of Cell Division in

Bacillus subtilis, Is Regulated Posttranslationally and Requires the Transmembrane Region for Activity. *Journal of Bacteriology*, 192(12), pp.3159–3173.

Modell, J.W., Hopkins, A.C. & Laub, M.T., 2011. A DNA damage checkpoint in Caulobacter crescentus inhibits cell division through a direct interaction with FtsW. *Genes & Development*, 25(12), pp.1328–1343.

Mott, M.L. & Berger, J.M., 2007. DNA replication initiation: mechanisms and regulation in bacteria. *Nature Reviews Microbiology*, 5(5), pp.343–354.

Rajagopalan, M. et al., 2005. Genetic evidence that mycobacterial FtsZ and FtsW proteins interact, and colocalize to the division site in Mycobacterium smegmatis. *FEMS Microbiology Letters*, 250(1), pp.9–17.

Rajagopalan, M. et al., 2010. Mycobacterium tuberculosis origin of replication and the promoter for immunodominant secreted antigen 85B are the targets of MtrA, the essential response regulator. *Journal of Biological Chemistry*, 285(21), pp.15816–15827.

Rico, A.I., Krupka, M. & Vicente, M., 2013. In the Beginning, Escherichia coli Assembled the Proto-ring: An Initial Phase of Division. *Journal of Biological Chemistry*, 288(29), pp.20830–20836.

Rowlett, V.W. & Margolin, W., 2013. The bacterial Min system. *Current Biology*, 23(13), pp.R553–R556.

Santi, I. & McKinney, J.D., 2015. Chromosome organization and replisome dynamics in Mycobacterium smegmatis. *mBio*, 6(1), pp.e01999–14.

Sassetti, C.M., Boyd, D.H. & Rubin, E.J., 2003. Genes required for mycobacterial growth defined by high density mutagenesis. *Molecular Microbiology*, 48(1), pp.77–84.

Schenk, K. et al., 2017. Rapid turnover of DnaA at replication origin regions contributes to initiation control of DNA replication W. F. Burkholder, ed. *PLoS Genetics*, 13(2), p.e1006561.

Singh, B. et al., 2013. Asymmetric growth and division in Mycobacterium spp.: compensatory mechanisms for non-medial septa. *Molecular Microbiology*, 88(1), pp.64–76.

Slayden, R.A., Knudson, D.L. & Belisle, J.T., 2006. Identification of cell cycle regulators in Mycobacterium tuberculosis by inhibition of septum formation and global transcriptional analysis. *Microbiology (Reading, England)*, 152(Pt 6), pp.1789–1797.

Thanbichler, M. & Shapiro, L., 2006. MipZ, a Spatial Regulator Coordinating Chromosome Segregation with Cell Division in Caulobacter. *Cell*, 126(1), pp.147–162.

Trojanowski, D. et al., 2015. Choreography of the Mycobacterium replication machinery during the cell cycle. *mBio*, 6(1), pp.e02125–14.

Vijay, S. et al., 2014. Asymmetric cell division in Mycobacterium tuberculosis and its unique features. *Archives of Microbiology*, 196(3), pp.157–168.

Wakamoto, Y. et al., 2013. Dynamic Persistence of Antibiotic-Stressed Mycobacteria. *Science*, 339(6115), pp.91–95.

Warner, D.F., Evans, J.C. & Mizrahi, V., 2014. Nucleotide Metabolism and DNA Replication. *Microbiology Spectrum*, 2(5).

Wolański, M. et al., 2014. oriC-encoded instructions for the initiation of bacterial chromosome replication. *Frontiers in microbiology*, 5, p.735.

World Health Organization, 2016. Global Tuberculosis Report 2016. *WHO Library Cataloguing-in-Publication Data*.

Wu, L.J. & Errington, J., 2011. Nucleoid occlusion and bacterial cell division. *Nature Reviews Microbiology*.

Xie, Y. & He, Z.-G., 2010. Characterization of physical interaction between replication initiator protein DnaA and replicative helicase from Mycobacterium tuberculosis H37Rv. *Biochemistry. Biokhimiia*, 74(12), pp.1320–1327.

Zawilak-Pawlik, A. et al., 2005. Architecture of bacterial replication initiation complexes: orisomes from four unrelated bacteria. *Biochemical Journal*, 389(Pt 2), pp.471–481.

Chapter 3

ClpC, ClpP, and ClpX play different roles in the cell

Abstract

The model bacterium *Caulobacter crescentus* generates phenotypically distinct daughter cells in part through asymmetric division and partitioning of key cell cycle regulators. In *Caulobacter*, the essential housekeeping protease ClpXP degrades a key DNA replication regulator to initiate the cell cycle (Jenal & Fuchs 1998; Iniesta & Shapiro 2008). Because mycobacteria also grow and divide asymmetrically, I postulated that similar proteolytic mechanisms might underlie asymmetric growth and division in mycobacteria.

To test this hypothesis, I systematically evaluated *Mycobacterium smegmatis* (Msm) cells depleted of ClpP, ClpC, and ClpX using the suite of imaging tools described in Chapter 2. In this chapter, I present data suggesting the requirements for all three Clp family members for *in vitro* growth of Msm is due to their different roles in the cell, as suggested by the significant differences in phenotypes with depletion of each protein. This is the first study of mycobacterial Clp family members to propose a mechanism for their non-redundant essentiality.

Introduction

Mycobacterium tuberculosis (Mtb)—and the model organism *Mycobacterium smegmatis* (Msm)—grows and divides asymmetrically, leading to differential susceptibility to antibiotics (Aldridge et al. 2012). This bet-hedging strategy allows for the rapid creation of phenotypically different cell types with each cell division. Each subsequent division adds an additional layer of complexity by "aging" the cell wall and pole, so that with only two divisions, there are three different classes of cells. Because this diversification happens with every cell division, it is a phenotype with high penetrance.

Previously, Aldridge and colleagues showed how the effectiveness of key antibiotics used in the clinic was correlated, at the single cell level, to pole and cell wall age (Aldridge et al. 2012). However, despite the high penetrance of this phenotype and its potential importance in combatting tuberculosis, the molecular mechanisms driving asymmetry have not been elucidated.

Like mycobacterial species, the model bacterium *Caulobacter crescentus* generates phenotypically distinct daughter cells in part through asymmetric division and partitioning of key cell cycle regulators. In *Caulobacter*, the essential housekeeping protease ClpXP degrades a key cell cycle regulator, DNA replication inhibitor CtrA, to begin a new round of DNA replication and reenter the cell cycle from G_0 to S (Jenal & Fuchs 1998; Iniesta & Shapiro 2008) (Figure 3.1).

ClpP is the proteolytic subunit, which auto-assembles into a homo-tetradecamer in *Caulobacter*. In mycobacteria, two separate proteins—ClpP1 and ClpP2—form homo-heptamers that assemble into the functional tetradecamer (Akopian et al. 2012), referred to as ClpP hereafter. The assembly of a functional protease from distinct heptamers requires a AAA+ protein (Schmitz & Sauer 2014). In addition, AAA+ ATPases provide recognition and unfolding

of substrates and delivery to ClpP. These ATPases are ClpX or ClpA in *Caulobacter* and ClpX or ClpC in mycobacteria. In mycobacteria, all three (C, X, P) are essential.

ClpAP is also implicated in regulation of DNA replication in *Caulobacter*. ClpAP degrades DnaA (Liu et al. 2016; Bhat et al. 2013) to prevent ectopic initiation events. It is important to note that in *Caulobacter*, ClpA is non-essential. Its role in DNA replication control is dispensable, as the primary inhibitor of this process is CtrA. Intriguingly, in mycobacteria, both ClpP-associating ATPases, ClpC and ClpX, are essential.

Contrast this DNA replication regulatory role of Clp proteins in *Caulobacter* to other model bacteria such as *E. coli* and *B. subtilis*, where non-essential ClpX or ClpXP are instead implicated in inhibition of cell division by direct interaction with FtsZ (Pazos et al. 2013; Camberg et al. 2009; Sugimoto et al. 2010; Weart et al. 2005; Haeusser et al. 2009) (Figure 3.1).

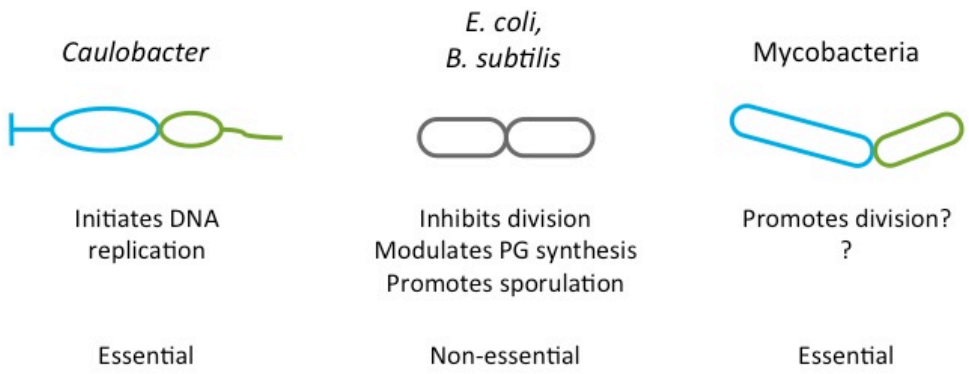

Figure 3.1 The role of Clp proteins in disparate bacterial species.

In *B. subtilis*, $ClpCP_{BS}$ has been shown to negatively regulate peptidoglycan (PG) biosynthesis by degrading MurAA, the enzyme catalyzing the first step in the PG pathway (Kock et al. 2003) (Figure 3.1). $ClpCP_{BS}$ has also been implicated in asymmetric division, as its role in

degrading the anti-sigma factor SpoIIAB is required for sporulation to occur (Pan et al. 2001) (Figure 3.1).

In mycobacteria, less is known about the role of Clp proteins in the cell. The essentiality of ClpP has been demonstrated (Raju et al. 2012), but the essentialities of ClpC and ClpX have not been shown experimentally. Functional and descriptive experiments for Clp ATPases have also been lacking.

To understand the essential roles of ClpC, ClpX, and ClpP in the mycobacterial cell, we systematically depleted each from the cell and assayed the phenotypes using the suite of tools described in the previous chapter. The data is summarized in this chapter.

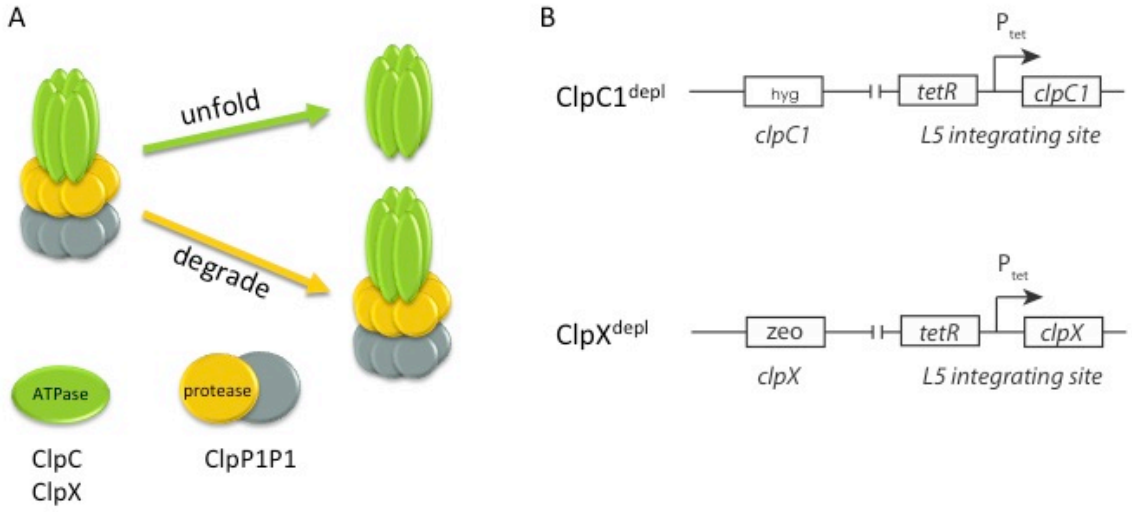

Figure 3.2 Genetic approach to testing role of Clp family in cell cycle control. A) Clp family members in mycobacteria include ATPases ClpC and ClpX, and the proteolytic subunit ClpP1P2 (ClpP). **B)** ClpC1 and ClpX depletion schema. ClpP depletion was constructed similarly (Raju et al. 2012).

Materials and Methods

Bacterial strains and culture conditions.

Performed as described in Chapter 2.

Depletion of essential genes: Depletion line cultures were grown with the addition of anhydrotetracycline (aTc) at a final concentration of 100ng/mL. Depletion was performed by washing logarithmically growing culture pellets in a volume of PBS supplemented with 0.05% Tween20 (PBS-T) equal to original culture twice before resuspending in growth media +/- aTc supplementation.

Engineering of Clp depletion lines.

The **ClpP depletion** line used was a generous gift from Ravi Raju in Eric Rubin's lab at Harvard University, Boston, MA, USA. It was made using a tetracycline-inducible promoter, as described in their published work (Raju et al. 2012).

To make the **ClpX depletion** line, *ClpX* was inserted into the L5 site of mc^2155 Msm under a tetracycline-inducible promoter using the nourseothricin resistance marker (Nat). In the merodiploid, I then deleted *ClpX* from the chromosome using recombineering and replacing it with a zeocin (Zeo) resistance marker. Doubly-resistant (Nat and Zeo) Msm cells were then selected. To prevent a high rate of escape mutants, I then added an episomal streptomycin-resistant plasmid containing several continuous tetR repeats (tetR plasmid gift of Kadamba Papavinasasundaram in Christopher Sassetti's lab at UMass Medical School, Worcester, MA, USA).

The **ClpC1 depletion** line was a generous gift from Cara Boutte in Eric Rubin's lab at Harvard University, Boston, MA, USA and was made as the ClpX depletion line, without the additional replicating TetR plasmid.

Microscopy, time-lapse imaging, and image analysis.

Msm imaging performed as described in Chapter 2.

Dendra2-Wag31 quantification was performed in ImageJ. Image analysis was performed at the slice immediately prior to cell division. A circle was drawn around the pole, and the measure function was used to determine the Integrated Intensity in the GFP channel.

Mtb imaging was performed at the Ragon BioSafety Level 3 facility in Cambridge, MA, USA. 10mL of logarithmically growing Mtb cells were washed twice in PBS-T and resuspended in 1mL 7H9 +Tween80 +OADC. Cells were imaged using CellASIC microfluidic system (EMD Millipore, Billerica, MA). Cells were grown under continuous flow of 7H9 ±1uM drug (gift of Tatos Akopian from Alfred Goldberg's lab at HMS, Boston, MA, USA). Images were taken every 60 minutes for 3 days, captured by Nikon Eclipse TI microscope by CoolSNAP camera using the 100x objective. Focus was maintained throughout experiment using PerfectFocus.

Data representation and statistical analysis

As described in Chapter 2.

Results

We hypothesized that the Clp system might be required for cell cycle regulation in mycobacteria. To test this hypothesis, I created or obtained depletion lines of all three essential family members (ATPases: ClpC, ClpX; protease: ClpP; Figure 3.2) and used my suite of phenotypic evaluation tools to assay for changes with their loss.

As a first pass, I used pulse-chase labeling of Msm cells depleted individually of each Clp protein, and imaged over time. ClpC- and ClpP-depletions had morphologies similar to each other, while ClpX-depleted cells had unique morphologic changes (Figure 3.3). Specifically, depletion of ClpX did not appear to perturb cell growth. When comparing growth plots directly, ClpX depleted cells appear similar to WT, with a loss of division evident as a continuation of growth past 300+ minutes. In contrast, ClpC and ClpP depleted cells have a noticeable slope change to the old pole indicating slowed growth. In addition, ClpC and ClpP depleted cells displayed polar bulging while ClpX depletion led to filamentation and branching. Due to these distinct morphologic phenotypes between ClpCP and ClpX, I pursued each separately using unique assays. In-depth descriptions are presented below.

3.1 ClpC and ClpP are required for asymmetric growth and division.

In Chapter 2, I described the instantaneous growth rate, where measurements of new cell wall are taken every 10 minutes. This is an extremely low-throughput method, as all measurements must be done by hand. To expand measurements to more cells and increase the power, here we use a growth rate approximation. The new, undyed cell wall is measured at each pole at the first and last frame of a cell cycle (rather than at every frame in between). This total growth is then

divided by the total time taken for this growth, yielding a measurement with units length/time (μm/hr).

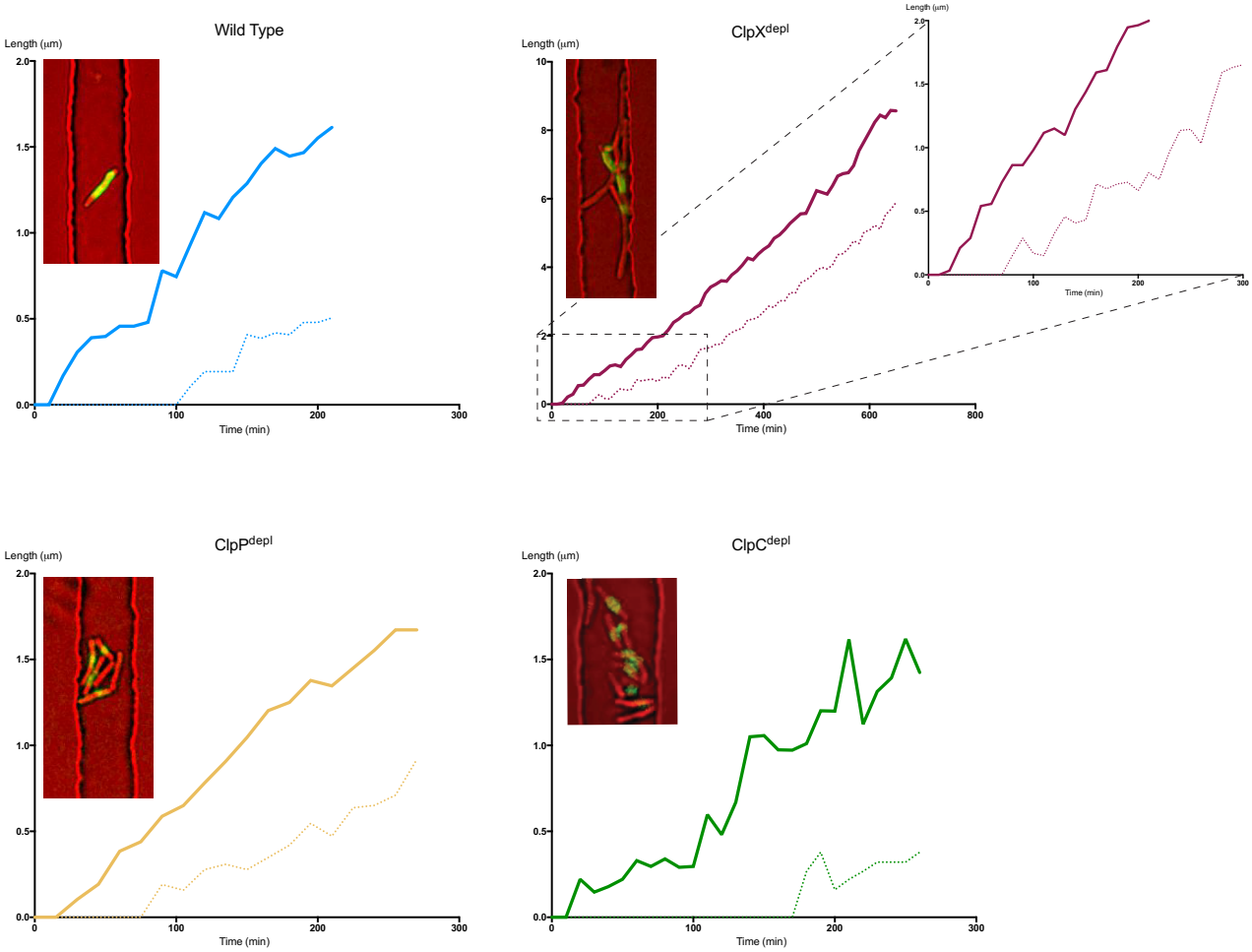

Figure 3.3 Clp family member depletion phenotypes. Representative graphs of instantaneous growth rates from indicated cell type. Solid lines represent old pole traces. Dotted lines show new pole traces. Inset images are stills from timecourse movies, demonstrating differences in total growth and gross morphology changes with depletion.

Using this measurement, we find old and new pole rates in WT cells are asymmetric; this is because we include the lag phase in the denominator for the new pole growth measurement (Figure 3.4A,B). When ClpC1 (ClpC) and ClpP1P2 (ClpP) are depleted individually from the cell, new and old pole growth rates are nearly equal. In fact, the ratio of old rate to new rate,

which is >2 for WT cells, is ~1 for ClpC and ClpP depletion (Figure 3.4A). This symmeterization comes from a loss of growth "boost" from the old pole, as the old pole growth rate is reduced in ClpC and ClpP depleted cells relative to WT cells (Figure 3.4B). Because the loss of asymmetry is due to a change in growth from the old pole rather than the new pole, this use of total growth is accurate.

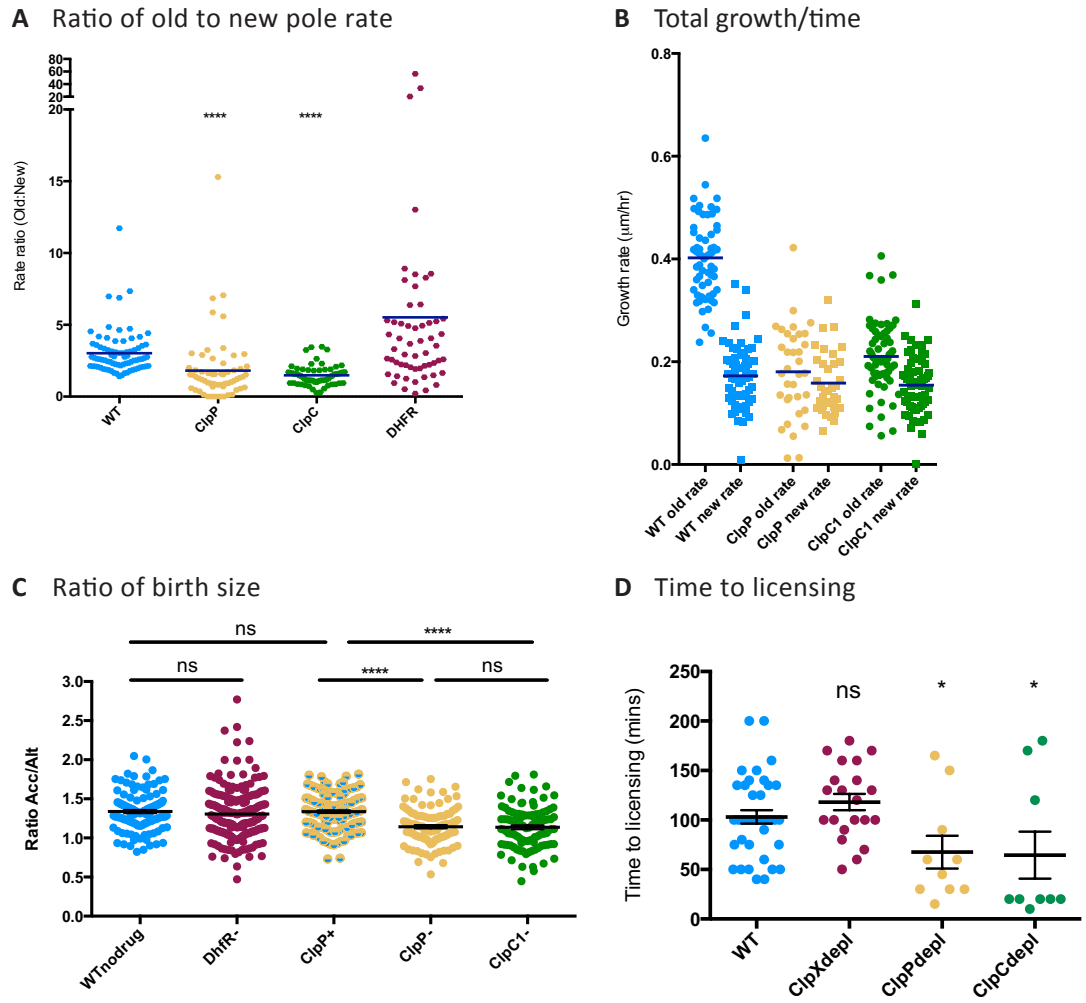

Figure 3.4 ClpC and ClpP are required for asymmetric growth and division. (A) Ratio of growth rates, based on total growth from old and new poles divided by total time. ClpP and ClpC depletions, but not depletion of another essential protein DhfR, reduces ratio to near 1. **(B)** Growth per pole using same measurement as in A: total growth per pole divided by total time. **(C)**. Loss of ClpC and ClpP, but not another essential protein DhfR, leads to symmetry of cell division. ClpP+ is the depletion strain +aTc. **(D)** Licensing time with loss of ClpX is unchanged, while ClpC- and ClpP-depletion cells license significantly sooner than WT cells.

WT Msm cells also divide asymmetrically, with the cell inheriting the older pole born ~25% larger than the cell inheriting the newer pole (Figure 3.4C). ClpC- and ClpP-depleted daughter cells are nearly equal in size (Figure 3.4C). Neither symmeterization effect is a direct result of death alone, as the depletion of an unrelated essential protein, DhfR (encoded by *dfrA*), does not affect asymmetry of growth or division (Figure 3.4C). Taken together, these data implicate ClpC and ClpP in asymmetric growth and division in mycobacteria.

Growth is driven by the set of proteins collectively referred to as the elongasome. The first protein to visibly localize to the pole and the nucleator of polar growth is the DivIVA homolog, Wag31 (Jani et al. 2010). In other work, Wag31 has been used as a marker for cell wall growth at both the pole and septum (Kang et al. 2008; Joyce et al. 2012; Wakamoto et al. 2013). We asked if Wag31 localization might differ with the loss of asymmetric growth seen in ClpP depletion by imaging dendra2-Wag31 in the presence and absence of ClpP. We find ClpP is required for asymmetric partitioning of Wag31, which is in agreement with our growth rate assays (Figure 3.5).

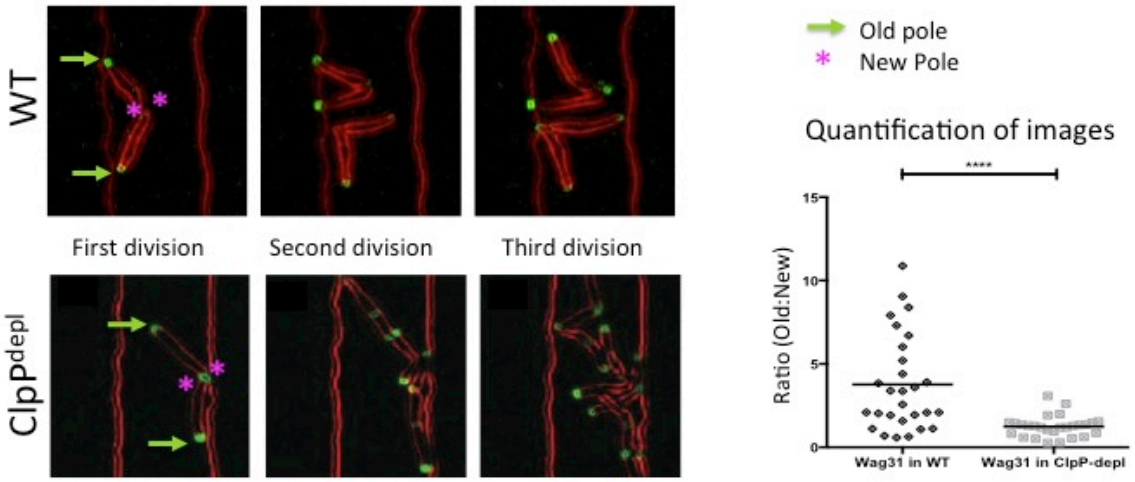

Figure 3.5 Asymmetry of growth machinery requires ClpP. Upper panel: In WT cells, dendra2-Wag31 is asymmetrically associated with the old to the new pole. **Lower panel:** With depletion of ClpP, dendra2-Wag31 asymmetry is lost. **Graph:** Images are quantified in the graph.

Similarities between Msm and Mtb

Asymmetric growth and division are correlated with the ability of mycobacteria to withstand antibiotics currently in use (Aldridge et al. 2012). It is therefore possible that changes to asymmetry might effect changes to MIC. In fact, we found a 14-fold increase in MIC with ClpP-depletion in Msm for meropenem (data not shown). ClpP-depleted cells have slowed growth, which could cause a shift in MIC independent of the specific role of ClpP in the cell. Therefore we were unable to conclude if the change in MIC was due to slowed growth or specific to ClpP-depletion.

To test if the role of ClpP is similar in Mtb as in Msm, I imaged treated and untreated Mtb in BioSafety Level 3 for 3 days with a new ClpP inhibitor #4283 (gift of Tatos Akopian in Alfred Goldberg's lab at HMS). I find a similar morphology from ClpP inhibition in Mtb as with ClpP depletion in Msm (Figure 3.6), suggesting combinatorial therapies with new ClpP inhibitors will need to be cognizant of the potential for homogenization of cells. Clearly, further work in TB is needed to understand the potential for drug interactions.

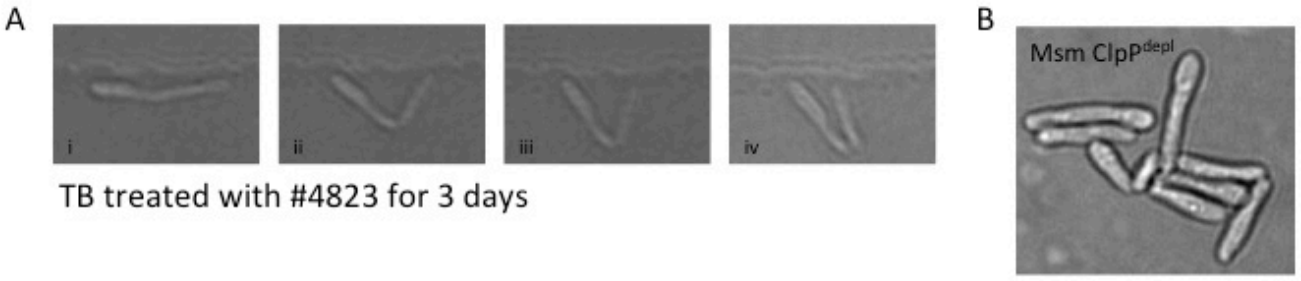

Figure 3.6 Pharmacological ClpP inhibition in *Mtb* phenocopies depletion in *Msm*. (A) Mtb treated with compound #4823 for 3 days and imaged every hour. **(B)** Msm depleted of ClpP for 18hrs.

3.2 ClpX is implicated in cell division or DNA maintenance.

ClpX depletion had no effect on the delay of new pole growth. After the lag phase, both poles grew at near WT rates. ClpX-depleted cells no longer divided, rendering measuring asymmetry of division moot.

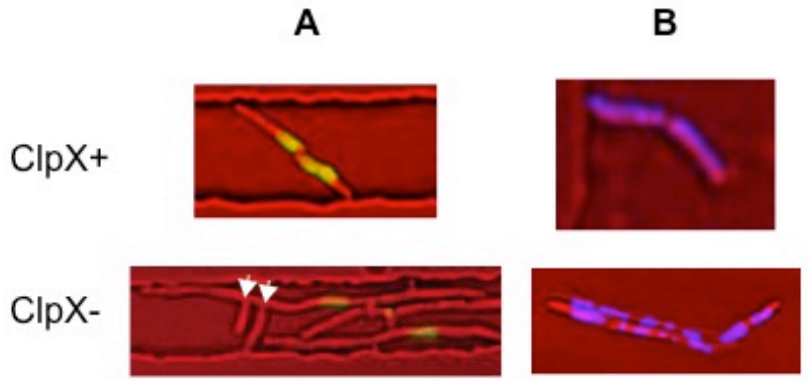

Figure 3.7 Summary of ClpX depletion phenotypes. (A) Cell wall dyes reveal continued polar and branched growth. **(B)** DAPI staining shows discontinuous chromosomes.

To understand the role of ClpX in the cell, we used microscopy to further phenotype these cells. ClpX depletion leads to filamentation in all surviving cells, branching with 42.5% penetrance, and eventual lysis and death. Filamentation and branching are shown in Figure 3.7A. In contrast, when we used DAPI to observe DNA within depleted cells, we find discontinuous genetic material (Figure 3.7B), possibly indicative of lost DNA integrity. These data suggested a role for ClpX in DNA maintenance and cell division.

FtsZ dynamics with and without ClpX.

In our observations of FtsZ-mCherry localization in WT cells, we found two distinct Z-ring phases. The first was about ¼ into the cell cycle. Here, Z-rings localize faintly to mid-cell and flicker on and off. The second phase is approximately ¾ into the cell cycle and lacks the

dynamism seen in the first ring phase. This second phase forms stable, brighter rings, and these rings do not disperse until cell invagination is visible in WT cells. This FtsZ-mCherry dynamism has not been described in mycobacterial species before, though FtsZ dynamics have been beautifully described in E. coli (Sun & Margolin 1998).

With ClpX loss, FtsZ rings continue to localize at or near midcell, with the same dynamic formation, dispersion, and reforming as with WT. Yet, division is absent. After a period of time, each single FtsZ-mCherry ring at midcell disappears and two new rings are formed closer to the poles (Figure 3.8, upper panels). We assume this is the location of septa in the daughter cells, if the first had division occurred.

Although it is not possible to combine FtsZ-mCherry and ZipA-GFP in the same strain with ClpX-depletion due to over-engineering of that strain, imaging each separately was feasible. ZipA-GFP imaging in ClpX-depletion has fewer foci (Figure 3.8 lower panels) than FtsZ-mCherry, even in a cell matched for depletion time and similar in size. This suggests Z rings are not fully maturing, as ZipA is a marker of late division.

Taken together, our ClpX depletion microscopy data suggest a role for ClpX in cell division, DNA maintenance, or both.

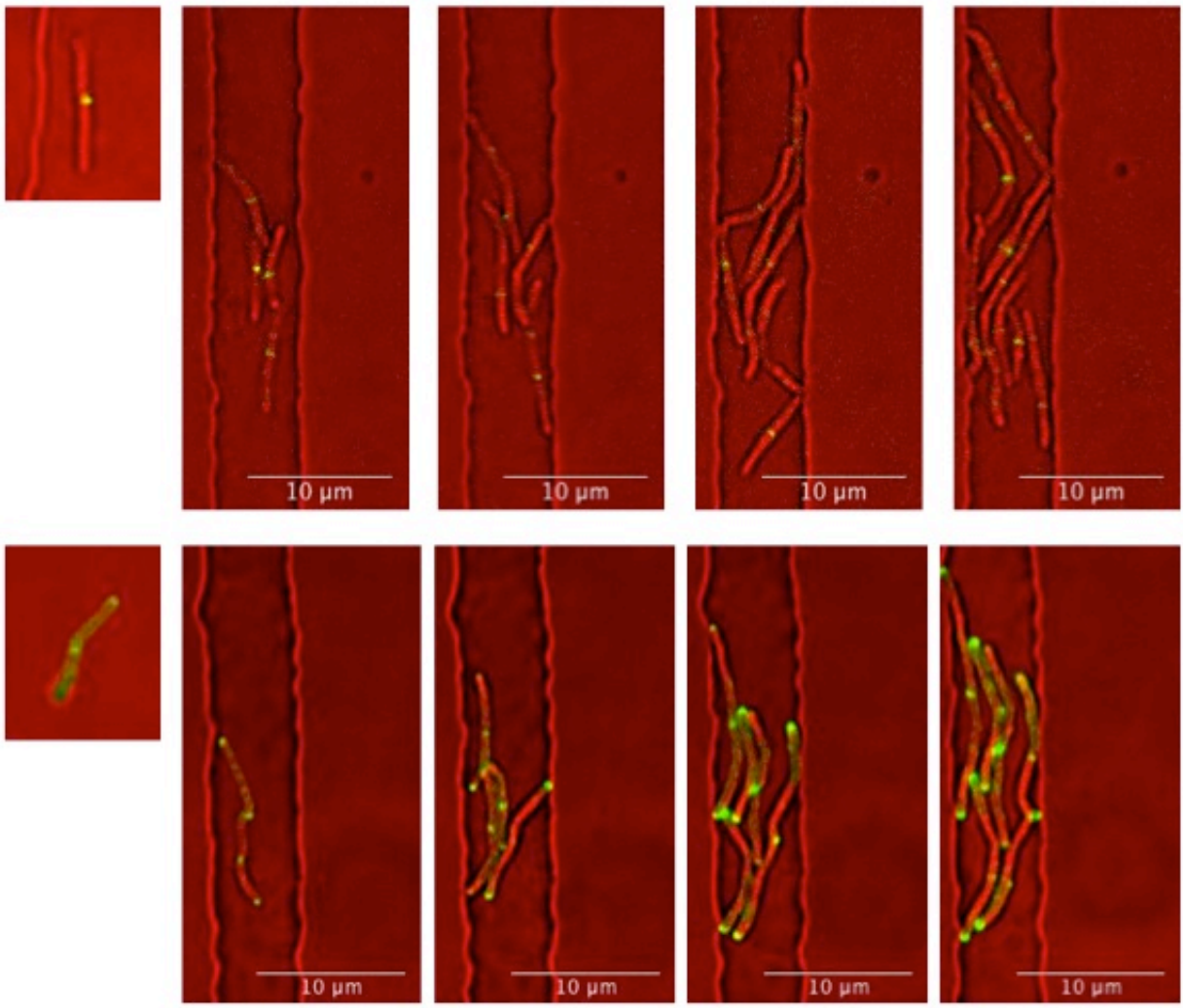

Figure 3.8 Division dynamics with ClpX depletion. Upper panels: FtsZ-mCherry with (left) and without (right) ClpX. **Lower panels:** ZipA-GFP with (left) and without (right) ClpX.

Discussion

My studies of the Clp family of proteins implicate ClpC and ClpP in asymmetric patterning. Our data implicate a requirement for ClpC and ClpP in creating the "boost" in total growth and instantaneous rate to the old pole. This boost is irrespective of lag phase, as lag phase relates only to the new pole.

As ClpCP functions together in the cell as a AAA+ protease, we expect there to be a set of substrates of ClpCP. The depletion phenotype of ClpC or ClpP is expected to be similar to that of overexpression of a target specific to ClpCP's role in polarization of growth. Further work in the lab is ongoing to identify potential substrates of ClpCP in growth and division asymmetry.

ClpX was implicated in cell cycle control, specifically by maintaining DNA integrity or promoting cell division in an indispensable way. These roles are not mutually exclusive; it is possible ClpX promotes both DNA stability and cell division, directly or indirectly. However, a direct role for ClpX on FtsZ seems unlikely, given the cell's ability to form Z rings in the absence of ClpX. It is more likely that cell division is failing at a later point, either because of a requirement for ClpX or because of inhibition due to another cell issue.

It is well established that a bacterium's failure to faithfully replicate its chromosome will inhibit cell division. While ectopic cell division can lead to genomic instability, as seen with chromosomal guillotining or anucleate cell production, we have observed no evidence of either phenotype with ClpX loss. Therefore, I believe it is more likely ClpX plays a role in genomic stability, though I cannot rule out a direct role for ClpX in cell division based on phenotyping alone. We used molecular, biochemical, and microscopy-based assays to distinguish these two hypotheses, described in Chapter 4.

References for Chapter 3

Akopian, T. et al., 2012. The active ClpP protease from M. tuberculosis is a complex composed of a heptameric ClpP1 and a ClpP2 ring. *The EMBO Journal*, 31(6), pp.1529–1541.

Aldridge, B.B. et al., 2012. Asymmetry and Aging of Mycobacterial Cells Lead to Variable Growth and Antibiotic Susceptibility. *Science*, 335(6064), pp.100–104.

Bhat, N.H. et al., 2013. Identification of ClpP substrates in Caulobacter crescentus reveals a role for regulated proteolysis in bacterial development. *Molecular Microbiology*, 88(6), pp.1083–1092.

Camberg, J.L., Hoskins, J.R. & Wickner, S., 2009. ClpXP protease degrades the cytoskeletal protein, FtsZ, and modulates FtsZ polymer dynamics. *Proceedings of the National Academy of Sciences of the United States of America*, 106(26), pp.10614–10619.

Dziedzic, R. et al., 2010. Mycobacterium tuberculosis ClpX Interacts with FtsZ and Interferes with FtsZ Assembly D. M. Ojcius, ed. *PLoS ONE*, 5(7), p.e11058.

Haeusser, D.P. et al., 2009. ClpX Inhibits FtsZ Assembly in a Manner That Does Not Require Its ATP Hydrolysis-Dependent Chaperone Activity. *Journal of Bacteriology*, 191(6), pp.1986–1991.

Iniesta, A.A. & Shapiro, L., 2008. A bacterial control circuit integrates polar localization and proteolysis of key regulatory proteins with a phospho-signaling cascade. *Proceedings of the National Academy of Sciences*, 105(43), pp.16602–16607.

Jani, C. et al., 2010. Regulation of Polar Peptidoglycan Biosynthesis by Wag31 Phosphorylation

in Mycobacteria. *BMC Microbiology*, 10(1), p.327.

Jenal, U. & Fuchs, T., 1998. An essential protease involved in bacterial cell-cycle control. *The EMBO Journal*, 17(19), pp.5658–5669.

Joyce, G. et al., 2012. Cell division site placement and asymmetric growth in mycobacteria. *PLoS ONE*, 7(9), p.e44582.

Kang, C.M. et al., 2008. Wag31, a homologue of the cell division protein DivIVA, regulates growth, morphology and polar cell wall synthesis in mycobacteria. *Microbiology*, 154(3), pp.725–735.

Kock, H., Gerth, U. & Hecker, M., 2003. MurAA, catalysing the first committed step in peptidoglycan biosynthesis, is a target of Clp-dependent proteolysis in Bacillus subtilis. *Molecular Microbiology*, 51(4), pp.1087–1102.

Liu, J. et al., 2016. ClpAP is an auxiliary protease for DnaA degradation in Caulobacter crescentus. *Molecular Microbiology*, 102(6), pp.1075–1085.

Pan, Q., Garsin, D.A. & Losick, R., 2001. Self-reinforcing activation of a cell-specific transcription factor by proteolysis of an anti-sigma factor in B. subtilis. *Molecular Cell*, 8(4), pp.873–883.

Pazos, M., Natale, P. & Vicente, M., 2013. A specific role for the ZipA protein in cell division: stabilization of the FtsZ protein. *Journal of Biological Chemistry*, 288(5), pp.3219–3226.

Raju, R.M. et al., 2012. Mycobacterium tuberculosis ClpP1 and ClpP2 function together in protein degradation and are required for viability in vitro and during infection. *PLoS*

Pathogens, 8(2), p.e1002511.

Schmitz, K.R. & Sauer, R.T., 2014. Substrate delivery by the AAA+ ClpX and ClpC1 unfoldases activates the mycobacterial ClpP1P2 peptidase. *Molecular Microbiology*, 93(4), pp.617–628.

Sugimoto, S. et al., 2010. AAA+ chaperone ClpX regulates dynamics of prokaryotic cytoskeletal protein FtsZ. *Journal of Biological Chemistry*, 285(9), pp.6648–6657.

Sun, Q. & Margolin, W., 1998. FtsZ dynamics during the division cycle of live Escherichia coli cells. *Journal of Bacteriology*, 180(8), pp.2050–2056.

Wakamoto, Y. et al., 2013. Dynamic Persistence of Antibiotic-Stressed Mycobacteria. *Science*, 339(6115), pp.91–95.

Weart, R.B. et al., 2005. The ClpX chaperone modulates assembly of the tubulin-like protein FtsZ. *Molecular Microbiology*, 57(1), pp.238–249.

Chapter 4

ClpX is a master regulator of the mycobacterial cell cycle

Abstract

In collaboration with Olga Kandror in Alfred Goldberg's lab at HMS, and using an ATP analog and tandem MS/MS, I have isolated and identified proteins associating in an ATP-dependent manner with ClpX hexamers in *Mycobacterium smegmatis* (Msm) cell lysates. With help from Mike Chase in the Fortune lab, I analyzed the raw data and identified 188 high-confidence ClpX-specific putative substrates for followup. KEGG enrichment analysis of these candidates, combined with our phenotypic analysis data from Chapter 3, suggested a role for ClpX in DNA replication. We therefore selected single-stranded DNA binding protein (SSB), a top hit and essential DNA-related protein, for validation.

Using purified *Mycobacterium tuberculosis* (Mtb) SSB protein (SSB_{TB}) from Meindert Lamers' lab at MRC, we show that SSB_{TB} stimulates the ATPase activity of ClpX *in vitro*. This activation extends to a small but repeatable increase in degradation of the only known *in vitro* substrate of ClpXP, GFP-SsrA. SSB does not stimulate ATPase activity of ClpC, suggesting this activation is specific to ClpX. We show SSB stimulation is mediated by the C-terminal phenylalanine, as deletion of this residue from C-terminal peptides abrogates the ATPase increase. Finally, phenotypic data support a role for ClpX and SSB in maintaining genomic integrity, as loss of ClpX leads to decreased time for active replication, multiple replisome and *oriC*-proximal foci, and an overabundance of *ori*-proximal relative to *ter*-proximal genes.

We propose ClpX is an essential modulator of DNA replication in mycobacteria. This study is the first to identify an activator of ClpX in mycobacteria, and the first to describe an essential role for ClpX in the cell.

Introduction

AAA+ (ATPases associated with diverse cellular activities) are housekeeping enzymes found across all domains of life. AAA+ proteins bind and hydrolyze ATP to power their unfoldase activity. They can function on their own, termed chaperones, or be coupled to proteases. AAA+ proteases harness ATP hydrolysis to drive proteolytic cleavage of substrates. AAA+ proteases can be coupled to their protease internally, as with Lon, or externally, as with ClpXP.

The ClpX hexamer is a AAA+ protein implicated in maintaining homeostasis and recovering from heat shock and other stress conditions. ClpX can function alone as an unfoldase or disaggregase, or in conjunction with the protease ClpP to identify, unfold, and degrade targets (reviewed in (Olivares et al. 2016)).

Frequently, recognition sequences or motifs provide substrate specificity. ClpXP is known to free ribosomes from stalled translation events in a process called trans-translation. In this process, a peptide tag, the SsrA tag, is added to the C-terminus of a nascent peptide on a stalled ribosome by charged *ssrA* RNA. ClpXP recognizes this SsrA tag, and the peptide is degraded. For mycobacteria, the SsrA tag is a twelve amino acid sequence (A)ADSHQRDYALAA (Personne & Parish 2014). Beyond this SsrA tag, no recognition sequence has been identified in mycobacteria for ClpC or ClpX.

ClpXP-dependent degradation of SsrA-tagged substrates is frequently carried out with the aid of the adaptor protein stringent starvation protein B (SspB). SspB binds the SsrA tag itself and shuttles the peptide to ClpXP for degradation. Though mycobacteria utilize ClpXP for degradation of SsrA-tagged proteins, no SspB homolog has been identified.

All known SsrA systems—even those of mycobacteria—require small protein B (SmpB) for trans-translation to succeed (Karzai et al. 2000). SmpB binds to RNA, forming an *ssrA*-SmpB

complex to deliver *ssrA* to ribosomes (Karzai et al. 2000). Thus, SmpB is not a ClpX adaptor; no Clp adaptors have been found in mycobacteria.

In most bacteria studied, adaptors bind a specific substrate to increase its accessibility or appeal to AAA+ proteases (Flynn et al. 2004; Donegan et al. 2014; Hou et al. 2008; Engman & Wachenfeldt 2014). Contrastingly, in *Caulobacter* the adaptor CpdR has been shown to function directly on ClpXP (Lau et al. 2015), making it the first adaptor identified with a broad range of substrates on which it can act.

Another well-described AAA+ adaptor is ClpS. While mycobacteria have an annotated ClpS, its deletion has no phenotype (my unpublished work and personal correspondence with Alfred Goldberg, HMS) suggesting it no longer plays a role in Clp functionality. Additionally, ClpS has previously been shown to modulate activity with ClpA rings (Hou et al. 2008); as mycobacteria do not contain a ClpA homolog, ClpS is unlikely to modulate ClpX or ClpXP activity.

What is the essential role of ClpX in mycobacteria? Our phenotypic data (Chapter 3) suggested a role for ClpX in DNA replication (based on genomic fractioning) or cell division (as depletion causes filamentation and branching). Previous work investigating the role of ClpX on cell division found a loss of cell division with depletion of *clpX* by siRNA and overexpression of a truncated ClpX (Dziedzic et al. 2010). However, Dziedzic et al. provide no direct biochemical evidence for an interaction of ClpX with FtsZ.

To clarify the role of ClpX, and identify other substrates or adaptors of ClpX, we performed an unbiased screen to find proteins associated with ClpX in the cell.

Materials and Methods

Screen methodology

The screen was performed in collaboration with Olga Kandror in Alfred Goldberg's lab in the department of Cell Biology at Harvard Medical School, Boston, MA, USA. Two technical replicates of two biological replicates each of logarithmically growing 1.5L cultures of ClpX-His and WT control cells were lysed by French press in the presence of ATPγS:ATP (100:1) and Dnase I at 4°C. Lysates were bound to Ni-NTA agarose beads (ThermoFisher, Catalog number: R90101) overnight with shaking at 4°C. Elutions were performed in increasing concentrations of imidazole (0-200mM in elution buffer). 100mM and 200mM elutions were collected, ultracentrifuged and concentrated by TCA. Next, short gels were run and the entire lysate band was sent for MS/MS analysis by John Leszyk at UMASS Medical Center, Worcester, MA, USA. We identified peptides in a data-dependent manner by nanoflow LC/MS/MS on an orbitrap (QExactive) and quantitated their relative abundances based on spectral counts (the number of MS/MS events) and precursor intensity (MS1 integrated peak intensity) (B. Zhang et al. 2006). We then used Mascot software in the Scaffold viewer to assign spectra to *Msm* proteins and quantify relative abundances of individual proteins between the samples.

Bacterial culture conditions.

M. smegmatis mc^2155 was cultured in Middlebrook 7H9 salts supplemented with 10% ADC (5:2:3 albumin:dextrose:catalase), 0.25% glyercol, and 0.05% Tween-80 or plated on Middlebrook 7H10 agar supplemented with ADC, 0.25% glycerol, and 0.05% Tween-80. All cultures were grown at 37°C, unless otherwise noted.

Depletion of essential genes: Clp family depletion line cultures were grown with the addition of anhydrotetracycline (aTc) at a final concentration of 100ng/mL. Depletion was performed by washing logarithmically growing culture pellets in a volume of PBS supplemented with 0.05% Tween20 (PBS-T) equal to original culture twice before resuspending in growth media ±aTc supplementation. Depletion of FtsZ was performed in the same manner, with the substitution of acetamide for aTc, at a final concentration of 0.2% by volume.

KEGG pathway analysis.

Gene set enrichment analysis was performed using KEGG annotation (Kanehisa & Goto 2000) on the DAVID Bioinformatics Resources platform v6.8 from NIAID, NIH (Huang et al. 2008). Significance was set to ≥3.5 fold and <0.01.

Recombinant DNA and protein constructs.

MCtH::ptb21-FLAG-SSB was constructed using the Gateway Multisite system, as described in Chapter 2. **SSB peptides** were synthesized by Genscript, Piscataway, NJ, USA. To make the **ClpX depletion** line, *clpX* was inserted into the L5 site of mc^2155 Msm under a tetracycline-inducible promoter using the nourseothricin resistance marker (Nat). In the merodiploid, I then deleted *clpX* from the chromosome using recombineering and replacing it with a zeocin (Zeo) resistance marker. Doubly-resistant (Nat and Zeo) Msm cells were then selected. To prevent a high rate of escape mutants, I then added an episomal streptomycin-resistant plasmid containing several continuous tetR repeats (tetR plasmid gift of Kadamba Papavinasasundaram in Christopher Sassetti's lab at UMass Medical School, Worcester, MA, USA).

Biochemical validation.

Expression and purification of proteins: N-terminally 6His-tagged truncated form of ClpX (lacking first 60 amino acids) and C-terminally 6His-tagged ClpP1, ClpP2 and ClpC1 were expressed from pTrc99 in E. coli BL21 ΔclpXP and purified as described previously (Akopian et al. 2015). SSB_{TB} was a generous gift of Meindert Lamers at MRC, Cambridge, UK.

ATPase assay (PK-LDH): ATP hydrolysis was measured with the enzyme-linked assay using pyruvate kinase and lactic dehydrogenase (PK/LDH). 2 μg of pure ClpC1 or ClpX were mixed with 100 μl of the assay buffer B containing 1 mM phosphoenolpyruvate (Sigma, catalog number 860077); 1 mM NADH (Sigma, catalog number N8129); 2 units of pyruvate kinase/lactic dehydrogenase; 4 mM MgCl2 and 1 mM ATP, and the ATPase activity was followed by measuring the oxidization of NADH to NAD spectrometrically at 340 nm. Measurements were performed in triplicate, which agreed within 5%.

Proteinase assay: ClpXP1P2 was assayed continuously in 96-well plates using the fluorescent protein substrate, GFP-SsrA. To measure GFP-SsrA degradation by the ClpXP1P2 complex, each well contained 500 nM GFP-SsrA, 75-100 nM ClpP1P2 tetradecamer and 300-400 nM ClpX hexamer, and 2 mM Mg-ATP in 100 μl of buffer A (20 mM phosphate buffer pH 7.6 with 100 mM KCl, 5% glycerol and 2 mM Bz-Leu-Leu). GFP-SsrA fluorescence was measured at 509 nm (Ex at 440 nm).

Protein analysis by western blotting

Protein lysates were extracted using bead beating in FLAG or His buffer. Whole cell lysates were run on NuPAGE 4-12% Bis-Tris Protein Gels (ThermoFisher, Catalog number: NP0322BOX).

For **FLAG western blotting**, we used primary mouse anti-DYKDDDDK (FLAG epitope tag) Antibody, clone 2EL-1B11 (EMD Millipore, catalog number: MAB3118) at 1:500. For secondary blotting, we used WesternBreeze Chromogenic Kit, anti-mouse (ThermoFisher, Catalog number: WB7103) according to manufacture's instructions.

For a **loading control**, we used anti-GAPDH (Ga1R) Loading Control Mouse Monoclonal Antibody from Pierce Chemical, catalog number: MA515738 at 1:5000. For secondary blotting, we used Goat anti-Mouse IgG (H+L) Secondary Antibody, HRP, Catalog number: 32430, at 1:5000.

Imaging and analysis

Devices: As previously described (Aldridge et al. 2012), microfluidic devices were made of polydimethylsiloxane (PDMS) bonded to #1.5 cover glass substrates using soft lithography techniques. Additional baking in a conventional oven at 65 ºC for at least one week aided in reducing background fluorescence.

Microscope: As previously described (Aldridge et al. 2012), time-lapse images were acquired at 60X (Plan APO NA 1.42) using a DeltaVision PersonalDV microscope with an automated stage enclosed in an environmental chamber warmed to 37°C, unless otherwise noted. We used the InsightSSI Solid State Illumination system (461-489 nm; Applied Precision, Inc.) to illuminate and a CoolSnap HQ2 camera (Photometric) to take pictures. We used the Ultimate Focus System (Applied Precision, Inc.) to maintain focus in time-lapse imaging. Images were acquired every 10 or 15 minutes for 18-24 hours.

Data representation and statistical analysis

Prism 6.0a software (GraphPad Software, La Jolla, CA) was used to graph all data. Statistical tests of measurements were used from the Prism suite as noted in figure legends. Significance is indicated by p values as follows: *<0.05, **<0.01, ***<0.001, ****<0.0001.

Statistical analysis of **mass spectrometry** data was performed as described within the text below.

qPCR and qRT-PCR assays

Genomic DNA extraction was performed using the lab's phenol chloroform method as previously described (Shell et al. 2013).

Quantitative PCR (qPCR) was performed on 20ng of gDNA using in-house primer sets. All primer sets were tested and matched for efficiency using a standard curve of known target concentration prior to use in this assay. Detection of product amplification was by iTRAQ Universal SYBR green Supermix (Bio-RAD, catalog number: 1725121) on an Applied Biosystems 7300 Real Time PCR System. Expression values are a product of the ΔΔCt method, normalized to *dnaA* and using time 0 as the control.

RNA was extracted using the standard TRIzol (ThermoFisher, Catalog number: 15596026) method with the addition of 45s and 30s bead-beating in a FastPrep24 (MP Bio, Santa Ana, CA, USA) to aid in lysis. DNA was removed by the addition of 10U DNase Turbo (Ambion, catalog number: AM2238) for 1 h and purified with RNeasy (Qiagen, catalog number: 74104) according to the manufacturer's instructions.

cDNA synthesis was performed with SuperScript III First-Strand Synthesis (ThermoFisher, Catalog number: 18080051) and random hexamers, according to product manual.

Quantitative reverse transcriptase PCR (qRT-PCR) was performed as qPCR above, using cDNA instead of gDNA. Expression values are a product of the ΔΔCt method, normalized to *sigA* and using -aTc as the control.

Results

4.1 Novel screen allows for identification of interactors of essential ATPases.

Our phenotypic data (Chapter 3) suggested a role for ClpX in DNA replication (genomic fractioning by DAPI staining) or cell division (filamentation and branching) or both. To differentiate these possibilities, we undertook to identify the set of substrates of ClpX within the mycobacterial cell. We hypothesized there would be a protein(s) whose interaction with ClpX might explain the essentiality of ClpX and its specific cellular role.

From other bacteria, we know there are additional proteins involved in ClpXP-dependent degradation, called adaptors. These can act on ClpX directly, as with CpdR in *C. crescentus* (Lau et al. 2015) or on the substrate, as with RSSB on RpoS in *E. coli* (Zhou et al. 2001). No known adaptors have been identified in mycobacteria to date. In order to capture potential adaptor proteins, we used whole cell lysates rather than purified proteins.

Previously, several labs have identified the substrates of AAA+ proteases from whole cell lysates. Owing to the non-essential nature of ClpXP in these bacterial systems, proteolytic traps were available for *S. aureus* (Feng et al. 2013) and *E. coli* (Flynn et al. 2003). Although ClpP is essential in *C. crescentus*, the Chien lab was able to introduce a degradation-null ClpP ($ClpP_{TRAP}$) in a ClpP-WT depletion background, thus enriching for $ClpP_{TRAP}$ (Bhat et al. 2013).

However, because of the difference in phenotype between ClpX and ClpP, we predicted ClpX's essential cellular role might be ClpP-independent. Therefore, in designing our screen, we wanted a method allowing us to capture substrates or adaptors of both ClpX alone and in conjunction with ClpP. ClpC depletion had a phenotype similar to that of ClpP; since we were following up on ClpX substrates, we did not want ClpC substrates. Therefore, a $ClpP_{TRAP}$ was not a viable option, as this would provide ClpC substrates as well as ClpX substrates.

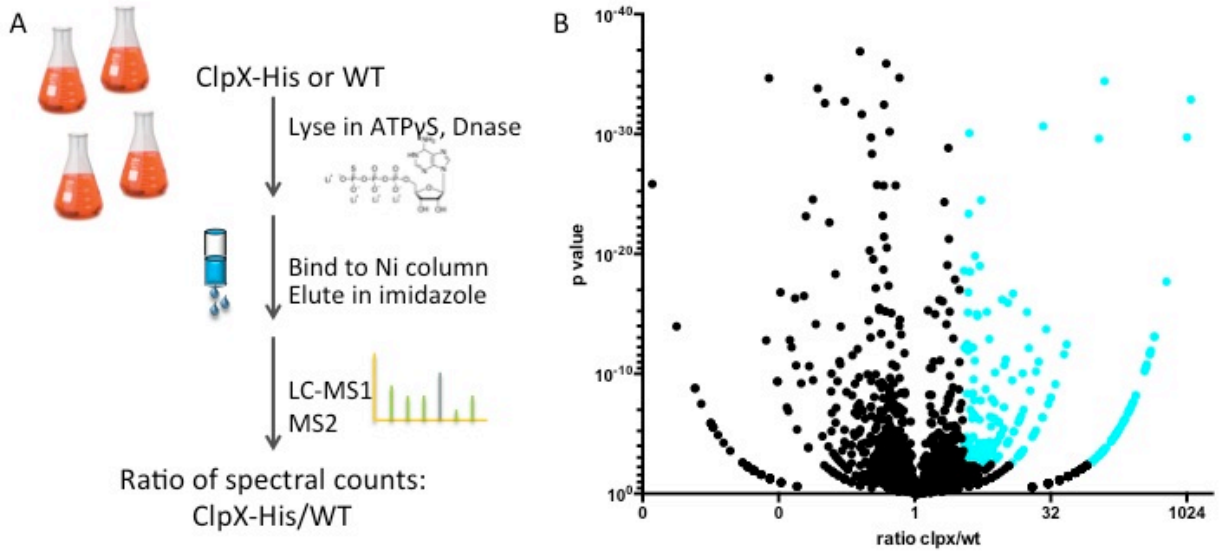

Figure 4.1 Unbiased screen identifies putative ClpX substrates/interactors. A) Diagram describing screen methodology. **B)** Volcano plot of all proteins identified, shown as log10 p value to log2 ratio of spectral counts of each protein from ClpX relative to WT. Teal represents proteins at least 3.5-fold higher in ClpX with a p value of ≤0.001.

An *in vivo* method previously used to identify AAA+ substrates utilizes mutations in the Walker B motif. These mutants can bind ATP and substrate, but cannot hydrolyze ATP. Thus, they are translocase-null. Unfortunately, even as a second copy in a WT background, Walker B *clpX* mutants were non-viable. Since we could use neither a $ClpP_{TRAP}$ nor a ClpX Walker B mutant, we chose a biochemical inhibition approach.

We used the non-hydrolyzable ATP analog ATPγS in an optimized ratio with ATP to create a pseudo-trap, allowing us to pull down from *M. smegmatis* whole cell lysates proteins whose association with the hexameric ClpX barrel is ATP-dependent. We had LC-MS/MS performed on all four replicates of each class and analyzed using spectral counting. Screen methodology is outlined in Figure 4.1A.

Statistical analysis of raw data finds 188 potential substrates.

We pooled spectral counts from all four replicates and took the ratio of peak intensity of ClpX-His:WT to obtain a relative abundance for each protein. Next, we excluded any protein not present in all 4 replicates of the class (WT or ClpX-His). We considered only proteins that had at least two spectra found, and required any change in abundance be in the same direction across all four replicates. This yielded 1,926 total proteins observed, irrespective of abundance change (Figure 4.1B, all points).

Next, we rank ordered by statistical significance (g test, corrected for multiple testing). ClpX was the second protein by significance. Setting a narrow cutoff of fold change of ≥3.5 and p-value≤0.001, we identified 188 high-confidence ClpX-specific putative substrates (Figure 4.1B, teal).

Selection of relevant candidates.

The phenotypic data of ClpX depletion (Chapter 3) suggested a role for ClpX in either cell division or DNA maintenance, possibly without ClpP involvement given the difference in phenotype. To narrow our search in an unbiased manner, we performed KEGG pathway analysis on all 188 proteins. Using DAVID online software, I identified KEGG terms enriched ≥3.5 over the entire genome with a p-value cutoff of <0.01 (Figure 4.2). The enriched terms are involved mainly in three pathways: DNA replication, DNA repair, and transcription, suggesting a role for ClpX in DNA maintenance. Nearly all terms were related to nucleotide/nucleoside binding, directing our focus to the DNA/RNA pathway-related putative substrates.

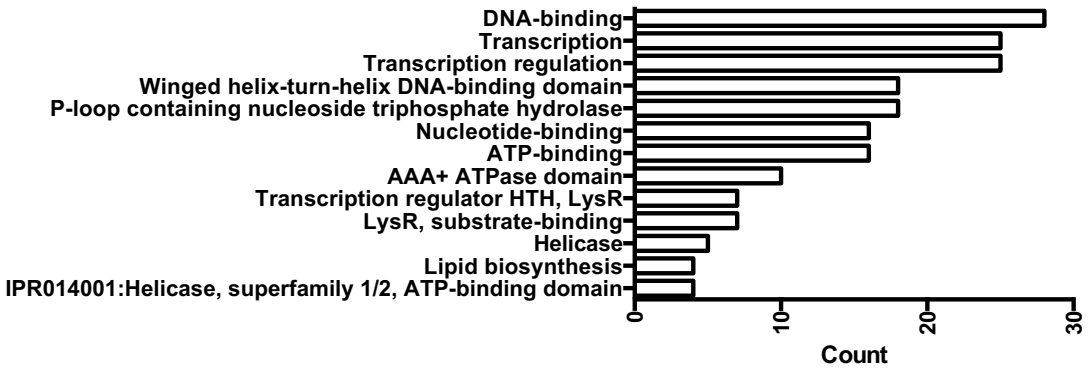

Figure 4.2 KEGG Analysis reveals abundance of DNA/RNA-associated proteins. All terms with p value <0.01 from IP list fold change ≥3.5, completed using DAVID online software.

4.2 SSB stimulates ClpX ATPase activity.

Once we narrowed our search to DNA replication, DNA repair, and transcription, we looked for high fold change candidate interactors that might be involved in one or more of these pathways. Single-stranded DNA binding protein (SSB) was a top hit with a 210-fold increase in abundance in ClpX-His to WT cells and an adjusted p-value of 0.001. SSB is an essential protein involved in all three pathways.

We first asked if SSB protein stimulated ClpX's ATP hydrolysis, as an indicator of interaction. We used the well-established PK-LDH assay, which measures the decrease of NADH as ADP increases as a proxy for the consumption of ATP (Figure 4.3A). We measured the rate of ATP hydrolysis for ClpX purified from Mtb ($ClpX_{TB}$) with and without SSB purified from Mtb (SSB_{TB}). We found SSB_{TB} stimulated $ClpX_{TB}$'s rate of ATP hydrolysis two-fold (Figure 4.3B). This effect is specific to these two proteins, as an unrelated control protein did not stimulate ATP hydrolysis of ClpX (Figure S.1) nor did SSB stimulate ClpC's hydrolysis activity (Figure S.2). SSB_{TB} therefore interacts with $ClpX_{TB}$.

SSB's C-terminus is sufficient for ClpX hydrolysis effect.

Our data suggest SSB activates ClpX ATPase activity. We next asked if this stimulation was mediated by SSB's C-terminus, as previous work has established this domain as critical for AAA+ ATPase interaction in other species (Shereda et al. 2008; Chen et al. 2016; Lecointe et al. 2007). Based on sequence alignment of Mtb SSB to *E. coli* and Msm, we hypothesized that either the terminal 10 or 19 residues would be sufficient to activate ClpX. In fact, this is what we find; the C-terminal 10- and 19-residue peptides increased ClpX ATP hydrolysis relative to scrambled. This is dependent upon the terminal phenylalanine (F), as peptides lacking the final F did not increase the rate (Figure 4.3C).

4.3 SSB stimulates ClpXP to degrade of GFP-SsrA.

Due to the design of our study, we expected to have pulled down all ATP-dependent interactors of ClpX in the cell. Additionally, SSB has been shown to stimulate ATPases of DNA maintenance proteins in Mtb and other bacterial species (H. Zhang et al. 2014; Chen et al. 2016; Slocum et al. 2007). Therefore, the stimulation of $ClpX_{TB}$ by SSB_{TB} might suggest SSB is a substrate or an activator. To distinguish between the two, we employed an established fluorimetric assay measuring the rate of GFP-SsrA degradation by its cognate protease ClpXP (Flynn et al. 2003; Akopian et al. 2015).

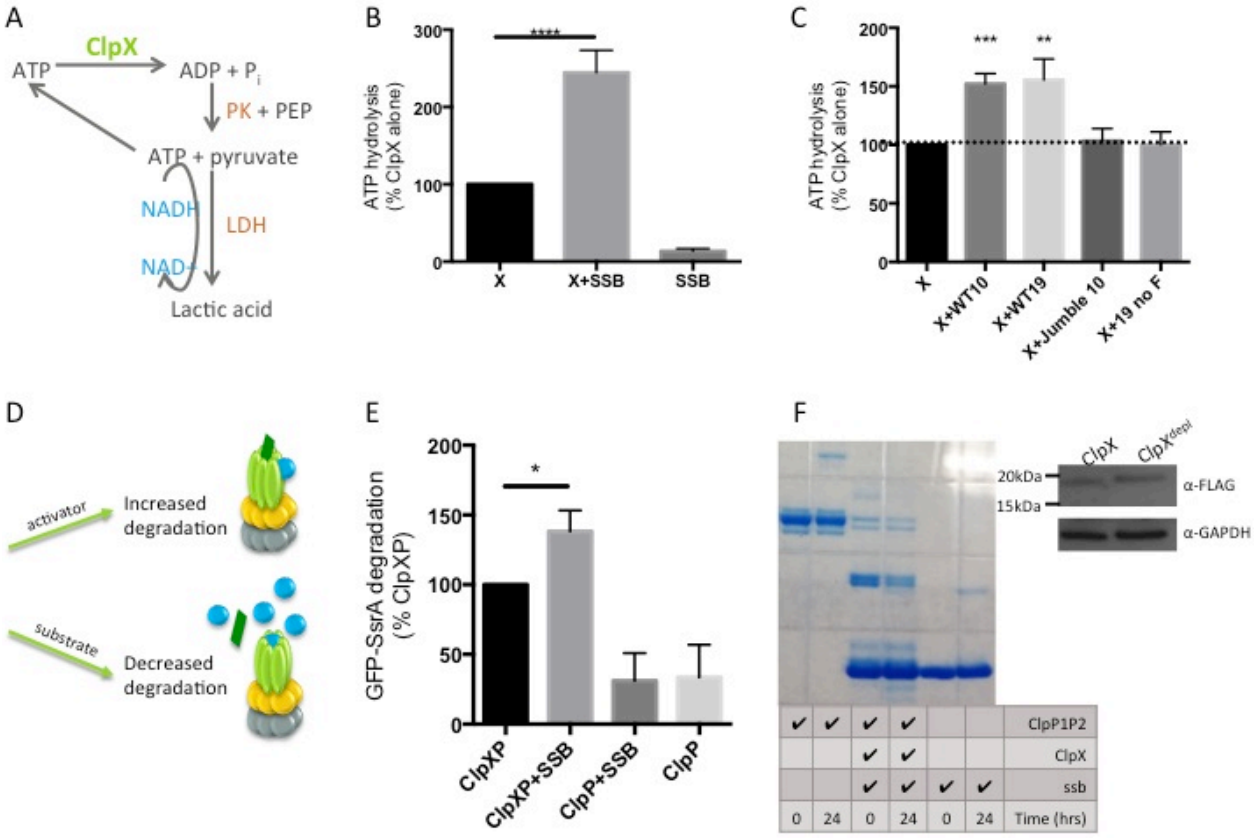

Figure 4.3 SSB activates ClpX ATPase activity. (A) Schematic of the PK-LDH assay. **(B)** PK-LDH data shown as a percent of ClpX ATP hydrolysis activity alone, using full length SSB_{TB}*. **(C)** PK-LDH data shown as a percent of ClpX ATP hydrolysis activity alone, using synthesized 10- and 19-aa peptides from the C-terminus of SSB_{TB}*. **(D)** Cartoon depicting expectations for GFP-SsrA degradation assay outcome. If SSB is an activator, it should increase the rate of degradation. **(E)** Proteinase assay shown as percent of GFP-SsrA degradation by ClpXP alone*. **(F)** SSB_{TB} incubated with $ClpXP_{TB}$ overnight (left). SSB_{SM} anti-FLAG western blot from Msm whole cell lysates. *Averages of three replicates, error bars represent SEM.

If SSB_{TB} is a substrate of ClpXP, we expect it to outcompete GFP-SsrA at its saturation point (Figure S.3). In contrast, if SSB_{TB} is an activator, it should instead increase the rate of GFP-SsrA degradation. A cartoon of this logic is shown in Figure 4.3D. We found that SSB_{TB} increases the rate of degradation of GFP-SsrA by ClpXP to a similar extent as for ATP

hydrolysis of ClpX (Figure 4.3E). This effect of SSB is specific to ClpXP, as there was no change in the rate of degradation of casein by ClpCP by the addition of SSB_{TB} (data not shown).

4.4 SSB is not degraded by ClpXP *in vitro* or *in vivo*.

This study has so far shown that SSB can activate ClpX. Because of the possibility that SSB is a substrate and therefore activating ClpX, we looked for changes to SSB levels *in vitro* and *in vivo*. We observed no change in SSB_{TB} with overnight incubation with ClpXP or FLAG-SSB following ClpX depletion from the cell (Figure 4.3F).

4.5 ClpX is required for the integrity of the DNA replication cycle.

We have successfully identified a protein with an ATP-dependent interaction with ClpX and validated it biochemically. We next sought to understand how the interaction of SSB with ClpX might affect cell cycle progression *in vivo*.

In Chapter 3, I described the effect of ClpX loss on cell growth and division. Briefly, ClpX-depleted cell growth is unperturbed and division loss is observed as early as 9 hours post removal of aTc. This loss of division appears to be post-FtsZ ring formation but before late events, as additional FtsZ rings form at their expected locations but no additional ZipA foci do appear. Additionally, I described the apparent loss of chromosome integrity using DAPI staining.

From work in this chapter identifying potential ClpX-interacting proteins and subsequent GSEA on the pathways represented, we find ClpX candidates are enriched for DNA maintenance. We therefore hypothesized ClpX plays a role in DNA maintenance, and turned to the DNA replication tools validated in Chapter 2 to assess.

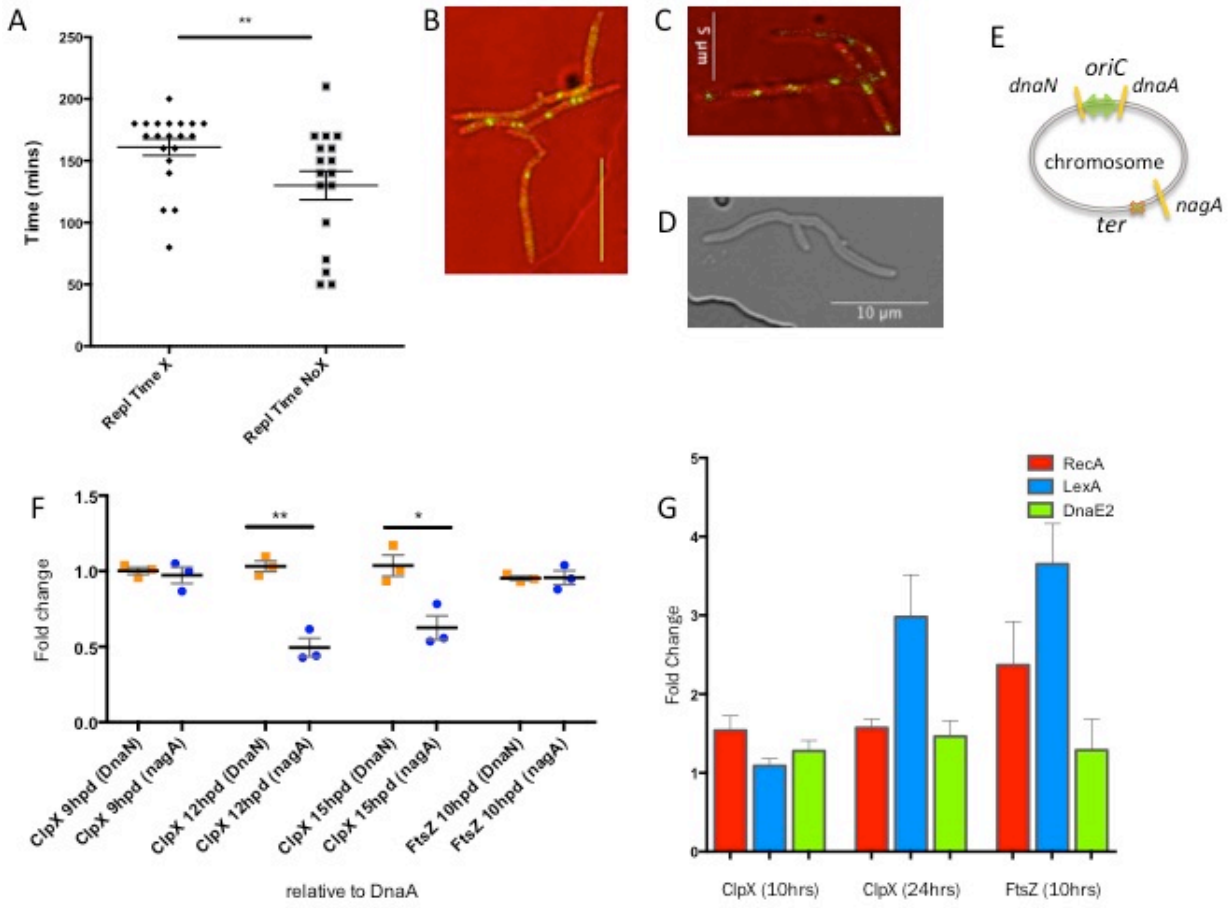

Figure 4.4 Phenotypic data support a role for ClpX in genomic stability. (A) Time between DnaN-ON to DnaN-OFF in cells with and without ClpX. Depletion time spans 10-18hrs post removal of aTc. Reduction with loss of ClpX is 19.3%. Significance by Mann-Whitney. **(B)** Representative image of DnaN-eGFP foci in ClpX-depleted cells. Scale bar represents 10um. **(C)** Representative image of ParB-mCherry in ClpX-depleted cells. **(D)** Representative image of FtsZ depletion after overnight growth without acetamide. **(E)** Cartoon depicting location of each gene used in qPCR. **(F)** Results of qPCR on gDNA. Fold change represents ΔΔCt method relative to *dnaA* and +aTc. **(G)** Results of qRT-PCR for SOS response genes. Fold change represents ΔΔCt method for depleted cells relative to *sigA* and time 0 (ClpX) or +ami (FtsZ).

We imaged DnaN-eGFP in ClpX-depleted cells. With ClpX loss, we find DnaN-ON (the appearance of DnaN-eGFP foci) occurs later, i.e., after visible cell division. DnaN-OFF (the resolution of DnaN-eGFP foci) occurs 19% earlier in cells without ClpX than in cells with ClpX

(Figure 4.4A). This indicates replisomes are active for 19% less time, suggesting ClpX-depleted cells might have unstable replisomes.

Following a period without DnaN-eGFP foci, new DnaN-eGFP foci appear. These new DnaN-eGFP foci are greater in number and unevenly spaced (Figure 4.4B). This could either indicate further rounds of DNA replication are initiated or DNA repair is underway. To distinguish, we used qRT-PCR on ClpX- cells compared to ClpX+ cells and looked for induction of three canonical SOS response pathway genes: *recA*, *lexA*, and *dnaE1*.

As a control, we used FtsZ depletion. FtsZ is an essential protein whose loss also leads to death by way of filamentation and branching (Figure 4.4D). We find no induction of these genes by ΔΔCt method for ClpX loss above induction in FtsZ loss (Figure 4.4G).

DnaN is present in both replisomes and sites of DNA repair, yet we observed no induction of canonical SOS response (Figure 4.4G). This suggests the DnaN foci represent replisomes rather than DNA repair sites, though we cannot exclude the possibility of non-canonical SOS induction (LexA/RecA-independent).

To investigate this, we used ParB-mCherry as a proxy to count *oriC*s. If the extra DnaN-eGFP foci represent additional rounds of DNA replication, there should be a concomitant increase in ParB-mCherry foci. We find a pronounced increase in ParB-mCherry foci with ClpX-depletion (Figure 4.4C), suggesting ClpX-depleted cells have more *oriC*s than cells with ClpX.

We have shown ClpX-depletion results in shorter open fork times, increased replisomes, and increased *oriC*s. As previously noted, ClpX-depleted cells eventually stop dividing. Taken together, these data suggest ClpX-depleted cells are competent in DNA replication initiation but replication fails at a later point. The alternative interpretation is that ClpX-depleted cells are chaining, with additional replisome foci representing continued normal DNA replication.

If ClpX-depleted cells fail to competently replicate their chromosome at a point after initiation, ClpX-depleted cells should have different copy numbers of *oriC* and *ter* regions of chromosomes relative to ClpX-competent cells. In contrast, chaining cells should have the same ratio of *oriC*/*ter* as cells pre-depletion. To test this, I created qPCR probes against the *ori*-flanking genes *dnaA* and *dnaN*, and the *ter*-proximal gene *nagA* (shown in Figure 4.4E). I performed qPCR on gDNA from ClpX+ and ClpX- cultures at 9, 12, and 15 hours post depletion and determined the fold change of *nagA* and *dnaN* relative to *dnaA* and time 0. I found a 50% reduction in *nagA* relative to *dnaA* with ClpX depletion compared to undepleted cells (Figure 4.4F). In the same assay, the two *oriC*-flanking genes *dnaA* and *dnaN* do not change in their relative abundance.

As a negative control, I performed the same assay in an FtsZ-depletion strain at a similar level of phenotypic advancement in depletion (Figure 4.4C). We find FtsZ loss has no effect on fold change of *nagA* relative to *dnaA* (Figure 4.4F). Taken together, these data suggest a role for ClpX in the integrity of the DNA replication cycle that is specific to ClpX, and not a general response to death by filamentation and branching.

Discussion

In this chapter I have described the isolation of proteins interacting in an ATP-dependent manner with the AAA+ ATPase ClpX. Statistical analysis narrowed 1,926 total proteins found to 188 high-confidence putative substrates of or adaptors for ClpX. GSEA using KEGG pathway annotation combined with our phenotypic data pointed us towards DNA replication, DNA repair, and transcription. We therefore proceeded to validate single-stranded DNA binding protein (SSB) due to its high fold change and position at the nexus of all three of these DNA-related pathways.

Using purified Mtb proteins we show that SSB_{TB} activates $ClpX_{TB}$ ATP hydrolysis, and that this interaction is dependent upon the terminal phenylalanine. Likewise, we show SSB_{TB} increases the rate at which $ClpXP_{TB}$ degrades GFP-SsrA, without SSB being degraded by ClpXP *in vitro* or *in vivo*.

Though both the ATP hydrolysis and GFP-SsrA degradation stimulations are small, changes of this magnitude have been established previously. The very well established ClpX adaptor SspB has only a mild effect on SsrA-tagged proteins *in vitro*; yet Chowdhury et al. observed pronounced enhancement of ClpXP degradation by SspB when using the weaker substrate of mutated SsrA tagged proteins (Chowdhury et al. 2010).

To understand the role of SSB-ClpX in the cell, we further parsed the phenotype of ClpX-depletion. Using translational fluorescent fusions, we find ClpX-depleted cells have DnaN-eGFP foci that appear late, disappear early, and return with increased numbers relative to ClpX-competent cells. ParB-mCherry foci also increase with loss of ClpX.

These data suggest either a chaining phenotype or loss of DNA replication completion. We show an increase in ratio of *ori*-proximal to *ter*-proximal genes with ClpX depletion, suggesting chromosome replication integrity is lost.

Towards a possible mechanism.

SSB's role at the nexus of several DNA maintenance pathways combined with our phenotypic data supporting a role in DNA replication and GSEA of other potential substrates combine to suggest a role for ClpX and SSB in DNA replication. We propose ClpX plays a role in maintaining the integrity of DNA replication.

One possible mechanism is for ClpX to function as a negative regulator of DNA replication initiation, as has been shown for ClpX on MuB transposase in Mu replication in *E. coli* (Kruklitis et al. 1996) and DnaA in *C. crescentus* (Gorbatyuk & Marczynski 2005). Our preliminary phenotypic and biochemical data on the replicative helicase DnaB agrees with this hypothesis (data not shown).

Alternately, ClpX might provide a maintenance function for stalled forks, allowing for fork progression to termination or aiding in restart of stalled forks. There are no homologs to known DNA replication termination factors in mycobacteria, suggesting a novel mechanism exists for the release of the replisome. Given the abundance of DNA replication- and RNA transcription-related proteins in our dataset, this hypothesis has potential. In support of this postulation, when we inhibit DNA replication termination by sub-inhibitory concentrations of the topoisomerase inhibitor moxifloxacin, Msm cells filament with no effect on licensing (Figure S.4), as with ClpX loss.

Outstanding questions.

In other systems, many roadblocks to successful DNA replication (including environmental stress, DNA damage, and over-firing of the *oriC*) induce an SOS response (Simmons et al. 2008). We propose ClpX is required for integrity of the DNA replication cycle. Yet, we do not observe induction of gene expression in three canonical SOS genes: *lexA*, *recA*, and *dnaE1* (Figure 4.4G) above what we find in FtsZ-depletion.

There are three possible explanations for this discrepancy. First, a robust response might not be possible without ClpX. There is evidence to suggest ClpX is required for a robust canonical SOS response in other systems (Neher et al. 2006; Nagashima et al. 2006). If this were true in mycobacteria as well, a lack of SOS in the absence of ClpX would not mean there is no DNA defect.

Second, there can be DNA instability without the SOS response. The SOS response is *almost* always induced when DNA replication fails. The exception to this rule is when replication fails due to a disruption of termination events. In *E. coli*, the presence of DinB is sufficient to prevent induction of the SOS response when termination fails (Mori et al. 2012). In this case, cell division is still prevented and cells filament. Mycobacteria encode a DinB homolog, which could participate in dampening the SOS response.

Finally, we may not have tested the "correct" genes. The SOS response in mycobacteria has been shown to be non-canonical (Brooks et al. 2001), with many SOS-induced genes lacking LexA binding sites. The authors found *recA* and *lexA* were driven by LexA binding, but many other SOS genes (including *ssB*, *dnaB*, *recN*, *recC*, and *dinPG*) were not. Therefore, transcript levels of *lexA* and *recA* may not reflect a response to this particular DNA error.

Currently, we are continuing work to validate other hits from our screen. In validating substrates, we aim to understand more of what ClpX does in the cell.

What makes SSB's modulation of ClpX special?

A homolog to the *E. coli* adaptor ClpS has been suggested in mycobacteria by sequence homology. ClpS has been shown to modulate ClpA in *E. coli*, a close relative to ClpC in Mtb. Therefore, I deleted the non-essential *clpS* gene from Msm and assayed the phenotype. Its deletion had no effect on growth or division asymmetry or on gross morphology (data not shown). As such, we believe SSB to be the first identified and experimentally tested adaptor of a Clp ATPase in mycobacteria.

The ClpX adaptor in *B. subtilis*, YjbH, mediates the degradation of a stress response transcription factor and is specific to this substrate (Garg et al. 2009). In *E. coli*, three ClpX adaptors have been identified, all with a role in aiding the degradation of stress response proteins (reviewed in (Kirstein et al. 2009)). These adaptors, SspB, RssB, and UmuD, are all specific for their cognate substrates: SsrA-tagged proteins, RpoS, and UmuD', respectively. In our work, SSB's effect on ClpX seems independent of substrate and protease, making it a unique system. Additionally, because ClpX and SSB are conserved across bacterial species, it is conceivable that SSB might act on ClpX in other systems. We are currently pursuing this possibility.

References for Chapter 4

Akopian, T. et al., 2015. Cleavage Specificity of Mycobacterium tuberculosisClpP1P2 Protease and Identification of Novel Peptide Substrates and Boronate Inhibitors with Anti-bacterial Activity. *Journal of Biological Chemistry*, 290(17), pp.11008–11020.

Aldridge, B.B. et al., 2012. Asymmetry and Aging of Mycobacterial Cells Lead to Variable Growth and Antibiotic Susceptibility. *Science*, 335(6064), pp.100–104.

Bhat, N.H. et al., 2013. Identification of ClpP substrates in Caulobacter crescentus reveals a role for regulated proteolysis in bacterial development. *Molecular Microbiology*, 88(6), pp.1083–1092.

Brooks, P.C., Movahedzadeh, F. & Davis, E.O., 2001. Identification of Some DNA Damage-Inducible Genes of Mycobacterium tuberculosis: Apparent Lack of Correlation with LexA Binding. *Journal of Bacteriology*, 183(15), pp.4459–4467.

Chen, S.H., Byrne-Nash, R.T. & Cox, M.M., 2016. Escherichia coli RadD Protein Functionally Interacts with the Single-stranded DNA-binding Protein. *Journal of Biological Chemistry*, 291(39), pp.20779–20786.

Chowdhury, T. et al., 2010. Versatile modes of peptide recognition by the ClpX N domain mediate alternative adaptor-binding specificities in different bacterial species. *Protein Science*, 19(2), pp.242–254.

Donegan, N.P., Marvin, J.S. & Cheung, A.L., 2014. Role of Adaptor TrfA and ClpPC in Controlling Levels of SsrA-Tagged Proteins and Antitoxins in Staphylococcus aureus. *Journal of Bacteriology*, 196(23), pp.4140–4151.

Dziedzic, R. et al., 2010. Mycobacterium tuberculosis ClpX Interacts with FtsZ and Interferes with FtsZ Assembly D. M. Ojcius, ed. *PLoS ONE*, 5(7), p.e11058.

Engman, J. & Wachenfeldt, von, C., 2014. Regulated protein aggregation: a mechanism to control the activity of the ClpXP adaptor protein YjbH. *Molecular Microbiology*, 95(1), pp.51–63.

Feng, J. et al., 2013. Trapping and proteomic identification of cellular substrates of the ClpP protease in Staphylococcus aureus. *J. Proteome Res.*, 12(2), pp.547–558.

Flynn, J.M. et al., 2004. Modulating substrate choice: the SspB adaptor delivers a regulator of the extracytoplasmic-stress response to the AAA+ protease ClpXP for degradation. *Genes & Development*, 18(18), pp.2292–2301.

Flynn, J.M. et al., 2003. Proteomic discovery of cellular substrates of the ClpXP protease reveals five classes of ClpX-recognition signals. *Molecular Cell*, 11(3), pp.671–683.

Garg, S.K. et al., 2009. The YjbH Protein of Bacillus subtilis Enhances ClpXP-Catalyzed Proteolysis of Spx. *Journal of Bacteriology*, 191(4), pp.1268–1277.

Gorbatyuk, B. & Marczynski, G.T., 2005. Regulated degradation of chromosome replication proteins DnaA and CtrA in Caulobacter crescentus. *Molecular Microbiology*, 55(4), pp.1233–1245.

Hou, J.Y., Sauer, R.T. & Baker, T.A., 2008. Distinct structural elements of the adaptor ClpS are required for regulating degradation by ClpAP. *Nature Structural & Molecular Biology*, 15(3), pp.288–294.

Huang, D.W., Sherman, B.T. & Lempicki, R.A., 2008. Systematic and integrative analysis of large gene lists using DAVID bioinformatics resources. *Nature Protocols*, 4(1), pp.44–57.

Kanehisa, M. & Goto, S., 2000. KEGG: kyoto encyclopedia of genes and genomes. *Nucleic Acids Research*, 28(1), pp.27–30.

Karzai, A.W., Roche, E.D. & Sauer, R.T., 2000. The SsrA-SmpB system for protein tagging, directed degradation and ribosome rescue. *Nature structural biology*, 7(6), pp.449–455.

Kirstein, J. et al., 2009. Adapting the machine: adaptor proteins for Hsp100/Clp and AAA+ proteases. pp.1–11.

Kruklitis, R., Welty, D.J. & Nakai, H., 1996. ClpX protein of Escherichia coli activates bacteriophage Mu transposase in the strand transfer complex for initiation of Mu DNA synthesis. *The EMBO Journal*, 15(4), pp.935–944.

Lau, J. et al., 2015. A Phosphosignaling Adaptor Primes the AAA+ Protease ClpXP to Drive Cell Cycle-Regulated Proteolysis. *Molecular Cell*, 59(1), pp.104–116.

Lecointe, F. et al., 2007. Anticipating chromosomal replication fork arrest: SSB targets repair DNA helicases to active forks. *The EMBO Journal*, 26(19), pp.4239–4251.

Mori, T. et al., 2012. Escherichia coli DinB inhibits replication fork progression without significantly inducing the SOS response. *Genes & genetic systems*, 87(2), pp.75–87.

Nagashima, K. et al., 2006. Degradation of Escherichia coli RecN aggregates by ClpXP protease and its implications for DNA damage tolerance. *The Journal of biological chemistry*, 281(41), pp.30941–30946.

Neher, S.B. et al., 2006. Proteomic Profiling of ClpXP Substrates after DNA Damage Reveals Extensive Instability within SOS Regulon. *Molecular Cell*, 22(2), pp.193–204.

Olivares, A.O., Baker, T.A. & Sauer, R.T., 2016. Mechanistic insights into bacterial AAA+ proteases and protein-remodelling machines. *Nature Reviews Microbiology*, 14(1), pp.33–44.

Personne, Y. & Parish, T., 2014. Mycobacterium tuberculosis possesses an unusual tmRNA rescue system. *Tuberculosis (Edinburgh, Scotland)*, 94(1), pp.34–42.

Shell, S.S. et al., 2013. DNA Methylation Impacts Gene Expression and Ensures Hypoxic Survival of Mycobacterium tuberculosis W. R. Bishai, ed. *PLoS Pathogens*, 9(7), p.e1003419.

Shereda, R.D. et al., 2008. SSB as an Organizer/Mobilizer of Genome Maintenance Complexes. *Critical Reviews in Biochemistry and Molecular Biology*, 43(5), pp.289–318.

Simmons, L.A. et al., 2008. The SOS Regulatory Network. *EcoSal Plus*, 2008.

Slocum, S.L. et al., 2007. Characterization of the ATPase activity of the Escherichia coli RecG protein reveals that the preferred cofactor is negatively supercoiled DNA. *Journal of Molecular Biology*, 367(3), pp.647–664.

Zhang, B. et al., 2006. Detecting Differential and Correlated Protein Expression in Label-Free Shotgun Proteomics. *J. Proteome Res.*, 5(11), pp.2909–2918.

Zhang, H. et al., 2014. Functional characterization of DnaB helicase and its modulation by single-stranded DNA binding protein in Mycobacterium tuberculosis. *The FEBS journal*,

281(4), pp.1256–1266.

Zhou, Y. et al., 2001. The RssB response regulator directly targets sigma(S) for degradation by ClpXP. *Genes & Development*, 15(5), pp.627–637.

Chapter 5

Discussion

Abstract

Tuberculosis (TB) remains a global health threat, with 10.4 million incident cases in 2015 (World Health Organization 2016). The WHO reports 580,000 newly multidrug resistant TB cases in the same year. Although TB treatment prevented an estimated 49 million deaths in the past 15 years (World Health Organization 2016), with 1.8 million deaths annually, we can surely do better.

In general, antibiotics target processes that together compose the cell cycle: cell growth, DNA replication, and cell division. Though these processes have been highly successful targets, with current drugs failing, new drugs and/or regimens will be required. One avenue to identification of new drugs or drug targets is to better understand regulators of the cell cycle in *Mycobacterium tuberculosis* (Mtb), the causative agent of TB.

In my dissertation, I defined the cell cycle using the model, non-pathogenic *Mycobacterium smegmatis* (Msm) and a suite of image-based analysis tools. I tested the hypothesis that Clp family proteins play a role in the mycobacterial cell cycle. I demonstrated a role for ClpCP in asymmetric cell growth and division, and provided evidence of a mechanism for ClpX regulation of DNA replication.

In addition to the intriguing cell biology of Clp family members, these proteins are actively being targeted with antibiotics (Brötz-Oesterhelt & Sass 2014; Famulla et al. 2016), yet we know very little about their function in mycobacteria. It is critical to understand Clp proteins' functions before targeting them in the clinic, in order to predict and prevent antibiotic resistance with rational drug combinations. Additionally, since host cells also contain ClpXP homologs in their mitochondria, chemical adaptations of drugs to increase specificity for bacterial ClpXP could aid in limiting patient side effects.

Results summary and perspective

To understand the regulators of the cell cycle, we first needed to develop a suite of tools with which to observe and quantify any changes to the cell cycle. Using fluorescent translational fusions and dyes in conjunction with quantitative image analysis, in Chapter 2 I ordered key events in the cell cycle relative to each other: DNA replication, cell division, and polar growth. I found DNA replication initiation occurs in the final 10% of the mother cell's cycle, completing in each daughter cell. This is in agreement with the data (Trojanowski et al. 2015) and interpretations (Santi & McKinney 2015) of previous studies. The time between completion of replication and initiation of a new round is indicated by the resolution of DnaN-eGFP foci (Santi & McKinney 2015) and the appearance of another focal point. This phase is likely when termination and segregation events occur, and it is possible there are cell cycle checkpoints embedded within.

Asymmetric division has been established in mycobacteria (Joyce et al. 2012; Vijay et al. 2014; Singh et al. 2013). Asymmetric growth has also been described, and shown to give rise to a phenotypically diverse population able to withstand multiple insults, including differential response to antibiotic treatment associated with birth order (Aldridge et al. 2012). In other work, both old and new poles were shown to have equal growth rates (Wakamoto et al. 2013). What is the reason for this seeming discrepancy? Because these two papers measured growth differently, it was not possible to directly compare their data.

In adapting our growth assay to include each slice in a timecourse, I was able to calculate growth rates from poles as the slope of a line. I found the new pole—the pole created by division itself—has a period without growth directly following visible separation of the cells. This time, which we termed the "lag phase", averages 100 minutes. While we have not identified the cause

of this delay, we assume there is a licensing event that must occur. We suspect this event to be related to the dispersal of the divisome and the coalescence of the polar growth apparatus, as *a priori* we can say this process must occur. Following this lag phase, growth rates from both poles are not significantly different. Thus, both papers are correct: the total growth from the old pole over time (μm/min) is greater than the total growth from the new pole, but the rate of growth (μm/min) from each pole after licensing occurs is indistinguishable.

What drives asymmetry of growth and division in mycobacterial species? To begin to answer this question, we looked to the well-characterized non-pathogenic bacterium *Caulobacter crescentus,* which likewise divides asymmetrically. *Caulobacter* utilizes a complex molecular circuit to control its cell cycle, beginning with regulated proteolysis of key cell cycle-governing proteins by the housekeeping protease ClpXP. Because the unique essentiality of ClpXP, the AAA+ ATP protease responsible for this step, is conserved between the phylogenetically different *Caulobacter* and mycobacteria, and because they both divide asymmetrically, we asked if Clp proteins might contribute to cell cycle regulation in mycobacteria as well.

To address this question, in Chapter 3 I systematically studied the phenotypes of *M. smegmatis* (Msm)—the non-pathogenic and faster growing model for Mtb—cells depleted for each essential part of the Clp system: ClpC and ClpX, the AAA+ ATPases, and ClpP, the proteolytic core. I found ClpC- and ClpP-depletion phenotypes to be highly similar, with each leading to loss of asymmetric growth and division. Specifically, depletion led to the significant reduction in old pole growth rate and total growth. In addition, ClpP was required for asymmetric localization of the growth marker Dendra2-Wag31. These data are in agreement with the hypothesis that ClpCP contributes to an old pole "boost" in growth under optimal conditions in wild type cells.

Asymmetric growth and division are a bet-hedging strategy, creating diversity in the population with each cell division (Aldridge et al. 2012). Because asymmetry is associated with differential survival of subpopulations of cells, it is important to understand the contribution to cell heterogeneity with the pharmacologic inhibition of ClpP. As a first pass, we looked for gross morphologic changes to Mtb in the presence of pre-market ClpP inhibitors. I treated Mtb with a ClpP inhibitor and imaged every hour in a microfluidic chamber for 3 days. These cells display a similar morphology to ClpP-depleted Msm, suggesting there might be other similarities between pharmacological inhibition and molecular depletion. We interpret this result as an indication that ClpP pharmacologic inhibition might lead to reduced heterogeneity in Mtb, as ClpP depletion did in Msm. This is important information for the rational design of drug regimens that include ClpP inhibitors.

In stark contrast to the ClpCP-depletion phenotypes, when I depleted ClpX from Msm, growth rates from the old and new poles were unchanged significantly from wild type. Licensing time was undisturbed as well, occurring ~100 minutes after division. I characterized the ClpX-depletion line using growth assays and DAPI staining. I found ClpX-depleted cells stop dividing and branch at a high penetrance. In addition, their genetic material appears segmented by DAPI staining.

To further investigate the loss of cell division, I imaged FtsZ-mCherry in ClpX-depleted cells. While there were increased FtsZ-mCherry foci, Z rings were distributed along the lateral cell wall as with ClpX+ cells, displaying no obvious defect in assembly. This suggests FtsZ ring formation is undisturbed. However, the late division marker ZipA-eGFP does not form increased foci, suggesting these Z rings are not maturing.

Is ClpX required for cell division, DNA maintenance, or both? Our efforts to distinguish the role for ClpX in DNA maintenance from cell division are the subject of Chapter 4. Using the most physiologically intact system to date, we pulled down proteins interacting with ClpX-His in an ATP-dependent manner by trapping potential interactors using ATPγS. Relative abundance proteomic analysis and robust statistical analysis gave us a candidate list of 188 proteins. We further narrowed our list by using KEGG annotation to perform gene set enrichment analysis, which revealed DNA-related proteins were significantly enriched in this data.

Of the candidates, we focused on single-stranded DNA binding protein (SSB) due to its role at the nexus of DNA repair and DNA replication. SSB_{TB} stimulated the ATPase activity of $ClpX_{TB}$ in the PK-LDH assay. SSB also increased degradation of GFP-SsrA by $ClpXP_{TB}$. Because SSB is not degraded by ClpXP *in vitro* and does not increase in abundance by western or proteomics upon depletion of ClpX (this study) or ClpP (Raju et al. 2014), we propose SSB is a *bona fide* activator of ClpX, the first of its kind identified in mycobacteria.

How do ClpX and SSB interact to affect DNA maintenance? SSB has been shown to stimulate other ATPases in mycobacteria and other systems. In mycobacteria, SSB stimulates the ATP hydrolysis and helicase activity of the replicative helicase, DnaB (Zhang et al. 2014).

In *E. coli*, SSB stimulates ATPase activity of DNA repair, replication, and recombination proteins (Chen et al. 2016; Shereda et al. 2008). Their interaction is dependent upon the C-terminus, in particular the terminal phenylalanine (F).

To test if the terminal F is also necessary for SSB_{TB}'s activation of $ClpX_{TB}$, we used short peptides of 10 and 19 residues, +/- the terminal F, and looked for stimulation by PK-LDH. We found that the terminal F was required for this activation, as the increase in ATP hydrolysis was absent without the terminal F or when the peptide sequence was jumbled.

Taken together, our phenotypic and biochemical data suggest a role for ClpX, mediated by SSB, in DNA maintenance. To test this hypothesis, we observed DNA replication via fluorescent fusions to the open fork protein DnaN and the kinetochore-like protein ParB, in cells with and without ClpX. We find ClpX-depleted cells have a decrease in open fork timing, both in minutes and percent of the extended cell cycle, suggesting they fail to complete DNA replication successfully. Depletion of ClpX also leads to an increase in DnaN-eGFP foci, likely from an increase in replisomes. Additionally, we find excess ParB foci, suggesting an increase in copy number of *parS* sequences, the centromere-like section of genomic DNA near the *oriC* to which ParB binds.

Our quantitative microscopy data point to increased origins of replication. To confirm this, I developed a quantitative PCR assay to measure the relative abundance of *ori*-proximal and *ter*-proximal sequences. This assay revealed a marked increase in the *ori*-proximal gene *dnaN* relative to the *ter*-proximal gene *nagA*, which agrees with our hypothesis that DNA replication is initiating but not completing in ClpX-depleted cells.

Future directions

The AAA+ proteins ClpC and ClpX are both essential for growth in mycobacterial species. In this work, I have provided evidence for this apparent redundancy—they perform non-redundant cellular functions. My data suggest ClpCP act together to drive elongasome activity to the old pole, increasing the growth rate and driving heterogeneity through asymmetric growth and division.

What might be the target of the ClpCP protease? In work continuing in the lab, we are using a Venus-tagged, mild overexpression library to screen for potential substrates of the ClpCP

protease. Depletion of protease and overexpression of target might show similar phenotypes. Therefore, we looked for proteins whose tagging and overexpression led to the same morphological changes as ClpCP depletion. To date, we have imaged fluorescent fusions to 295 proteins. Of those, only two proteins' overexpression displayed morphology similar to ClpP pharmacological inhibition and ClpCP depletion. Those are the glutamate synthesis pathway proteins GlnA and GlnE (Figure 5.1).

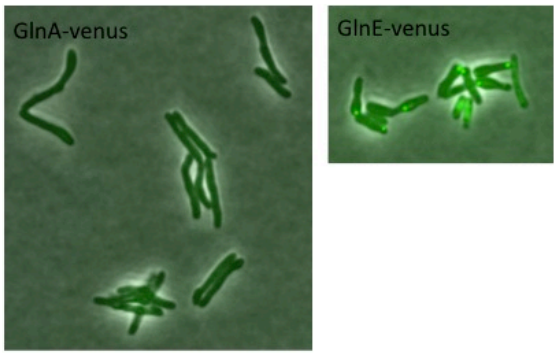

Figure 5.1 Localization and mild overexpression of glutamine biosynthesis pathway members.

Preliminary data suggest the glutamate synthase regulon as a potential target, as GlnE-mVenus and GlnA-mVenus cells display polar bulges. Glutamine biosynthesis has been shown to contribute to cell wall manufacturing in at least two steps in other systems (Cui et al. 2000), tying this pathway in with the ClpCP depletion phenotype. Additionally, GlnE-mVenus localizes to the peri-polar region of the new pole (Figure 5.1), which is where cell wall biosynthesis occurs in mycobacteria (Meniche et al. 2014). A role for ClpCP in driving glutamate biosynthesis to the peri-polar region of the old pole would be similar to the role of ClpCP in MurAA localization in *B. subtilis* (Kock et al. 2003). Ongoing work aims to test the interaction between ClpCP and GlnE/GlnA, and assay for their combined contribution to asymmetric growth.

In contrast to ClpCP, ClpX functions (with or without ClpP) to maintain DNA replication in conjunction with SSB. Ongoing work in the lab aims to biochemically validate additional hits from our screen, ultimately leading to the identification of substrates of ClpX-SSB involved in the process of DNA maintenance.

Identification of ClpC and ClpX substrates has the potential to lead to the discovery of a degron, or recognition sequence within substrates, for ClpC or ClpX. As a first pass, I aligned the top 25 hits from the ClpX-IP screen by ClustalW. I then used the BLOCKS database (Pietrokovski et al. 1996) to search for conserved motifs among these proteins. I found a highly hydrophobic sequence enriched in ClpX-associated proteins relative to total proteins identified (Figure 5.2A) bearing striking similarity to the minimum required SsrA sequence for recognition by ClpX, YALAA. The average fold change for proteins containing this motif was significantly higher than for proteins not containing the motif or total proteins (Figure 5.2B). In other words, ClpX-associated proteins are more likely to contain this motif than other proteins. Further work to test the ability of ClpX to recognize this motif is planned.

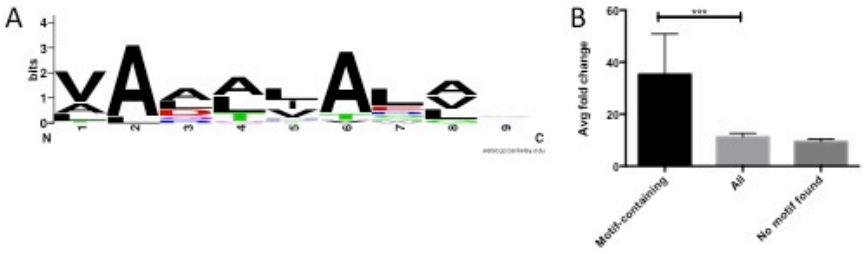

Figure 5.2 Putative recognition motif for ClpX in mycobacteria. (A) Recognition sequence presented as a WebLogo. Sequence was compiled from the top 25 hits from the ClpX-IP screen. **(B)** Motif-containing proteins have a significantly higher fold change ClpX pulldown relative to all proteins found or proteins lacking the motif.

Concluding remarks

This work contributes to the field of mycobacteriology in four key ways. First, I have provided a framework for understanding the unique essentiality of the Clp system in mycobacteria. ClpC and ClpX, both essential AAA+ ATPases, appear to play distinct roles in the cell cycle, thus explaining their seeming redundancy.

Second, I have provided evidence to suggest that pharmacologically targeting ClpP in the clinic may reduce cellular heterogeneity. This loss of diversity could affect MICs of other antibacterials currently in use, as I found with meropenem and ClpP-depletion. Rational deployment of Clp inhibitors will be needed in order to avoid drug synergies potentially leading to tolerant or resistant cells.

Third, we have developed and validated a novel methodology for the identification of proteins interacting with AAA+ ATPases. This methodology is unique in that it allows for *ex vivo* isolation of protein complexes using the full-length protein under near-normal cellular conditions. Due to the uniqueness of our screen, we were able to identify an adaptor molecule to an essential ATPase.

Finally, this work is the first to demonstrate a connection between the Clp system and the cell cycle in mycobacteria. While Clp proteins are already being targeted for antibiotic development, identification of Clp substrates and adaptors could also lead to new drug targets in the ongoing battle against Mtb.

References for Discussion

Aldridge, B.B. et al., 2012. Asymmetry and Aging of Mycobacterial Cells Lead to Variable Growth and Antibiotic Susceptibility. *Science*, 335(6064), pp.100–104.

Brötz-Oesterhelt, H. & Sass, P., 2014. Bacterial caseinolytic proteases as novel targets for antibacterial treatment. *International journal of medical microbiology : IJMM*, 304(1), pp.23–30.

Chen, S.H., Byrne-Nash, R.T. & Cox, M.M., 2016. Escherichia coli RadD Protein Functionally Interacts with the Single-stranded DNA-binding Protein. *Journal of Biological Chemistry*, 291(39), pp.20779–20786.

Cui, L. et al., 2000. Contribution of a thickened cell wall and its glutamine nonamidated component to the vancomycin resistance expressed by Staphylococcus aureus Mu50. *Antimicrobial Agents and Chemotherapy*, 44(9), pp.2276–2285.

Famulla, K. et al., 2016. Acyldepsipeptide antibiotics kill mycobacteria by preventing the physiological functions of the ClpP1P2 protease. *Molecular Microbiology*, 101(2), pp.194–209.

Joyce, G. et al., 2012. Cell division site placement and asymmetric growth in mycobacteria. *PLoS ONE*, 7(9), p.e44582.

Kock, H., Gerth, U. & Hecker, M., 2003. MurAA, catalysing the first committed step in peptidoglycan biosynthesis, is a target of Clp-dependent proteolysis in Bacillus subtilis. *Molecular Microbiology*, 51(4), pp.1087–1102.

Meniche, X. et al., 2014. Subpolar addition of new cell wall is directed by DivIVA in mycobacteria. *Proceedings of the National Academy of Sciences*, 111(31), pp.E3243–E3251.

Pietrokovski, S., Henikoff, J.G. & Henikoff, S., 1996. The Blocks database--a system for protein classification. *Nucleic Acids Research*, 24(1), pp.197–200.

Raju, R.M. et al., 2014. Post-Translational Regulation via Clp Protease Is Critical for Survival of Mycobacterium tuberculosis M. A. Behr, ed. *PLoS Pathogens*, 10(3), p.e1003994.

Santi, I. & McKinney, J.D., 2015. Chromosome organization and replisome dynamics in Mycobacterium smegmatis. *mBio*, 6(1), pp.e01999–14.

Shereda, R.D. et al., 2008. SSB as an Organizer/Mobilizer of Genome Maintenance Complexes. *Critical Reviews in Biochemistry and Molecular Biology*, 43(5), pp.289–318.

Singh, B. et al., 2013. Asymmetric growth and division in Mycobacterium spp.: compensatory mechanisms for non-medial septa. *Molecular Microbiology*, 88(1), pp.64–76.

Trojanowski, D. et al., 2015. Choreography of the Mycobacterium replication machinery during the cell cycle. *mBio*, 6(1), pp.e02125–14.

Vijay, S. et al., 2014. Asymmetric cell division in Mycobacterium tuberculosis and its unique features. *Archives of Microbiology*, 196(3), pp.157–168.

Wakamoto, Y. et al., 2013. Dynamic Persistence of Antibiotic-Stressed Mycobacteria. *Science*, 339(6115), pp.91–95.

World Health Organization, 2016. Global Tuberculosis Report 2016. *WHO Library Cataloguing-in-Publication Data*.

Zhang, H. et al., 2014. Functional characterization of DnaB helicase and its modulation by single-stranded DNA binding protein in Mycobacterium tuberculosis. *The FEBS journal*, 281(4), pp.1256–1266.

Supplemental Materials

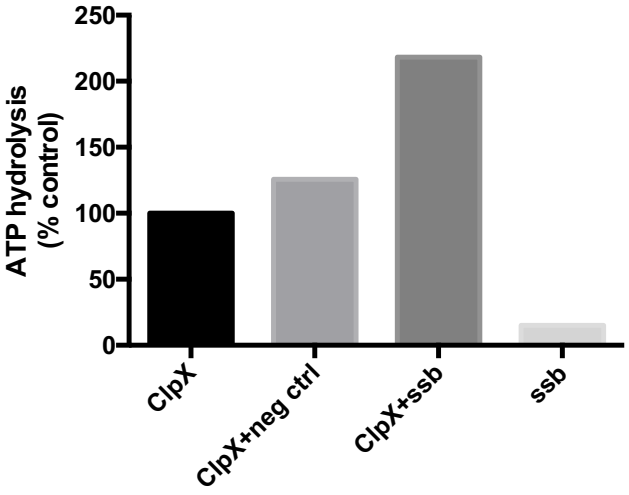

Figure S.1 Negative control for $ClpX_{TB}$ ATP hydrolysis assay. PK-LDH data shown as percent ClpX ATP hydrolysis alone. Negative control is ArnA, an *E. coli* decarboxylase.

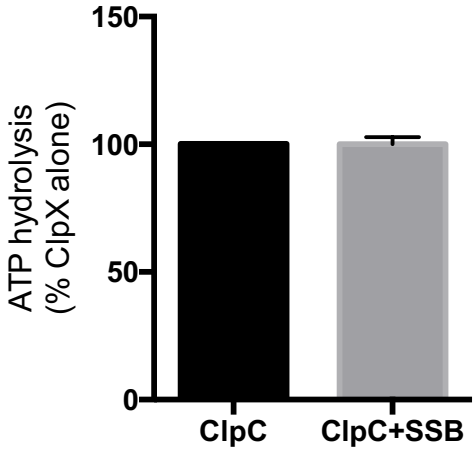

Figure S.2 SSB_{TB} does not stimulate $ClpC_{TB}$ ATP hydrolysis. PK-LDH data shown as percent ClpC ATP hydrolysis alone.

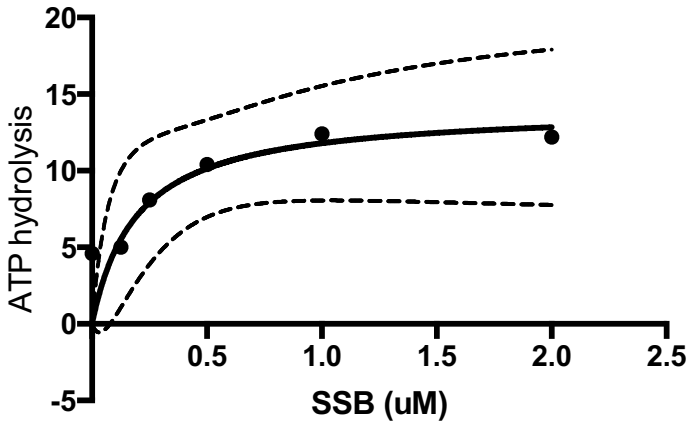

Figure S.3 SSB saturation kinetics. ATP hydrolysis activity of ClpX as a function of SSB concentration. 95% confidence intervals shown.

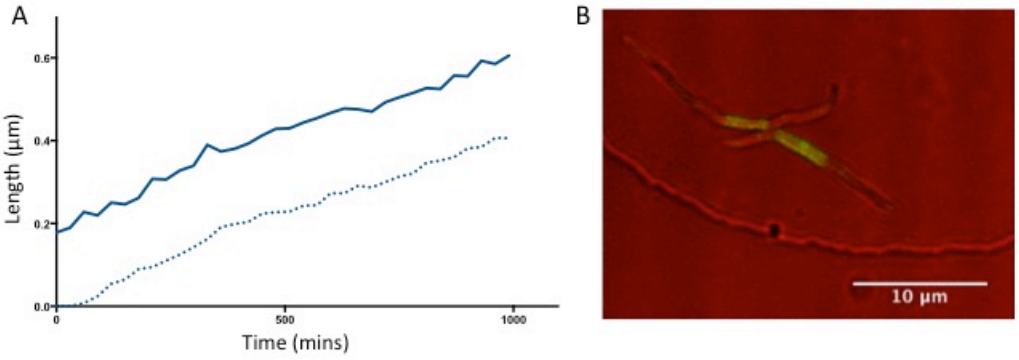

Figure S.4 *M. smegmatis* treated with moxifloxacin. (A) Representative tracings of old (solid line) and new (dashed line) pole growth during treatment. **(B)** Representative image of moxifloxacin-treated cells.